Cellular and cytotoxic mechanisms in cadmium exposed renal distal ephelial A6-cells

Faurskov Rasmussen, Brian

Publication date:
2000

Ph.D. Thesis:

CELLULAR AND CYTOTOXIC MECHANISMS IN CADMIUM EXPOSED RENAL DISTAL EPITHELIAL A6-CELLS

Brian Faurskov

Department of Life Sciences & Chemistry

Roskilde, May 2000

Roskilde University

The present thesis is based on the following articles/manuscripts:

I. Faurskov, B. & Bjerregaard, H. F. Effect of Cadmium on Active Ion Transport and Cytotoxicity in Cultured Renal Epithelial Cells (A6). *Toxicology in Vitro*, 11, 717-722, 1997.

II. Bjerregaard, H. F & Faurskov, B. Cadmium-induced Inhibition of ADH-stimulated Ion Transport in Cultured Kidney-derived Epithelial Cells (A6). *ATLA*, 25, 271-277, 1997.

III. Faurskov, B. & Bjerregaard, H. F. Effect of Cisplatin on Transepithelial Resistance and Ion Transport in the A6 Renal Epithelial Cell Line. *Toxicology in Vitro*, 13, 611-617, 1999.

IV. Faurskov, B. & Bjerregaard, H. F. Chloride secretion in kidney distal epithelial cells (A6) evoked by cadmium. *Toxicology and Applied Pharmacology*, 163, 267-278, 2000.

V. Faurskov, B. & Bjerregaard, H. F. Cadmium mobilizes intracellular calcium in a hormone-like manner in renal distal epithelial A6 cells. *In submission in American Journal of Physiology.*

VI. Bjerregaard, H. F. & Faurskov, B. Temporary entitled: "Nickel acts as an CaR activator in A6 cells". *In preparation.*

PREFACE

The present thesis is the result of work carried out at the department in the laboratory of assistant professor Henning F. Bjerregaard and in the laboratory of professor dr. rer. Wolfgang Clauss, Giessen University, Germany. The work began early 1996 where Henning introduced a research area totally new to me dealing with electrophysiological measurements. Very early, preliminary experiments with cadmium exposed epithelia cells displayed promising results that encouraged me to work further with this subject. In spring 1997 I went to dr. Clauss' laboratory to extend the electrophysiological experiments with noise analysis. I stayed four months in Giessen and I am deeply grateful for the hospitality and obligingness that I met from the hole staff. I still often think back and I sure miss them all. Especially, I would like to thank Mathias Rehn with whom I spend many good moments around the area of Giessen and when invited to his home. Matthias also showed the kindness to introduce me into the mystery of noise analysis and helped me a lot performing additional short-circuit-current experiments. Back in Denmark the project took a new angel when I realized that the observed cadmium-mediated effects involve calcium-mobilization. I therefore began additional experiments employing fluorescence techniques during 1998 and the early 1999.

I am truly grateful to the dear students who were involved in my research area. I supervised three groups of students. All of them were skilled, motivated and hard-working and provided me with very interesting results inspiring me to deepen more into the research area. Some of these results were published later or are presently part of submitted/accepted manuscripts.

As to my supervisor Henning I would like to thank him for always being obliging whenever I needed to discuss obtained results. I also thank Henning for encouraging me to do additional experiments whenever needed and inspiring me in everyday life. Also, thanks to the technician Anne who with (some) patience taught me to behave and survive in the laboratory. Moreover, I feel urgent to thank professor Ole Andersen for sharing the interest with me, reading my manuscripts and providing me with laboratory equipment to measure radioactivity of cadmium-isotopes. I am also my sister-in-law, Lærke truly grateful for her tremendous work correcting grammar in some of the manuscripts. My "office-mate" Bjarne, whom I also stayed at for half a year, gave me all the self-confidence that was needed to finish this ph.d.-work. I ow him a lot. Moreover, I am very grateful for the donation of 20.000 kr. that I received from Anna Hjerrilds foundation.

Finally, I am deeply grateful to my wife, Mette, who supported me in all aspects and encouraged me to continue my work in situations where things appeared hopeless. Without her and my two boys, Niels and Christen, completing the studies would not have been possible.

No one mentioned - no one forgotten.

ABBREVIATIONS

$\Delta I_{sc(Cd)}$	Cd^{2+} induced increase in I_{sc}
$[\Delta Ca^{2+}]_{Cd}$	Cd^{2+}-induced $Ca^{2+}{}_i$ mobilization
$[\Delta Cl^-]$	Change in Cl^- concentration pr. minute
$[\Delta Cl^-]_{Cd}$	Cd^{2+}-activated secretion
$[Ca^{2+}]_i$	Free calcium ions in the cytoplasm
AC	Adenylate cyclase
AVT	Arginine vasotocin
Cd-MT	Cadmium-metallothionein complex
ER	Endoplasmic reticulum
FFA	Flufenamic acid
G_{te}	Conductance
$H_{0.5}$	Half maximal stimulation concentration
IC_{50}	Half maximum inhibition concentration IC_{50}
I_{sc}	Short-circuit-current
MDR	Multi-drug resistance
NFA	Niflumic acid
NRS	Normal Ringer solution
NRS-Glu	NRS containing glucose
PB	Probenecide
PDE	Phosphodiesterase
PTWI	Tolerable weekly intake
R_{te}	Transepithelial resistance
TG	Thapsigargin

CONTENTS

1. DANSK RESUMÉ

Cadmium er en vigtig industriel og naturligt forekommende forureningskilde, som forårsager svær skade på flere organer, hvor især nyrerne er særlige sårbare. Størsteparten af optaget cadmium reabsorberes og akkumuleres i de proximale tubuli, men skader på de distale tubuli tyder på at cadmium også påvirker denne del af nyresegmentet. Almindeligvis har undersøgelser af cadmiumtransport, akkumulering og intracellulære effekter på den distale tubuli ikke modtaget stor opmærksomhed, hvorfor informationer herom på transporterende "tætte" epithelceller er yderst begrænsede. Formålet med dette studie var således at opnå (yderligere) kendskab til de mekanismer, hvormed cadmium (Cd^{2+}) påvirker de renale distale epithelceller, A6, med særlig fokus på basolaterale effekter og deraf følgende mulige cytotoksiske effekter.

Cytotoksiske undersøgelser viste, at cadmium virkede langt mere cytotoksisk når A6 celler blev eksponeret for cadmium fra den basolaterale side i forhold til apical eksponering af A6 monolag. Aktiv iontransport, der blev bestemt ved brug af kortslutningsstrømsteknikken (I_{sc}), viste at kun hvis Cd^{2+} blev tilsat den basolaterale side af A6 monolag førte dette til en prompte og forbigående stigning i kortslutningsstrømmen ($\Delta I_{sc(Cd)}$). Endvidere var $\Delta I_{sc(Cd)}$ dosis-afhængig, der udviste en halv-maksimal stimuleringskoncentration på 385,9 ± 10,7 µM og en maksimal stimuleringskoncentration på omtrent 1 mM. Nærmere undersøgelse af $\Delta I_{sc(Cd)}$ viste, at Na^+-transport ikke var involveret, men at $\Delta I_{sc(Cd)}$ alene var afhængig af Cl^- transport, hvilket blev yderligere underbygget af Cl^- tømnings- og Cl^--kanalhæmmerforsøg. Direkte bestemmelse af Cl^- transport ved brug af den Cl^- sensitive probe, SPQ, viste ligeledes at Cd^{2+} førte til Cl^- sekretion i A6 celler. Både i I_{sc}- og SPQ-forsøg var de to fenemater, flufenemat og nifluminat, der begge er i stand til at hæmme Ca^{2+} afhængige Cl^- kanaler, de mest effektive hæmmere af Cd^{2+} stimuleret Cl^- transport, hvilket indicerer at Ca^{2+} mobilisering er involveret.

Tømning af calciumlagre, anvendelse af thapsigargin (TG), der hæmmer Ca^{2+} ATPaser i endoplasmatisk reticulum, og anvendelse af Ca^{2+} ionophoren A23187 viste at Ca^{2+}-mobilisering spiller en vigtig rolle i $\Delta I_{sc(Cd)}$, og at denne Ca^{2+} stammer fra intracellulære lagre. Direkte bestemmelse af intracellulær $Ca^{2+}{}_i$ viste, at Cd^{2+} forårsager en kraftig forbigående hormonlignende top, der var dosis-afhængig. En nylig identificeret Ca^{2+}-følsom receptor (CaR) er blevet lokaliseret i parathyroidea og siden også i nyrerne. Denne receptor er muligvis ansvarlig for de observerede Cd^{2+}-afhængige effekter. Ekstracellulær $Ca^{2+}{}_o$ aktiverer CaR, hvorved phosphoinositid 4,5-diphosphat spaltes af phospholipase C (PLC) til 1,4,5-triphosphat (IP_3) og diacylglycerol. CaR genkender antagelig andre agonister end Ca^{2+}, f.eks. Mg^{2+} og Gd^{3+}, men også polykationer som f.eks. neomycin. PLC-hæmmeren, U73122, og CaR-agonisten, neomycin, påvirkede således begge Cd^{2+}-afhængig Ca^{2+}-stigning ($[\Delta Ca^{2+}]_{Cd}$), hvilket indicerer at CaR er involveret. Ligeledes reducerede TG $[\Delta Ca^{2+}]_{Cd}$, hvilket tyder på at $Ca^{2+}{}_i$ stammer fra intracellulære lagre. Følgelig viste direkte målinger af IP_3-niveauet, at dette øgedes 1,45 gange i forhold til basalniveauet når A6 celler blev eksponeret for Cd^{2+}. Endelig tyder observationerne på, at de nærtbeslægtede tungmetaller, zink (Zn^{2+}) og nikkel (Ni^{2+}), begge i kraftigere grad end Cd^{2+} kunne inducere Ca^{2+} mobilisering ($Zn^{2+} > Ni^{2+} > Cd^{2+}$). Zn^{2+} og Ni^{2+} øgede tillige IP_3-dannelsen signifikant over basalniveauet. Både Zn^{2+} og Ni^{2+} var i stand til fuldstændigt at fjerne $[\Delta Ca^{2+}]_{Cd}$, hvis disse metaller blev tilsat forud for Cd^{2+} tilsætning. Det er derfor sandsynligt, at Cd^{2+}, sandsynligvis også Zn^{2+} og Ni^{2+}, fungerer som en CaR-agonist, der ved aktivering fører til IP_3-afhængig frigørelse af Ca^{2+} fra intracellulære lagre.

Herudover viste undersøgelserne at Cd^{2+} reducerede det antidiuretiske hormonrespons ved at hæmme adenylatcyclase (AC) aktiviteten, hvorved det intracellulære cAMP-niveau faldt. Da CaR-aktivering medfører hæmning af AC og øget $Ca^{2+}{}_i$, tyder dette ligeledes på at basolateral Cd^{2+} fungerer som en CaR-agonist i A6-celler. Det er derfor tænkeligt, at Cd^{2+} virker toksisk i det

distale nepfronsegment og at vigtigheden af cadmiumforårsagede forstyrrelser af distal nefronfunktioner underestimeres pga. overvældende proximal tubulus beskadigelse. Efterfølgende forstyrrelser af calciumhomøostase og vand/elektrolyt balance i den distale tubulus medfører tillige diffuse symptomer, hvis oprindelse kan være svær at bestemme. Overordnet er det derfor sandsynligt at distal tubulus toksicitet indgår i de overordnede nyreskader, som observeres ved cadmiumeksponering.

2. ENGLISH SUMMARY

Cadmium is an important industrial and environmental pollutant that causes severe damage to a variety of organs, especially the kidney. Most cadmium is reabsorbed and accumulated in the proximal tubules. However, evidence for distal tubule toxicity suggests that cadmium may interfere at this nephron site too. In general, distal nephron studies of Cd^{2+} transport, accumulation and intracellular effects receive little attention and thus limited information regarding mechanisms and effects of inorganic cadmium on transporting tight epithelia cells is available. Hence, the aim of the presented work was to gain further knowledge of the mechanism by which Cd^{2+} acts on the distal renal epithelia A6 cells with special emphasis on the effects when applied to the basolateral surface of the epithelium and to evaluate possible concomitant cytotoxicity.

Cytotoxic studies demonstrated side-specific effects as Cd^{2+} was far more cytotoxic when applied to the basolateral side than to the apical side of A6 monolayers. Active ion transport measured as the short-circuit-current (I_{sc}) revealed that Cd^{2+} caused I_{sc} to increase promptly and transiently ($\Delta I_{sc(Cd)}$) only when applied to the basolateral surface of A6 monolayers. Furthermore, $\Delta I_{sc(Cd)}$ was dose-depended with a half-maximal stimulation concentration of 385.9 ± 10.7 μM and a maximal stimulation concentration of approximately 1 mM. Exploring the ionic nature behind $\Delta I_{sc(Cd)}$ demonstrated that Na^+- transport was not involved but that $\Delta I_{sc(Cd)}$ relied entirely on Cl^- transport. Additionally, Cl^-depletion and Cl^- channel inhibitor experiments supported this. Direct measurements of Cl^- secretion using the Cl^- sensitive probe, SPQ, also proved that Cd^{2+} evoked Cl^- secretion in A6 cells. Both I_{sc}- and SPQ-experiments showed that the two fenemates, flufenamic acid and niflumic acid, both known as inhibitors of Ca^{2+}-depended Cl^- channels, were the most potent inhibitors of Cd^{2+}-evoked Cl^-transport suggesting the involvement of Ca^{2+}.

Calcium-depletion, using thapsigargin (TG), an inhibitor of Ca^{2+} ATPases in endoplasmic reticulum and the Ca^{2+}ionophore, A23187, provided evidence for the involvement Ca^{2+} in $\Delta I_{sc(Cd)}$, which originated from internal stores. Direct measurements of intracellular $Ca^{2+}{}_i$ showed that Cd^{2+} produced a large transient hormone-like spike that was dose-dependent. Recently, a calcium-sensing receptor (CaR) has been identified in the parathyroid and later also in the kidney that may transduce the biological effects of Cd^{2+}. Activation of the receptor by increased levels of extracellular Ca^{2+} results in the breakdown of phosphoinositide 4,5-diphosphate by phospholipase C (PLC) and the formation of 1,4,5-inositol-triphosphate (IP_3) and diacylglycerol. CaR presumably recognizes other cations than Ca^{2+}, e.g. Mg^{2+} and Gd^{3+}, and even polycations such as neomycin. The PLC-inhibitor U73122 and the CaR-agonist, neomycin, both affected Cd^{2+}-evoked increase in intracellular Ca^{2+} ($[\Delta Ca^{2+}]_{Cd}$) suggesting the involvement of CaR in Cd^{2+}-mediated cell signalling. Further, TG significantly reduced $[\Delta Ca^{2+}]_{Cd}$showing that $Ca^{2+}{}_i$originates from internal stores. Extending these observations, IP_3-binding studies showed that the concentration of intracellular IP_3 underwent a 1.45-fold increase proportional to the resting level when exposed to Cd^{2+}. Finally, it was shown that the Cd^{2+}-related heavy metals, Zn^{2+} and Ni^{2+}, were even more potent inducers of Ca^{2+}-mobilization than Cd^{2+} with the following potency: $Zn^{2+} > Ni^{2+} > Cd^{2+}$. Zn^{2+} and Ni^{2+} also significantly increased the IP_3-generation above control level. Moreover, preexposure with Zn^{2+} and Ni^{2+} completely abolished $[\Delta Ca^{2+}]_{Cd}$. Thus, it is hypothesized that Cd^{2+}, possible also Zn^{2+} and Ni^{2+}, may act as a CaR-agonist leading to IP_3-mediated release of Ca^{2+} from intracellular stores.

Moreover, it was shown that Cd^{2+} significantly diminished the response of antidiuretic hormones by reducing the cAMP level through inhibition of the adenylate cyclase (AC) activity. CaR-activation leads to inhibition of the AC-activity and increased $Ca^{2+}{}_i$, which also suggests that basolateral Cd^{2+} may serve as a CaR-agonist in A6 cells. Accordingly, it is proposed that Cd^{2+} perhaps serves as a distal nephron toxicant and that the importance of cadmium-mediated

disturbances of distal nephron functions may be underestimated because of overwhelming proximal tubule damage. Subsequently, disturbances of calcium homoeostasis and water/electrolyte balance in the distal tubule cause nonspecific symptoms from which the origin is difficult to decide. Therefore, it is suggested that distal tubule nephrotoxicity may be a part of overall renal cadmium toxicity.

3. INTRODUCTION

3.1. Presentation

Cadmium is a recognized renal toxicant (WHO, 1992). The mechanisms behind the proximal tubular cell toxicity, due to exposure to Cd-complexes in urine, is rather well investigated (Nordberg, 1992). Cadmium may, however, have other effects on renal cells. The present thesis explores molecular mechanisms behind cadmium toxicity to distal renal culture cells. Please note that in the text the term "cadmium" is used when the specific chemical form of this metal is not known or when several cadmium species are to be considered. The term "Cd^{2+}" is used if the involvement of the free ion is known or suspected.

Preliminary studies at the laboratory using the Ussing technique soon demonstrated promising results regarding the effect of cadmium on electrophysiological endpoints in renal epithelial A6 cells. It was therefore decided to work further with this topic by extending and applying new techniques. However, before presenting the results obtained, the toxicity of cadmium will be introduced as this thesis deals primarily with effects of cadmium administration to A6 cells. In the following subjects dealing with cadmium in general, physio-toxicological aspects, considerations of apical and basolateral exposure, transport mechanisms and described cellular effects focussing primarily on *in vitro* studies in the kidney with special focuses on the distal nephron, will be covered. Furthermore, the use of A6 cells will be motivated and finally the purpose of this study will be outlined.

3.2. Cadmium sources

Unlike many other metals, cadmium has come to be used by man only relatively recently. It was discovered independently and almost simultaneously by the two German investigators, Strohmeier and Hermann in 1817. Its large scale use dates from the 1940's, and it is only during the last three decades that serious consideration has been given to cadmium as an environment contaminant (Aylett, 1979).

Cadmium is widely dispersed in the environment. Major sources of cadmium are found in the United States, Mexico, Canada, Australia and Japan. Environmental contamination because of human activities such as mining, smelting, fossil fuel combustion and industrial use may increase the flow of cadmium into ecological cycles. For example, goldmining in Brazil (Moreira, 1996) have caused massive cadmium contamination in the marine ecosystem that subsequently, due to up concentration in the food chain, may lead to health problems of the people in the polluted area. The main technical uses, important for emissions to air, water and land are steel production, metal production, refining, cement manufacture, pigment manufacture, cadmium plating and battery manufacture (Thornton, 1992). Table 3.1 gives an estimate of cadmium emission to the ecosystem in the EC.

Cadmium is present in all parts of the environment; It is present in all soils, sediments and unpolluted seawater at concentrations which are generally < 0.5 mg/kg, < 1 mg/kg and 1 μg/kg, respectively (Herber, 1994). In comparison, the cadmium concentration is 0.05-0.5 mg/kg in land fields, 0.03-0.1 μg/l in seawater and 0.015-0.05 μg/l in streams in Denmark (The Danish Environmental Protection Agency (EPA), Redegørelse fra Miljøstyrelsen, No. 1, 1995).

3.3. Food and daily intakes of cadmium

Human exposure to low levels of cadmium occur from inhalation from air and natural processes such as erosion of surface deposits of cadmium-containing minerals and subsequent uptake by plants and other edible organisms. The main parts of cadmium intake origins from vegetables and grain products. Offal also contributes to the cadmium intake. The highest cadmium concentrations are found in spinach, rice, wheat, shellfish, and kidney cortex of animals (Galal-Gorchev, 1993; Newberne, 1988; Sherlock, 1986). The daily intake of cadmium obviously depends on the personal diet. In uncontaminated areas the average daily intake is usually in the range 10-60 µg/day for a person of 70 kg. In rural "uncontaminated" areas in Japan the daily cadmium intake has been estimated at 59-113 µg, whereas in contaminated areas in Japan average daily intakes as high as 400 µg have been reported (Friberg, 1986).

Table 3.1. *Cadmium emissions (tonnes/year) to water, air and land in the EC. Data from Thornton, pp. 154, 1992.*

Source	Land	Air	Water
Metal production (iron and steel)	341	24	21.2
Refining nonferrous metals	338	31	27.3
Cement manufacture	261	-	-
Ashes from combustion	161	-	-
Oil combustion	-	28	-
Waste incineration	-	28	-
Coal combustion	-	21	-
Pigment manufacture	-	-	21.0
Cadmium platting	-	-	19.7
Battery manufacture	-	-	13.0

In 1989 WHO established a provisionally tolerable weekly intake (PTWI) for cadmium which, for adults, is of 7 µg/kg body weight corresponding to 400-500 µg/week for an adult Dane (the Danish EPA, Redegørelse No. 1, 1995 and publication No. 187, 1990). Measurements between 1983-1987 of cadmium intakes demonstrated that the average weekly intake of cadmium among the Danish people were about 140 µg, which corresponds to 30% of the PTWI-level (the Danish EPA, publication No. 187, 1990). Variations in intakes occur due to atypical dietary habits or because the food eaten is produced or grown in areas suffering from cadmium pollution. Accordingly, the average weekly intake of a small group of Danes is estimated at about 50 % of PTWI-level which is, according to the Danish EPA, "unacceptably high". Table 3.2 presents typical information on the dietary intakes of cadmium in various countries. All of the average weekly intakes presented in table 3.2 are below the PTWI, although national intake in Germany, Belgium and Italy appear to be close.

Besides intakes from food and drinking water (usually the concentration of cadmium does not exceed 5 µg/l), tobacco smoking, especially cigarettes, plays an important role in cadmium exposure of humans. In general, the cadmium load of smokers is twice that of nonsmokers. Smoking one cigarette, generally containing 1-2 µg cadmium, results in the inhalation of about 0.1-0.2 µg. The higher cadmium exposure among smokers is also reflected in higher cadmium

concentrations in blood. If it is assumed that about 10% of the cadmium present in cigarettes will be transferred into the blood (WHO, 1980), about 1 μg/day will be absorbed if a person smokes 15 cigarettes per day, which may result in an additional elevation of blood cadmium by 1 ng/ml (Friberg, 1986; Ikeda, 1992). Other lifestyle factors, besides diet and smoking, are far less important, however, the working environment can contribute considerably to cadmium intake in industries were technical and hygienic precautions are not implemented. Reported cadmium-blood levels for exposed workers generally lie between 5 and 50 μg/l (corresponding to 44 and 444 nM Cd^{2+}), but during extremely high exposures levels as high as 300 μg/l (2.7 μM) were reported (Herber, 1994). The average blood concentration is about 0.5-1.0 μg/ml (4-9 nM) in nonsmokers and twice as high in smokers (Alessio *et al.*, 1992; Friberg, 1986).

Table 3.2. Typical dietary intakes (mg/week) of cadmium (Sherlock, 1986).

Country	Intake
Australia	0.15
Belgium	0.35
Denmark	0.14*
Germany	0.40
Italy	0.38
Japan	0.27
New Zealand	0.11
United Kingdom	<0.15
USA	0.23

** The Danish EPA, publication No. 187, 1990.*

3.4. Metabolism of cadmium

Ingestion, distribution and excretion

Cadmium uptake occurs primarily via inhalation and ingestion whereas accumulation via the skin plays no role. The absorption of inhaled cadmium in air is 10-50% and from the gastrointestinal tract about 5% with a maximum of 20% in people with low iron stores (Nordberg *et al.*, 1985; Herber, 1994). The daily excretion via faeces and urine is only about 0.01-0.02% of the total human body burden of cadmium (Nordberg *et al.*, 1985). The excretion via urine increases with age and is proportional to the body burden of cadmium, thus, dramatic increases in urine-cadmium occur when renal damage appears (Friberg, 1986).

After absorption from the lungs or the gut, cadmium is transported via blood to other parts of the body. It is likely that cadmium is bound for at least 70% to the red blood cells why plasma and serum levels are very low. Binding in plasma may be to albumin, to SH-groups of other proteins or other ligands. In liver cadmium is taken up, possible after binding to albumin receptors, and induces the synthesis of the low-molecular-weight protein, metallothionein (MT) (Johnson, 1980; Klaassen *et al.*, 1999; Nordberg, 1992). Because of its low molecular weight, cadmium-MT (Cd-MT) is readily filtered through the glomeruli and taken up by tubular reabsorption in the renal tubule. Alternatively, when organisms are exposed to small amounts of

cadmium MT is induced in intestinal epithelia, and the resulting Cd-MT complex may act directly on the renal epithelia independently on the hepatic MT-induction (Andersen, 1992). Moreover, after subchronic or acute exposures direct transfer of cadmium, bound to small ligands such as cysteine, can occur from blood to kidney without any circulation of Cd-MT complex in plasma (Andersen, 1992; Foulkes, 1990a).

Cellular uptake

Cadmium uptake has been studied in several systems, and no general mechanism has emerged. Moreover, the mechanisms by which cadmium is taken up may vary from cell type to cell type. Although it has been stated often that ionic cadmium (Cd^{2+}) may diffuse across the plasma membrane into the cell, this route is not likely to occur because of the hydrophilic nature of Cd^{2+} and the binding of Cd^{2+} to serum and cell proteins. Accordingly, rather high concentrations of Cd^{2+} support a model involving a four-step process; 1) nonspecific electrostatic binding of Cd^{2+} to anionic sites at the mucosal membrane, or 2) temperature-sensitive (passive) internalization into epithelial cytoplasm by movement due to membrane fluidity, 3) diffusion through the cytoplasm and 4) completion of the absorptive process by transport across the basolateral membrane into serosal fluid (Andersen, 1992; Foulkes, 1988).

Furthermore, cadmium uptake can be described as a kinetic model of second order with an initial rapid membrane binding followed by a slow internalization process (Foulkes, 1988; Prozialeck, 1993; Shaikh, 1995; Templeton, 1990). Moreover, cadmium transport may involve one or more processes, including; 1) the use of a calcium transport pathway involving Ca^{2+}-binding protein, 2) a carrier-mediated (active transport and/or facilitated diffusion) extrusion across the basolateral membrane via, e.g. Ca^{2+}-ATPases, 3) the binding of Cd^{2+} to sulfhydryl groups on either the apical or basolateral surface of the cell (Pigman *et al.* 1997), 4) the use of already existing transport systems for essential metals, like Mg^{2+} (Quamme, 1992), and 5) facilitated transport via inorganic anion exchanger as observed in proximal renal epithelial LLC-PK_1-cells (Endo *et al.*, 1999). Even specific heavy metal ion transporter proteins have been characterized. They belong to the family of metal ion transporter CDF-proteins (the cation diffusion facilitator family) among which the P-type specifically catalyses either uptake or extrusion of Cd^{2+} or Cu^{2+} and a variety of mono- and divalent ions (Paulsen & Saier, 1997).

Apical versus basolateral uptake

Cadmium is believed to reach the kidney primarily, though not necessarily exclusively, as Cd-MT released to the plasma from the liver. Cd-MT is freely filtered at the glomerulus and reabsorbed from the lumen of the proximal tubule whereas (Friberg, 1986) Cd-MT apparently does not react with the basolateral membrane (for reviews see (Friberg, 1986; Herber, 1994;). However, renal uptake from peritubular blood has been demonstrated in cases where cadmium is complex bound with small ligand molecules, such as cysteine and glutathione, (Foulkes, 1990a).

As mentioned above a variety of mechanisms have been proposed to explain the uptake of cadmium by various types of cells. However, no single mechanism can adequately account for the uptake of Cd^{2+} by all cells. In hepatocytes about 30% of the cadmium transport was through the basolateral membrane. Moreover, total cadmium accumulation through the basolateral membrane of renal cortical epithelial cells was about twice that through the apical membrane (Shaikh, 1995). Consistently with this observation, a higher accumulation of cadmium from the basolateral compartment than from the apical compartment was demonstrated in LLC-PK_1-cells

(Bruggerman, 1990). In another study in LLC-PK_1-cells, the basolateral cadmium accumulation was about 3-4 times higher than the apical (Prozialeck, 1993). The uptake from the apical compartment may involve a somewhat different mechanism, as Prozialeck, (1993) and Templeton (1990) both showed relatively little cadmium bound to the apical cell surface of LLC-PK_1 cells, and as the small amount of surface binding that did occur did not precede cadmium-uptake.

It is unclear whether similar basolateral transport systems may play a role in Cd^{2+} transport *in vivo*. In general, most of the cadmium that reaches the tubular epithelia *in vivo* is bound to MT or other ligands, and the renal epithelium is exposed mainly from the apical cell surface. Apparently, there is some confusion about the specific species of cadmium that enters renal epithelia. The common theory is that cadmium enters the cells bound to ligands like MT, albumin etc. However, determination of the free cadmium uptake with the use of the fluorescence probe mag-fura-2 demonstrated that free cadmium is transported across the membranes into the intracellular space in renal MDCK epithelia cells (Quamme, 1992), supporting that Cd^{2+} may be accessible for the intracellular milieu and able to react with sensitive sites. Furthermore, it has been demonstrated that divalent Cd^{2+} may be nephrotoxic (Goyer *et al*, 1989) and that basolateral Cd^{2+} uptake may significantly contribute to the total renal burden of Cd^{2+} under certain conditions (Foulkes & Blanck, 1990b). Therefore, it is possible that under some conditions basolateral transport systems may contribute to the accumulation and toxicity of cadmium in some cells and tissues.

Biological half-time

The low excretion rate of cadmium leads to a very efficient retention in the body. The retention functions for cadmium are multiphasic and the half-time of the slowest compartment is usually more than 20% of the life-span for most animal species and humans (Nordberg *et al.*, 1985). The different compartments are likely to reflect retention in different tissues. Cadmium in the blood compartment may exchange with various tissues compartments as the binding of cadmium in the tissues is much stronger than in the blood (Herber, 1994). Human data suggest that the muscle depot of cadmium has one of the longest half-times, more than 30 years. Kidney-cadmium has a half-time of 10 to 30 years and liver-cadmium has a half-time of 5-15 years. The cadmium-accumulation curve for body burdens is almost straight from age 0 to about age 50 (Nordberg *et al.*, 1985). Because of these long half-times and continous transfer of cadmium from other tissues, cadmium accumulation in the kidney will take place during the whole life-span (Friberg, 1986).

3.5. Toxicological aspects

Acute effects

Exposure to high concentrations of fumes from heated cadmium or cadmiated compounds/items has led to acute poisoning and in some cases to death of workers. Principal symptoms reported were respiration distress due to pneumonitis and edema with secondary effects on the kidney (Friberg, 1986; Goyer, 1989). In the past (1940-1950) many cases of acute food poisoning occurred, but nowadays acute poisoning, apart from accidents, is rare (Friberg, 1986).

Chronic effects

Generally, the critical organ for cadmium exposure is the kidney due to lifelong accumulation, especially after extended low dose cadmium exposure. Thus, the most typical feature of chronic cadmium intoxication is kidney damage and clinical symptoms are related to the kidney damage, which in grave cases may lead to osteotoxicity and other calcium-related diseases as described below. In some cohorts with pulmonary exposure to cadmium, lung cancer and chronic bronchitis have been claimed to be increased (Kazantzis *et al.*, 1992). Studies in 1970's on chronic cadmium poisoning in man in Belgium showed that the earliest effect was a renal dysfunction with proteinuria. The proteinuria may be accompanied or preceded by a variety of other renal effects (Bernard *et al.*, 1992). After occupational exposure levels, workers have developed, besides proteinuria, renal glucosuria, aminoaciduria, hypercalciuria, phosphaturia, and polyuria. Some workers suffered from renal colic due to recurrent kidney stone formation (Friberg, 1986; Goyer, 1989; Herber, 1994). Long-term exposure to high dietary cadmium levels in a rural area of Japan has led to a renal disease of the same type as found with industrial long-term exposure, and to a severe osteomalacia-like bone disease known as *Itai-Itai* among middle-age and elderly women (Friberg, 1986; Kjellström, 1992).

As mentioned above the renal accumulation of cadmium is probably linear until the age of about 50. In humans the threshold for induction of kidney damage is considered to be a renal cortex level of 200 mg/kg (The Danish EPA, Redegørelse fra Miljø-styrelsen, No. 1, 1995). Measurements between 1981 and 1987 showed average cadmium concentrations in kidney cortex in 45 to 55 years old Danes of approximately 22 mg/kg (Hansen, 1989). Accordingly, cadmium evoked kidney damage in the average Dane is unlikely at the moment.

Extra renal effects & carcinogenicity

The suggestion that exposure to cadmium may be a causal factor in human hypertension is based mainly on animal experiments (Staessen et al., 1992). Most human studies, however, are hampered by the fact that confounding variables such as smoking and dietary habits, and other air pollutants make it difficult to draw solid conclusions about this effect (Ala-Opas, 1995; Friberg, 1986; Herber, 1994). Also, information on the genotoxicity and carcinogenicity of cadmium is still incomplete. In human beings, interest has mainly focussed on cancer in the prostate and lungs. There is a general understanding that data on a relationship between cadmium and prostatic cancer are inconclusive, mainly due to confounding factors such as cigarette smoking, diet and coexposure to other compounds (Herber, 1994; Nordberg, 1992; Tsuchiya, 1992). Also, increased mortality from lung cancer among workers exposed to cadmium has been observed in several occupational cohorts. Most studies found an increase in lung cancer risk of the order 25-50% (Bofetta, 1992; Friberg, 1986; Kazantzis *et al.*, 1992). Lung cancer evoked by cadmium inhalation in experimental animals is apparently restricted to the rat, as no cadmium-related tumours occur in hamsters and mice (Heinrich, 1992; Maximilien *et al.*, 1992). In general, cadmium compounds are considered as weak mutagens. However, cadmium at non-cytotoxic doses interferes with DNA-repair processes and enhances the genotoxicity of directly acting mutagens (Hechtenberg *et al.*, 1996). Hence, the inhibition of repair and detoxifying enzymes by cadmium may partially explain the observed weak genotoxic properties of this metal (for reviews see Beyersmann & Hectenberg, 1997; Hartwig, 1994; Rossman *et al.*, 1992; Smith, 1994).

3.6. Renal handling of calcium and Ca^{2+} homoeostasis

Prolonged exposure to elevated concentrations of cadmium cause disturbance of Ca^{2+}-homoeostasis, which can lead to various bone diseases and influence the level of Ca^{2+} in the blood. Some important symptoms and diseases are *Itai-Itai*, osteoporosis, calcuria, kidney stone formation etc.(Friberg, 1986; Goyer *et al.*, 1994; Järup *et al.*, 1998; Savolainen, 1995). The impact of cadmium on Ca^{2+}-homoeostasis is of major interest for this thesis why the subject will be discussed in more details.

The kidney is important in maintenance of calcium homoeostasis as this organ is responsible for the "fine tuning" of blood calcium (for reviews see (Bindels, 1993; Friedman & Gesek, 1993; Seldin, 1999) and bone calcium net flux (Kjellström, 1992). To maintain a net Ca^{2+} balance, more than 98% of the filtered load of Ca^{2+} must be reabsorbed along the nephron. There are two potential pathways through which net Ca^{2+} reabsorption can occur. First, a paracellular and passive route that predominates in the proximal tubules and thick ascending limb of Henle's loop. Micropuncture studies have shown that approximately 55-65% of the filtered Ca^{2+} is reabsorbed in the proximal tubule (Costanzo & Windhager, 1992). Passive driving force coupled to Na^+ transport are the major determinants of Ca^{2+} transport in this nephron segment (Bindels, 1993). Secondly, a transcellular, active transport against an electrochemical gradient is responsible for Ca^{2+} reabsorption in the distal nephron. The distal tubule is the main site of active transcellular Ca^{2+} transport and determines the fine tuning of Ca^{2+} excretion with the urine (Friedman & Gesek, 1993). In the distal convoluted and connecting tubule, active Ca^{2+}-reabsorption amounts to about 10% of the filtered load. A final of 1-3% of filtered Ca^{2+} is reabsorbed in the cortical collecting tubule (figure 3.1) (Costanzo & Windhager, 1992).

Transcellular Ca^{2+} transport, as it occurs in the distal segment, is a two-step process, which involves passive influx via Ca^{2+}-channels across the luminal membrane driven by a steep electrochemical gradient (electronegative cell interior) and active extrusion across the peritubular membrane driven by, e.g. Ca^{2+}-ATPase (Carafoli & Stauffer, 1992; Doucet & Katz, 1982) and Na^+/Ca^{2+} exchange mechanisms (figure 3.1) (Friedman, 1998; White *et al.*, 1996). Moreover, the renal Na^+/Ca^{2+} exchange system is apparently restricted to the distal tubule, at least in the rabbit kidney (Ramachandran & Brunette, 1989).

The distal convoluted tubule is the principal site for controlling the rate of active Ca^{2+} transport primarily by the calciotropic hormones, i.e. parathyroid hormones (PTH), calcitonin and 1,25-dihydroxyvitamin D_3 (Bindels, 1993; Brown *et al.*, 1999; Seldin, 1999). PTH stimulates calcium absorption primarily in the distal nephron through dihydropyridine-sensitive calcium channels. Also, the mechanism of calcitonin action on Ca^{2+} transport, though not fully understood, might be identical to that of PTH (Friedman & Gesek, 1993). Additionally, 1,25-dihydroxyvitamin D_3 appears to modulate PTH-dependent Ca^{2+} entry in a non-additive manner in distal epithelia (Friedman & Gesek, 1993; Hebert *et al.*, 1997). Overall, a fall in the extracellular Ca^{2+} (Ca^{2+}_o) levels triggers the release of PTH, which increases the renal absorption of Ca^{2+} and osteoclast-mediated Ca^{2+} mobilization from bone. PTH also stimulated 1-α-hydroxylase activity in the renal proximal tubule and thus, the synthesis of 1,25-dihydroxyvitamin D_3 which promotes absorption of Ca^{2+} from the intestine to the blood (Brown, *et al.*, 1999). A rise in Ca^{2+}_o triggers the secretion of calcitonin from thyroid follicular cells, which decreases the resorption of bone and increases the loss of Ca^{2+} in the urine (for review see figure 3.2 and (Champe & Harvey, 1987; De Luca & Baron, 1998)).

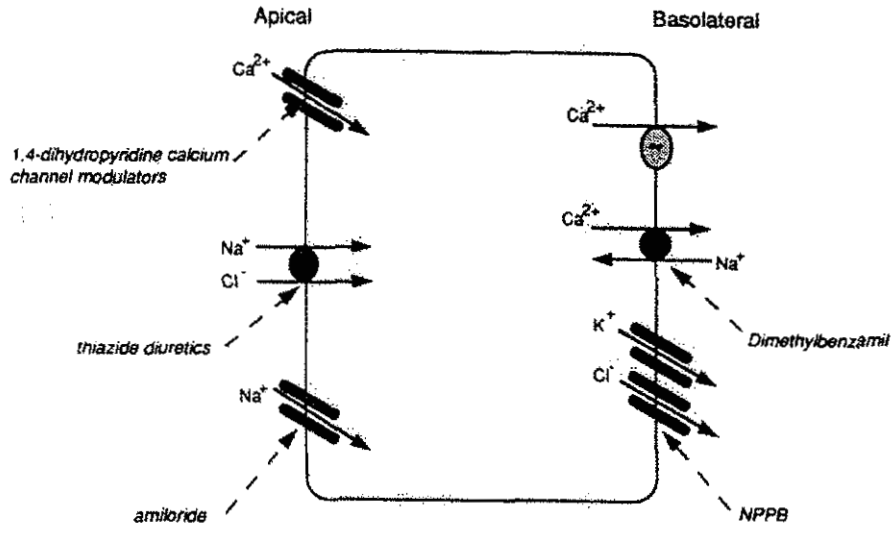

Figure 3.1. Model of cellular absorption in distal convoluted tubules. Transport mechanisms involved in apical calcium entry and basolateral efflux are depicted. Other transport proteins whose action impinges on calcium absorption (apical NaCl cotransport, Na^+ channels; basolateral Cl^- channels) are shown. Drugs that modify these transporters are shown in italics. NPPB, 5-nitro-2-(3-phenylpropylamino) benzoic acid. From Friedman & Gesek, (1993).

Due to the nonspecific action of cadmium on proteins, ligands etc. the effects of cadmium exposure are expected to be versatile covering organs especially important for the maintenance of Ca^{2+}-homoeostasis, e.g. the bones, intestine and the kidney. The different possible points of action of cadmium on calcium and vitamin D metabolism are depicted in figure 3.2.

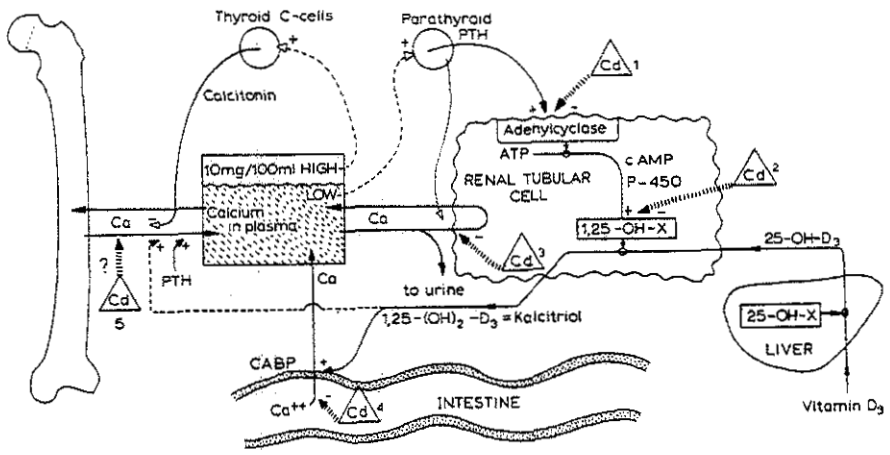

Figure 3.2. Schematic drawing of those aspects of calcium and vitamin D that may be affected by cadmium. Cadmium may in number order; 1) decrease PTH stimulation of adenylcyclase, 2) inhibits renal hydroxylation of 25-OH-D_3, 3) increase urinary calcium excretion, 4) decrease gastrointestinal calcium absorption, 5) affects bone mineralization directly (?). CABP = calcium binding protein. From: Kjellström (1985).

Calcium-sensitive receptors

As indicated in the section above the calciotropic hormones play an important role in the regulation of renal Ca^{2+} (mineral ions) handling. However, in the absence of PTH and vitamin D a positive relationship between urinary Ca^{2+} excretion and circulating Ca^{2+} concentrations is still present (Hebert *et al.*, 1997), which indicates that $Ca^{2+}{}_o$ itself is crucial in regulation of Ca^{2+}-balance.

The ability of parathyroid cells to recognise and response to small changes in the extracellular Ca^{2+} concentration plays a crucial role in Ca^{2+} homoeostasis. Recent studies have provided indisputable evidence that Ca^{2+} besides serving as an intracellular second messenger also serves a hormone-like role as an extracellular "first-messenger". Evidence for that came along with cloning of an extracellular Ca^{2+}-sensing receptor (CaR) from bovine parathyroid gland (Brown *et al.*, 1993). This receptor plays a central role in the homoeostatic system responsible for maintenance of constant blood Ca^{2+}-levels. When subjected to increased levels of $Ca^{2+}{}_o$ (and $Mg^{2+}{}_o$), cells expressing CaR respond with activation of phospholipase C (PLC) leading to accumulation of inositol-1,4,5-trisphosphate (IP_3) and consequent release of Ca^{2+} from intracellular stores (figure 3.3). Accordingly, the CaR belongs to the seven-membrane spanning family found in all G-protein-coupled receptors (Jackson, 1991) showing low-affinity binding of cationic agonists. The CaR responds only in the millimolar ion concentration range that reflects the physiologically relevant Ca^{2+} concentration for extracellular fluid (Hebert & Brown, 1996).

The CaR, which is expressed on the surface of parathyroid cells, provides the principal mechanism for $Ca^{2+}{}_o$ "sensing" in the parathyroid gland (see figure 3.2 and for reviews see (Brown *et al.*, 1998; Brown, 1999; Hebert & Brown, 1995). Moreover, the kidney like the parathyroid responds directly to alterations in $Ca^{2+}{}_o$ with the resultant modulation of mineral ion transport (see refs. Baum & Harris, 1998; Chattopadhyay, Yamaguchi *et al.*, 1998; Hebert, 1996). Also, it is likely that CaR is expressed in many different nephron segments and that the polarity varies with cell type along the nephron, e.g. CaR is exclusively expressed at the basolateral surface of distal tubule cells (Riccardi *et al.*, 1998).

Thus, elevations of $Ca^{2+}{}_o$ activate the CaR in the thick ascending limb (TAL)/distal segment and lead to reduced reabsorption of Ca^{2+} (and Mg^{2+}) and hence increased Ca^{2+}/Mg^{2+} excretion in the urine. High concentrations of urinary Ca^{2+} can enhance the risk of stone formation. The absolute concentration of urinary Ca^{2+} is reduced by two mechanisms. First, NaCl transport by TAL is reduced as CaR activation lead reduction in levels of cyclic AMP which normally induce NaCl transport by activation of K^+-channels and Na^+-K^+-$2Cl^-$-coporter (Amlal *et al.*,, 1996; Friedman, 1988; Hebert & Andreoli, 1984). Accordingly, the counter current is reduced and hence urinary concentrating ability. Also, the CaR-activation reduces antidiuretic hormone-stimulated water reabsorption leading to a more dilute lumen (Baum & Harris, 1998). Second, the lumen-positive potential decreases (Hebert & Andreoli, 1984), which is the driving force for Ca^{2+}. The result of these actions would be that Ca^{2+} is excreted at concentrations below saturation (see figure 3.4 and for reviews see(Chattopadhyay *et al.*, 1997; Chattopadhyay *et al.*, 1998; Hebert, 1996).

Strong support for a key role of CaR in the regulation of Ca^{2+}-homoeostasis has been provided by analyses of several mutations of the CaR gene that causes well-known human clinical disorders of Ca^{2+} homoeostasis (for reviews see Brown, 1999; Brown *et al.*, 1998). Familial hypocalciuric hypercalcemia (FHH) and neonatal severe hyperpara-thyroidism (NSHPT) are the heterozygous and homozygous forms, respectively, of inactivating CaR mutations that demonstrates an altered set point for Ca^{2+}-regulated PTH release (Pollak *et al.* 1993). Patients with FHH are generally asymptomatic whereas NSHPT is a life-threatening neonatal disorder. Another

inherited human disorder of Ca^{2+} homoeostasis is autosomal dominant hypocalcemia (ADH) caused by CaR overactivity (Pollak *et al.*, 1994). ADH patients demonstrate hypercalciuria that occasionally leads to formation of kidney stones (Brown, 1999). Thus, renal tubular transport mechanisms in FHH and ADH patients seem to manifest alterations in renal calcium handling, which suggest that the CaR present in their kidney tubules also exhibit increased set point (loss of function) or decreased set point (gain of function) identically to those present in parathyroid tissue CaR (Baum & Harris, 1998).

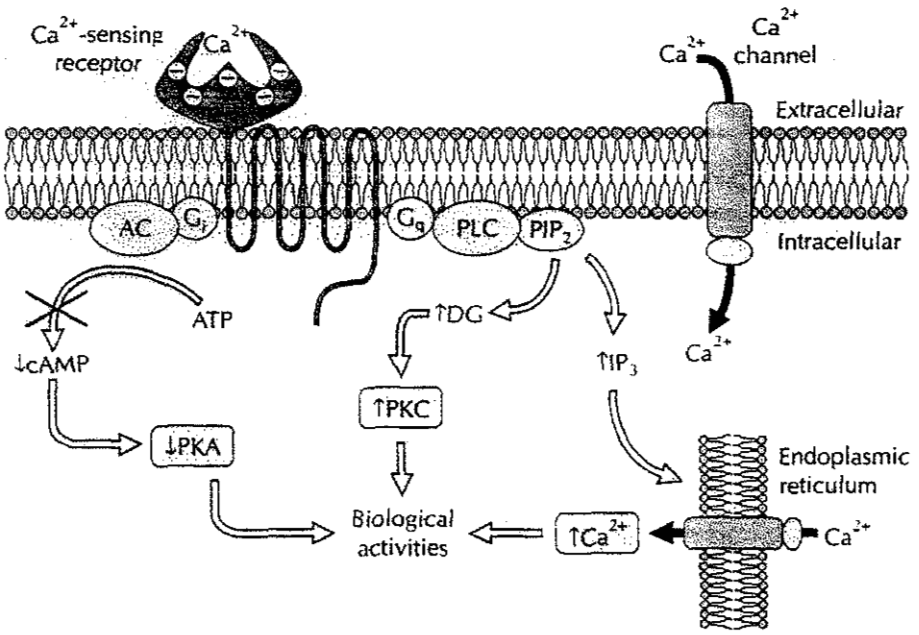

Figure 3.3. *Ca^{2+}-sensitive receptor (CaR)-dependent regulation by extracellular Ca^{2+} (Ca^{2+}_o). CaR is depicted with a large extracellular domain, 7 transmembrane-spanning domains, and a cytoplasmic domain. Increases in [Ca^{2+}_o] activate CaR linked, by G proteins (G_i and G_q), to inhibition of adenylate cyclase (AC) and stimulation of phospholipase C (PLC). A net result of CaR-activation is an increase in intracellular [Ca^{2+}_i], which results from mobilization of Ca^{2+}_i and influx of Ca^{2+}_o though voltage-insensitive channels. Ins(1,4,5)P_3, inositol 1,4,5-trisphosphate; DG, diacylglycerol; PIP_2, phos-phatidylinositol 4,5-diphosphate. From Hebert & Brown, 1995.*

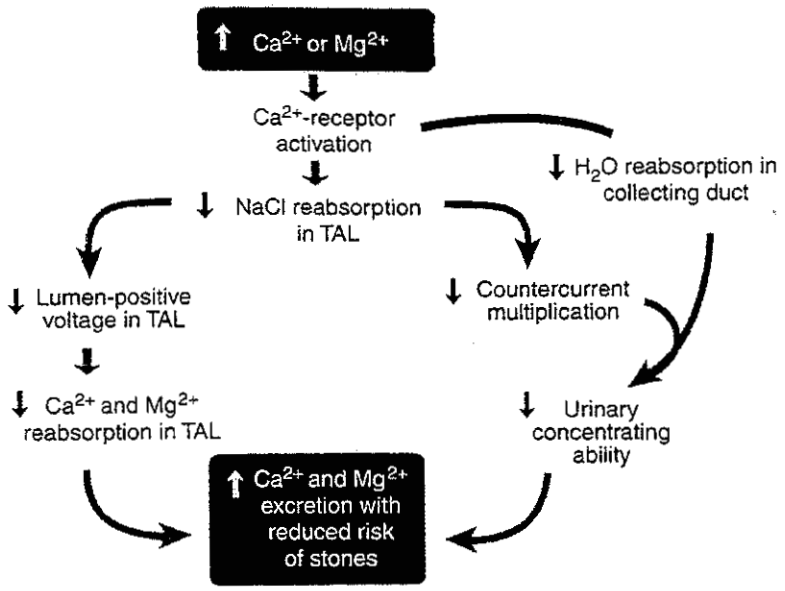

Figure 3.4. *Proposed model for integrating Ca^{2+}-Mg^{2+} and water handling by the kidney via extracellular Ca^{2+}-sensing receptor (CaR). With physiological transient hypercalcemia, the CaR-mediated reduction in concentrating ability would provide a regulatory mechanism helping to promote excretion of increased delivery of Ca^{2+} and Mg^{2+} from the thick ascending limb (TAL) to the collecting duct in a more dilute urine, by that decreasing the risk of stone formation (from Hebert, 1997).*

Cadmium interference with cellular signalling/Ca^{2+} homoeostasis

When it comes to the clinical symptoms of cadmium intoxication the knowledge is well-documented (discussed above). It is commonly believed that cadmium in its free form is responsible for the damage observed followed by heavy cadmium load (Nordberg, 1992). However, the mechanisms underlying cadmium-induced nephrotoxicity are largely unknown.

Cellular Ca^{2+} homoeostasis and Ca^{2+}-mediated functions are being increasingly recognized as sensitive and critical targets for the action of toxic metal compounds (Beyersmann & Hectenberg, 1997; Rossi, 1991). Due to its high affinity to proteins, cell membranes and other ligands, cadmium and other heavy metals can interact with cell surface receptors, Ca^{2+} influx channels and intracellular Ca^{2+} transport systems. Cadmium concentrations in the low micromolar range provoke the formation of IP_3 in human skin fibroblasts (Smith, 1989), bovine chromaffin cells (Yamagami *et al.*, 1998)and neuroblastoma cells (Benters, 1997), causing a large transient hormone-like mobilization of intracellular Ca^{2+}, supporting that Cd^{2+} interferes with receptors responsible for IP_3-dependent Ca^{2+}-signalling, e.g. the CaR protein. Regarding plasma membrane Ca^{2+}-channels, Cd^{2+} is a well-known blocker of Ca^{2+} influx into cells (for reviews see Kiss & Osipenko, 1994). Voltage-operated Ca^{2+}-channels may be most sensitive to blockade by Cd^{2+} (Jones, 1998; Lansman, 1986). Once taken up, cadmium interferes with the functions of several enzymes and regulatory proteins involved in intracellular Ca^{2+} signalling. Cadmium interferes with ATP-driven Ca^{2+} transport systems in the plasma membrane and intracellular stores in intestinal and kidney epithelia (Schoenmakers, *et al.*, 1992; Verbost, 1987). Also, Na^+/Ca^{2+}-exchanger, which is abundant in the distal nephron, is inhibited by Cd^{2+} in fish intestines

(Schoenmakers *et al.*, 1992). The overall effect is that the Ca^{2+} extrusion capacity of the cell is reduced leading to a sustained rise in $Ca^{2+}{}_i$.

Disturbance of Ca^{2+} homoeostasis resulting in modulation of various cell functions as $Ca^{2+}{}_i$ is perhaps the most important second (and first) messenger in regulating cellular processes. It is, however, beyond the scope of this thesis do discuss in detail the importance of Ca^{2+} in cell signalling as the interest of this subject has been intense and widespread (for reviews see Berridge, 1997; Clapham, 1995). As mentioned above Cd^{2+} can interfere with Ca^{2+} metabolism at several steps modulating Ca^{2+}-homeostasis, which would lead to a wide-range of cellular events. For instance Cd^{2+} disrupts intercellular junctions in renal proximal epithelia cells, LLC-PK_1, causing the transepithelial resistance to decrease (Prozialeck, 1991). In this regard, the findings that Cd^{2+} interferes with Ca^{2+} homoeostasis may be physiologically relevant since Ca^{2+} plays a key role in the formation, maintenance and regulation of structural proteins (Cereijido *et al.*, 1998; Jovov, 1994). In addition, Cd^{2+} perturbs the Ca^{2+} metabolism in bone cells via activating PKC-dependent processes (Long, 1997). Moreover, as discussed above cadmium has been postulated to be involved in the pathogenesis of hypertension. Nevertheless, cadmium-induced hypertension of rats has demonstrated that the action of cadmium may be due to cytosolic Ca^{2+} mobilization of the erythrocytes rather than a direct cadmium effect (Erkilic *et al.*, 1996). Cadmium is also considered as a carcinogenic agent known to increase the expression of several protooncogenes in a variety of cells (for review sees Beyersmann & Hectenberg, 1997). Even so the link between Ca^{2+}-homoeostasis and proto-oncogene expression still needs to be elucidated. However, cadmium-induced expression of proto-oncogenes requires intracellular Ca^{2+} mobilization and occurs in part by PKC-dependent pathways (Matsuoka, 1995), which may in part explain the suggested carcinogenicity of cadmium.

Thus, many reported physiological effects upon Cd^{2+} exposure might go through the modulation of Ca^{2+}-homoeostasis and because of cellular malfunctions, it may in severe cases lead to toxic events, e.g. it is well-known that $Ca^{2+}{}_i$ play a significant role in the transduction of apoptogenic signals (Alison, 1995; Koudrine, 1998; Kroemer, 1995). In fact, some cytotoxic actions of Cd^{2+} might be due the induction of apoptosis caused by Cd^{2+}-mediated Ca^{2+}-mobilization (Koudrine, 1998). Hence, cellular malfunctions due to the disturbance of Ca^{2+} homoeostasis seem universal and independent of cell types representing different tissues.

3.7. Interactions with Zinc

Zinc, Zn^{2+}, belongs to the same group of transition metals as Cd^{2+} and accordingly similar effects are expected. Contrary to Cd^{2+}, Zn^{2+} at low concentrations is essential for cellular growth and differentiation (Abdel-Mageed & Oehme, 1990; Solomons, 1988). Several studies have proved that Zn^{2+} and related metals competitively decrease the cellular uptake of Cd^{2+}, thereby protecting cells from the toxic effect of this metal (Benters, 1997; Blazka, 1991; Blazka & Shaikh, 1992; Endo, 1996; Gachot & Poujeol, 1992; Goyer, 1997; Kimura *et al.*, 1996; King *et al.*, 1998; Templeton, 1990). Like cadmium, zinc also induces MT, in fact, zinc is the most abundant metal bound to MT allowing Zn^{2+} to be transferred among the body compartments where it is needed (Klaassen *et al.*, 1999). Apparently, the Zn^{2+}-mediated induction of MT play a minor role in Zn-protection of Cd^{2+}-toxicity as Zn^{2+} protects MT-null mice (do not express MT) against cadmium-toxicity, probably by displacing Cd^{2+} from Cd-MT (Tang *et al.*, 1998). Additionally, tolerance to cadmium cytotoxicity is induced by Zn^{2+} via MT-independent mechanisms, such as decreasing intracellular cadmium as well as MT-induction at the cell level in LLC-PK_1-cells (Mishima *et al.* 1997). At the cell surface, Zn^{2+} competitively inhibits Cd^{2+} evoked Ca^{2+}-release (Dwyer *et al.*,

1991; Smith, 1989; Yamagami *et al.,* 1998), thus potentially protecting against cadmium-mediated Ca^{2+} mobilization.

3.8. Proximal versus distal effects

As mentioned above cadmium is believed to exercise its nephrotoxic actions mainly at the proximal tubule. As also mentioned above, cadmium accumulation by proximal tubules results from uptake of inorganic cadmium and of other small cadmium complexes and of the cadmium-metallothionein complex. Because proximal tubules reabsorb the bulk of ultrafiltered cadmium, most studies of cadmium transport, accumulation and intracellular effects have focussed on this nephron segment. Consequently, only limited information regarding the toxicity, mechanisms, and regulation of cadmium uptake and transport by distal tubules is available. However, evidence for distal tubule toxicity suggests that cadmium may also act at this nephron site (Friedman, 1994). In addition, immunohistochemical localization of cadmium-induced MT in rat kidney revealed intense staining in the distal tubule, that was often more intense than in the proximal tubule (Tohyama, 1988; Zhang, 1995). Also, studies in kidney cell lines of proximal ($LLC\text{-}PK_1$) and distal (MDCK) tubular origins exposed to cadmium demonstrated that not only the proximal cell line but also, however to a lesser extend, the distal cell line accumulated cadmium (Zhang, 1995) In an *in vivo* study, in cadmium-exposed rats, cadmium failed to induce hypertension but demonstrated increased urinary kallikrein excretion (Girolami, 1989)}, which predominantly originates from the distal nephron tubule (Vio & Figueroa, 1985). As mentioned above, the hypertensive effect of cadmium is questionable, however, kallikrein-excretion suggest that cadmium may display nephrotoxic effects at the distal nephron level. Hence, it seems likely that distal cadmium toxicity also qualitatively contributes to the overall nephrotoxic effects. However, it remains to be defined whether and how fare distal cadmium toxicity contributes quantitatively to cadmium nephrotoxicity in general.

Hormonal regulation of electrolytes in renal distal nephron

Distal cadmium toxicity might play a physiological important role as disturbance of the function at this nephron site can lead to widespread consequences. The distal nephron and the collecting duct are the main sites for hormonal regulation of ion and water transport.

In general, there are two steps in the transepithelial ion movement across the distal (and other) epithelium. In Na^+ absorption, one is the entry step of amiloride-sensitive (Na^+-channel blocker) Na^+ across the apical membrane and the other is the extrusion step of Na^+ across the basolateral membrane, which is referred to as the two-membrane model (figure 3.5). It is generally accepted that the entry of Na^+ across the apical membrane is the rate-limiting step and that Na^+ channels in the apical membrane play an important role as an entry site for Na^+ regulated by hormones. The two main hormones controlling salt and water homoeostasis are aldosterone and the antidiuretic hormone (ADH), respectively.

The aldosterone action on epithelial Na^+ transport occurs at two different sites: 1) an activation of apical amiloride-sensitive Na^+ channels (~1-4 h) and 2) an increase in the expression of basolateral Na^+-K^+-ATPase (4h-2 days) (Paccolat *et al.*, 1987; Verrey, 1995). How aldosterone increases apical membrane Na^+ entry in distal A6 cells is controversial since it is reported that aldosterone increases the probability of Na^+ channels being open (Kemendy *et al.*, 1992) or increases the density of Na^+-channels (Helman, 1994).

Vasopressin, the mammalian antidiuretic hormone and vasotocin (AVT), its equivalent in amphibian and other vertebrates, are among the most important antidiuretics. In A6 cells AVT acts via the V_2 receptor mainly located in renal collecting ducts, which activates AC resulting in an increase in cytosolic cAMP (Hays, 1996; Lang *et al.*, 1986). In A6 cells, vasopressin and cAMP increase the number of open apical Na^+ channels, whereas cAMP increases the open probability of apical Cl^- channels (Chalfant, 1993; Nakahari & Marunaka, 1994) and thereby increases the reabsorption of water. Besides that vasopressin increases the water permeability of the apical membrane of the distal nephron leading to increased water absorption (Marunaka, 1997). The water permeability increases when vasopressin via V_2 receptors mediates the transfer of water channels, aquaporins (AQP2), from a store in intracellular vesicles to the apical plasma membrane (Marples *et al.*, 1999).

Moreover, reabsorption of calcium in distal nephron segments is relatively modest, but it is physiologically regulated by PTH and is central to the renal component of calcium homeostasis (debated above). The presence of CaR in the distal tubule and scarcely in the proximal tubule (Hebert & Brown, 1995; Riccardi *et al.*, 1998) supports the idea that regulation and maintenance of Ca^{2+}-homoeostasis is extra-proximal and that the distal tubule form an active part of the Ca^{2+}-regulating apparatus. The "sensing" mechanism seems to be exclusively at the blood side in the distal tubule as CaR has been recognized only at the basolateral membrane in this nephron segment (Riccardi *et al.*, 1998).

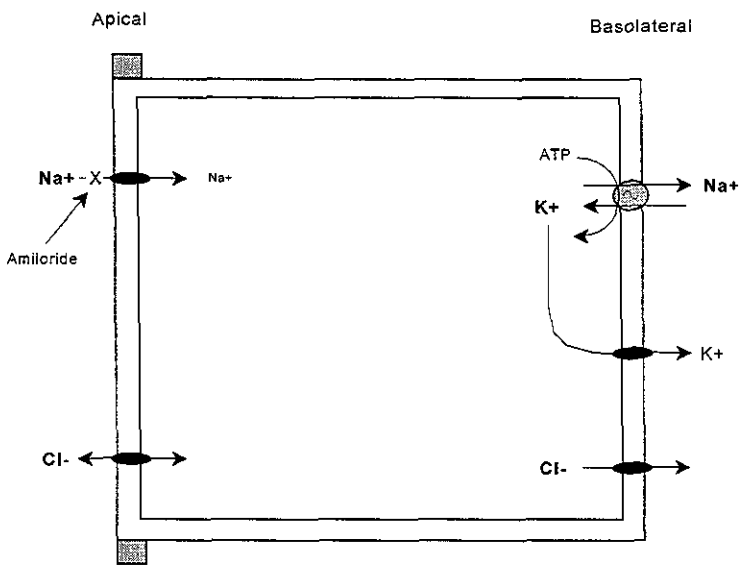

Figure 3.5. *A two-membrane model of transepithelial Na^+ transport in distal nephron. The apical Na^+ channel has an amiloride-sensitive Na^+ channel. Cl^- acts as a major counter ion. Na^+ absorption is indirectly linked to K^+ secretion driven by the basolateral Na^+-K^+-ATPase. Grey boxes at apical side indicate tight junctions.*

Hence, in contrast to the proximal tubule cadmium-evoked disturbances in the distal tubule function may introduce widespread effects due to the importance of the distal nephron in regulating electrolyte and water levels in the organism. However, because of the nonspecific effects, identification of the origin in cadmium-mediated malfunctions of the distal nephron would probably be difficult.

3.9. A6 cell culture

Whether distal nephron segments accumulate or transport cadmium or whether they represent a site of cadmium-induced nephrotoxicity has received little attention. However, as pointed out

above, some studies have shown that cadmium accumulates in this nephron segment too. Since this part of the kidney is the main site for hormonal regulation of electrolyte and water transport, it is of main interest to explore the qualitative and quantitative effects of cadmium exposure to the distal tubule. In the present thesis the cultured toad kidney epithelial cell line A6 was used as this cell model exhibits morphological and functional properties of the mammalian distal epithelium (Perkins, 1981).

A6 cells were initially cultured from the kidney of the South African clawed toad *Xenopus laevis* (Rafferty, 1969). Under optimal conditions A6 cells grow rapidly with a doubling time of 24 h's in a log phase growth. Within 6-7 days A6 cells form a polarised, highly differentiated epithelium with a large transepithelial resistance, R_{te} (> 1000 $\Omega \cdot cm^2$), and a large transepithelial potential (the basolateral surface being positive) of about 9 mV (Perkins, 1981). Dome formation, evidence of epithelium transport, is observed when cells are grown to confluence in culture flasks. Compared with mammalian cell cultures, the A6 cell line is more easy to handle, as this cell culture needs a humidified atmosphere with 5% CO_2 at room temperature (optimal 25-27 °C). Because of the high R_{te}, A6 cells are excellent for investigation of ion transport because high R_{te} indicates that the paracellular route is negligible allowing only transepithelial transport to occur. Furthermore, R_{te} serves as a sensitive marker for determination of cell integrity since low levels of R_{te} may suggest that tight junctions are leaky or that the cell membranes are being destroyed.

A6 cells display active and electrogenic amiloride-sensitive Na^+ absorption (BlazerYost & Helman, 1997; Rehn *et al.*, 1996; Sariban-Sohraby, 1983) and secrete Cl^- (Chalfant, 1993; Zeiske *et al.*, 1998) via two types of Cl^--channels controlled by Ca^{2+} and/or cAMP (Marunaka, 1990). Moreover, A6 cells (Chalfant, 1993) are for instance sensitive to PTH (Rodriguez-Commes, 1995), aldosterone (Bindels, 1988; Helman, 1994; Helman, 1995) and the diuretic hormone (Bindels, 1988; Verrey, 1993; Verrey, 1994). Therefore, this renal cell line provides an excellent model for distal tubular cells in the kidney that is useful in studies attempting to characterize mechanisms of epithelial transport and hormone action.

3.10. Purpose of the studies

The aim of the presented work was to gain further knowledge of the mechanism by which Cd^{2+} acts on the distal renal epithelia A6 cells with special emphasis on the effects when applied to the basolateral surface of the epithelium and to evaluate possible concomitant cytotoxicity. Additional work, in some cases carried out in cooperation with students, that is not published or put into manuscripts will also be presented and discussed according to the relevance of the subject in this thesis. The following aspects were studied in detail:

- The cytotoxicity of Cd^{2+} when applied at both surfaces of A6 cells
- Cadmium-evoked transepithelial ion transport measured by the short-circuit-current technique and the exploration of the ion transport behind.
- Cl^- secretion in A6 cells by Cd^{2+} and related divalent metals with special emphasis on the involvement of Ca^{2+}-mobilization.
- The effects of Cd^{2+} on intracellular Ca^{2+}, interaction between related divalent metals and studies of mechanisms behind with special emphasis on Cd^{2+} as a potential CaR-agonist.
- The effect of Cd^{2+} on ADH-exposed A6 cells and possible intracellular mechanisms.
- Additional results obtained with A6 cells; 1) effect of Cd^{2+} on Na^+-K^+-ATPase activity, 2) $^{109}CdCl_2$ studies, 3) multi-drug resistance experiments, 4) confocal laser microscopy experiments, 5) the effect of the anti-tumour agent, cisplatin, on ion transport capacity.

4. METHODS

For particular methods, reference is made below to the relevant article/manuscript using its number in Roman numerals. Methods not presented in articles/manuscripts attached to the section "additional experiments" in Results, yet too important to be excluded, will be presented using the notion: → results.

4.1. Cell culture and culture methods

A6 cells, a line derived from the distal tubule of *Xenopus laevis* kidney, were purchased from the American Type Culture Collection (Rockville, MD, USA), at serial passage 67. Cytotoxic experiments (I & II), ADH-experiments (III) and cisplatin experiments (IV) where conducted at passages 70-80, whereas fluorescence experiments (VI & VII) were conducted with cells at passages 80-113 (for exact cell passages please refer to the articles/manuscripts in the appendices). Cells were grown at 26 °C in a humidified atmosphere of 5% CO_2 in air in plastic culture flasks (25 cm^2, Costar, Northumbria Biologicals, Cramlington, Northumbria, UK) with 10 ml of Dulbecco's modified Eagle's medium, DMEM, (Gibco, Grand Island, NY, USA) adjusted with 20% distilled water to an osmolarity of 225-255 mOsm/kg, which is appropriate for amphibian cells (Perkins, 1981). The medium was supplemented with 100 IU/ml penicillin, 100 μg/ml streptomycin, and 10% (v/v) fetal bovine serum (Gibco). Twice a week the growth medium was replaced with a fresh medium. When cells were confluent and exhibited dome formation (5-10 days), they were subcultured by incubation in 2 ml Ca^{2+}-Mg^{2+}-free amphibian salt solution with 0.25% (w/v) trypsin containing 110 mM NaCl, 2.5 mM $NaHCO_3$, 3 mM KCl, 1 mM KH_2PO_4, 1 mM EGTA and 5 mM glucose (pH 7.6). Upon the detachment from the culture flask (3-5 minutes), the subculture medium was removed. Five to ten minutes later, the effect of trypsin was neutralized by adding 5 ml culture medium. The cells were resuspended and used for experiments.

4.2. Electrophysiological measurements

Cells were seeded onto membrane inserts in snap wells (Transwell, 1 cm^2, 0.45 μm poresize, Costar) at a seeding density of about $\frac{1}{2} \cdot 10^6$ cells/well. The cells were supplemented with growth medium for 7-8 days to obtain confluent monolayers. The ion transport capacities were improved by preincubation of the epithelia with 1 μM aldosterone 24 hours before performing the experiments (Bjerregaard, 1992). Active transepithelial ion transport was measured as I_{sc} according to the technique of Ussing and Zerahn (figure 4.1) (Ussing, 1953). Briefly, active transepithelial ion transport was studied on monolayers of cells mounted in a modified Ussing chamber bathed from both sides in aerated normal Ringer solution (NRS) as described below and kept at room temperature. Each half-chamber housed a potential-sensing KCl-electrode (agar bridge saturated with KCl) and an Ag-AgCl current passing electrode. All electrodes were connected to a multichannel Voltage/Current Clamp amplifier (WPI EVC-4000) enabling one to measure the potential difference and I_{sc} across the monolayer. Conductance (G_{te}) was determined at defined intervals by passing a 10-mv pulse of 3 sec durations. The I_{sc} and G_{te} were continuously recorded on a strip-chart recorder. Cell integrity was assessed by monitoring the transepithelial resistance (R_{te}) giving that G_{te} equals $1/R_{te}$.

Data handling: The time of basolateral addition of 1 mM $CdCl_2$ to the time when R_{te} started to decrease markedly was about 40 minutes (article I). Therefore, to assure that cell integrity during

I_{sc}-experiments was not influenced by Cd^{2+}, all experiments were terminated within 40 minutes after addition of Cd^{2+}. The increase in I_{sc} (ΔI_{sc}) was calculated as the difference in I_{sc} before addition of the agent and the steady or maximal I_{sc} level reached after addition of the agent. At least one monolayer from the same plating served as control for the other monolayers.

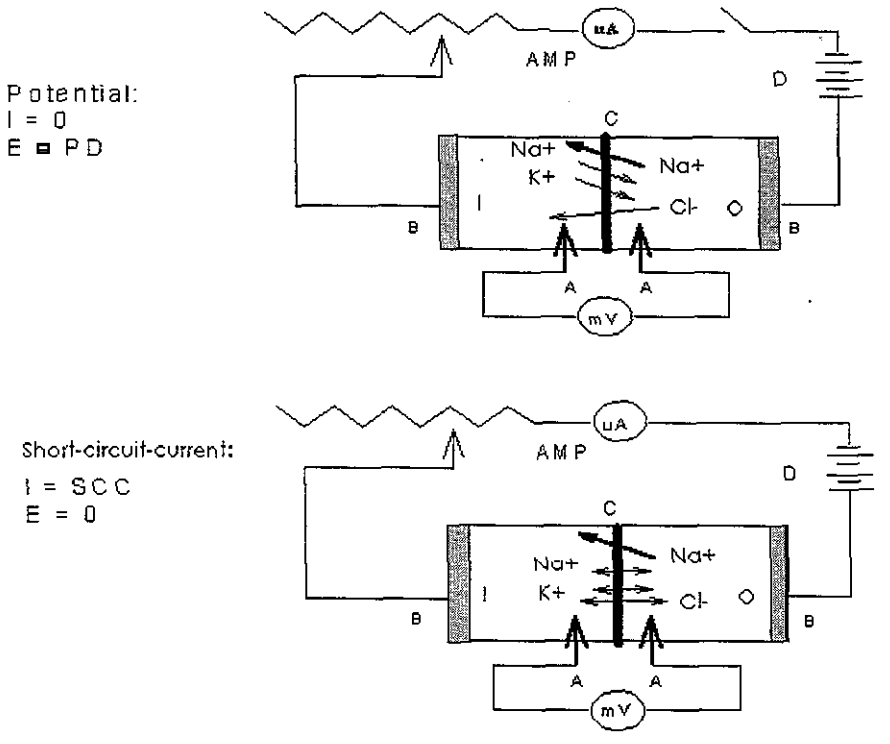

Figure 4.1. Short-circuit-current setup showing potential (top) and short-circuit-current (bottom) mode: A; agar bridges saturated with KCl, B; Ag-AgCl current passing electrodes, C; monolayer of confluent cells, D; Voltage source (voltage/current amplifier), I; the inner side of monolayer, O; the outer side of monolayer.

4.3. Epithelial function studies

Cells were grown on snap wells until confluence. In some experiments (II & IV) the integrity of cell-cell junctions was assessed by monitoring R_{te} as described above. Short-term effects were estimated by adding a fixed concentration of a test-agent to the basolateral side of the monolayer upon which successive R_{te}-measurements was performed. Long-term effects (24 hours) were estimated by determination of the half maximum inhibition concentration (IC_{50}) by increasing the concentration of test agents added to serum-free medium (73 % DMEM, 25 % milli-pore water and 2 % penicillin/streptomycin) on either the basolateral or apical sides of A6 monolayers. The cells were not pre-incubated in aldosterone as for electrophysiological measurements. After 24 hours, R_{te} was measured using an epithelium-volt-ohmmeter with chopstick electrodes (Millicell-ERS).

Data handling: The results were calculated as ohms·cm^2 of cell growing surfaces, after subtracting the values for the resistance measured in cell-free filter inserts. The results were expressed as percentages of the control values (no Cd exposure) taking into account the changes in control levels within 24 hours, and % control was calculated as $R_{te,24h}$/corrected $R_{te,control}$ for each dose. Corrected $R_{te,control}$ was expressed as $R_{te,control,\ time=24\ hours}/R_{te,control,\ time=0\ hours}$ in untreated

cells. IC_{50} tests were performed with cells of the same passage. IC_{50} values were calculated by intrapolation of the % inhibition-concentration relationship at 50% inhibition of R_{te}. The IC_{50} tests were obtained from cells of the same passage.

4.4. Morphological observations

In cisplatin experiments (IV) electrochemical functional studies were supplemented with morphological observations to picture the cytotoxic effect of cisplatin on A6 cells. Subcultured cells were seeded in petri dishes containing either 0, 200 or 400 μM cisplatin dissolved in NaCl-Ringer and exposed for 1, 3, 6, 24, 48 and 75 hours before evaluation. Morphological changes were examined in a Leica microscope at 200 or 400 × magnifications using the following criteria to distinguish effects of cisplatin; cell division, formation of pseudopodia and sheets of cells. The effects were compared with effects of control cells unexposed to cisplatin, but otherwise treated in same manner.

4.5. Protein determination

For determination of protein concentrations, a commercial kit purchased from Bio-Rad (Cat. # 500-0007) based on the method of Bradford (1976) was used. It involves the addition of an acidic dye to protein solution, and subsequent measurement at 595 nm using a micro plate reader (Elisa reader, Inter Med. Tim-2000). Bovine serum albumin was used as standard. The cells were degraded by adding 0.5 M NaOH for minimum 2 minutes after which 0.5 M HCl was added to neutralize the protein solution before the protein content was determined.

4.6. Measurements of cAMP, adenylate cyclase & phosphodiesterase activity

In some experiments (III & IV) cAMP content, activity of adenylate cyclase (AC) and phosphodiesterase (PDE) were measured in A6 cell homogenates as described in the following. Suspended epithelial cells were homogenised at 0-4 °C in a glass homogeniser with 2 ml of 10 mM Tris-HCl buffer (pH 7 5), containing 0.1 mM $CaCl_2$.The homogenate was centrifuged at 20.000 g for 30 minutes. The supernatant was used to measure PDE-activity and the pellet (composed of cell membranes) was resuspended in 1 ml of 5 mM Tris-HCl (pH 7.5) containing 0.25 M sucrose for measurement of AC-activity. Both suspensions were stored at -80 °C until use. The activity of AC was measured in a reaction mixture with a final volume of 500 μl, containing 150 mM N-morpholinopropane sulphonic acid (MOPS), 83 mM Tris-HC1, 10 mM theophylline, 2 mM $MgCl_2$, 1 mM EGTA, 1 mM dithiothreitol and membrane preparation (60-90 μg protein). The assay mixtures with cadmium or cisplatin, agents and membrane preparations (30-50 μg protein) were pre-incubated at 30 °C for 5 minutes. The assays were started by the addition of 1 mM ATP. The reactions were allowed to proceed at 30 °C for 20-30 minutes, and stopped by boiling the incubates for 3 minutes, whereupon they were centrifuged at 2000 g for 20 minutes at 4 °C. The content of cAMP in the supernatant was determined using a protein binding assay, by displacement of radioactive cAMP, as described by (Geisler *et al.*, 1977). The activity of "warm" cAMP was determined on a liquid scintillation counter, Wallack model 1409.

The activity of PDE was measured in a mixture with a final volume of 500 μl containing, at final concentrations: 40 mM Tris-HCl, 10mM $MgCl_2$ and 1 mM dithiothreitol (pH 8.0). The assay mixtures with test agents and the cytoplasmic preparations (50-100 μg protein) were pre-incubated at 30°C for 5 minutes. The assay was initiated by adding 1 μM cAMP, and stopped

after 30 minutes by boiling the incubates for 3 minutes. The incubates were centrifuged at 2000 g for 20 minutes at 4°C and the content of cAMP in the supernatant was determined, as noted above. The PDE-activity was measured as the theophylline (10mM)-sensitive decomposition of cAMP.

4.7. Measurements of Na^+-K^+-ATPase activity using nystatin

In vitro measurements of Na^+-K^+-ATPase activity was performed in intact A6 cell monolayers using, nystatin (experiment IV and additional experiments → results). Nystatin, known as an ionophore, can be used to determine the Na^+-K^+-ATPase activity since apical nystatin mediates a passive entry of Na^+ down its electrochemical gradient at the apical membrane (Wills, 1981). Charge transfer across the basolateral membrane is achieved through the basolateral Na^+-K^+-ATPase Pump (active contributions of ions as the system is in I_{sc}-mode). Thus, if it is assumed that nystatin reduces the resistance of the apical membrane, I_{sc} becomes a function primarily of the transport capacity in the basolateral membrane, i.e. the Na^+-K^+-ATPase pumps. Nystatin was dissolved in ethanol and had an activity of 300 U/ml.

Data handling: The amplitude of I_{sc} when nystatin ($\Delta I_{sc(Nys)}$) is added apically to the monolayers is proportional to the activity of Na^+-K^+-ATPase. Ouabain-pretreated (a specific inhibitor of Na^+-K^+-ATPase) monolayers were used to decide the lowest $\Delta I_{sc(Nys)}$ ($\Delta I_{sc(ouabain)}$) obtainable due to the specific inhibition of Na-K-ATPase. $\Delta I_{sc(ouabain)}$ was subtracted all $\Delta I_{sc(Nys)}$-values to allow measurement of ATPase-sensitive activity only. The pump activity was calculated by determining the fraction of ouabain-corrected $\Delta I_{sc(Nys)}$ with and without a test-agent present.

4.8. Measurements of Cd^{2+} accumulation in cell suspensions using $^{109}CdCl_2$

The extend of Cd^{2+} accumulation in A6 cells exposed to basolateral Cd^{2+} was roughly estimated by using the radioactive isotope, $^{109}Cd^{2+}$ (Du Pont, 9.94 MCi/ml, New Life Science products, Belgium)(additional experiments → results). The procedure was as follows: Cell suspension was washed 2 times in NRS (composition stated below) containing 5 mM glucose (NRS-Glu). 400 µl $^{109}Cd^{2+}$-stock solution (1 mM $CdCl_2$ containing 5 µCi $^{109}CdCl_2$) was added to 1 ml cell suspension achieving a final concentration of 400 µM Cd^{2+} and 2 µCi $^{109}Cd^{2+}$/ml. Next, the cell suspensions were exposed for ½, 5, 15, 30 and 60 minutes, respectively. At the pre-requested time, 100 µl EGTA (50 mM in milli-pore water) was added and the suspension was washed twice in 500 µl MOPS-EGTA solution (125 mM NaCl, 5 mM KCl, 1 mM $MgCl_2$, 3 mM EGTA and 10 mM MOPS, pH 7.4) at 800 g for two minutes. The cells were then lysed in 500 µl milli-pore water or by ultrasound. The lysate was fractionated by centrifugation at 20.000 g for 20 minutes at room temperature. 400 µl supernatant was decanted for isotope readings in a γ-counter and a small aliquot was taken for protein determination. Likewise, the pellet was resuspended in 500 µl milli-pore water for γ-counting and a small aliquot was taken for protein determination.

Data handling: The accumulation of Cd^{2+} was calculated from the sample counts using the specific activity of the $^{109}Cd^{2+}$-stock solution. Thus, when the activity of the stock solution is known (cpm/ml), the amount of "warm" $^{109}Cd^{2+}$-solution is known (here: 400 µl), the final concentration of Cd^{2+} (here: 400 µM), the molar activity can be calculated having the unit's cpm $\cdot$ $nmol^{-1} \cdot ml^{-1}$. From the molar activity, the sample count and protein content of supernatant/pellet

the specific activity, pmol · mg^{-1} can be calculated. Finally, all specific activities were expressed as fraction of control values of cell suspension not exposed to $^{109}Cd^{2+}$.

4.9. Assessment of multi-drug-resistance activity in A6 cells

Qualitative determination of the transport of Cd^{2+} was attempted using the Cd^{2+}-specific fluorescence probe, APTRA-BTC/AM (Molecular Probes, Leiden, NL)[1]. The loading of the probe was, however, unsuccessful due to lack of sensitivity of the probe. Cd^{2+} binds to a variety of cellular components reducing the intracellular concentration of free cadmium below the sensitivity level of APTRA-BTC (k_d = 1 μM). The quantitatively most important factor contributing to the lack of sensitivity of APTRA-BTC, was most likely the presence of multi-drug resistance (MDR) activity in A6-cells, which is responsible for the extrusion of the probe from the intracellular milieu. So far, the results indicate that APTRA-BTC serves as an excellent marker for MDR-activity in A6-cells (additional experiments → results), however, due to ongoing investigations of patent possibilities this subject will only be discussed briefly: Cells were cultured and processed as described previously. *In Cd^{2+} transport experiments,* 4 ml cell suspensions were washed in DMEM and then resuspended in 4 ml NRS-Glu. Prior to the loading of cells, APTRA-BTC/AM was mixed 1:1 with pluronic acid, a mild nonionic surfactant (Molecular Probes, Leiden, NL), to increase uptake of the dye. The final concentration of APTRA-BTC/AM:pluronic acid was 5 μM. After 60 minutes loading on a rocking device, the isolated cells were washed twice in NRS-Glu (1000 rpm for 1 minute). Aliquots of 500 μl were decanted for measurements in a Perkin Elmer LS50B luminescence spectrophotometer at excitation wavelengths' 380 and 460 nm and at emission wavelength 500 nm with a sampling rate of 3.5 seconds. *In MDR-experiments*, 2 ml cell suspensions were washed once in NRS-Glu and then resuspended in 300 μl NRS-Glu. 2 × 5 μl was decanted for protein determination. The rest was transferred to a quartz cuvette for measurements in a Perkin Elmer LS50B luminescence spectrophotometer (apparatus setups like transport experiments). The following agents were used to depress the MDR-activity: sulfinpyrazone, 50 mM and probenecide, 250 mM, both dissolved in NRS with NaOH, then adjusted to pH with HCl, and verapamil, 100 mM were dissolved in ethanol and then diluted with NRS to 1 mM.

The viability of the cells upon treatment with MDR-suppressors was assessed by the tryphane blue dye exclusion test incubating 50 μl cells with 50 μl tryphane blue for 10 minutes. Under the given conditions, no cells were stained meaning that the MDR-inhibitors at the used concentrations were nontoxic for the cells.

Data handling: When Cd^{2+} and APTRA-BTC/AM are added to the cell suspension MDR-activity results in a steady increase in fluorescence. The effects of MDR-suppressors were assessed by determining the slope of Cd^{2+}-mediated fluorescence increases at control conditions and then comparing that to the slopes at increasing concentrations of MDR-suppressors. The effects were expressed by the IC_{50}-level.

---

[1]APTRA-BTC/AM is cell permeable due to the attached hydrophobic AM (acetomethyl)-group. When passing the cell membrane, AM group is hydrolysed by esterases resulting in hydrophilic non-permeable form, APTRA-BTC that is sensitive to Cd^{2+}. APTRA-BTC is a dual-wave indicator, i.e. binding of Cd^{2+} shifts the excitation maximum from 380 to 420 nm, which can be detected by a fluorescence spectrophotometer.

4.10. IP_3-binding studies

Usually, 8 ml cell suspensions were centrifuged and resuspended in 3 ml NRS-Glu. Then the cell suspension was divided into 10 parts of 300 µl upon which the experiments were executed. The A6 cells were subcultured as described above and $0.8 \cdot 10^6$ cells/300 µl were prepared according to the guidelines given for the assay system (Kit: TRK 1000) purchased from Amersham (Life Science, UK). Shortly, 300 µl cell suspensions were mixed with 0.2 volumes ice-cold 20% perchloric acid, and incubated on ice for 20 minutes. 20 µl was taken for protein determination (sees flow-diagram 4.1). The cell suspension was then centrifuged at 2000 g for 15 min. at 15°C whereupon the supernatant was decanted into plastic tubes and neutralized with ice-cold 10 M KOH to pH 7.5. Finally, the neutralized supernatant was diluted 4 × in milli-pore water before running the assay.

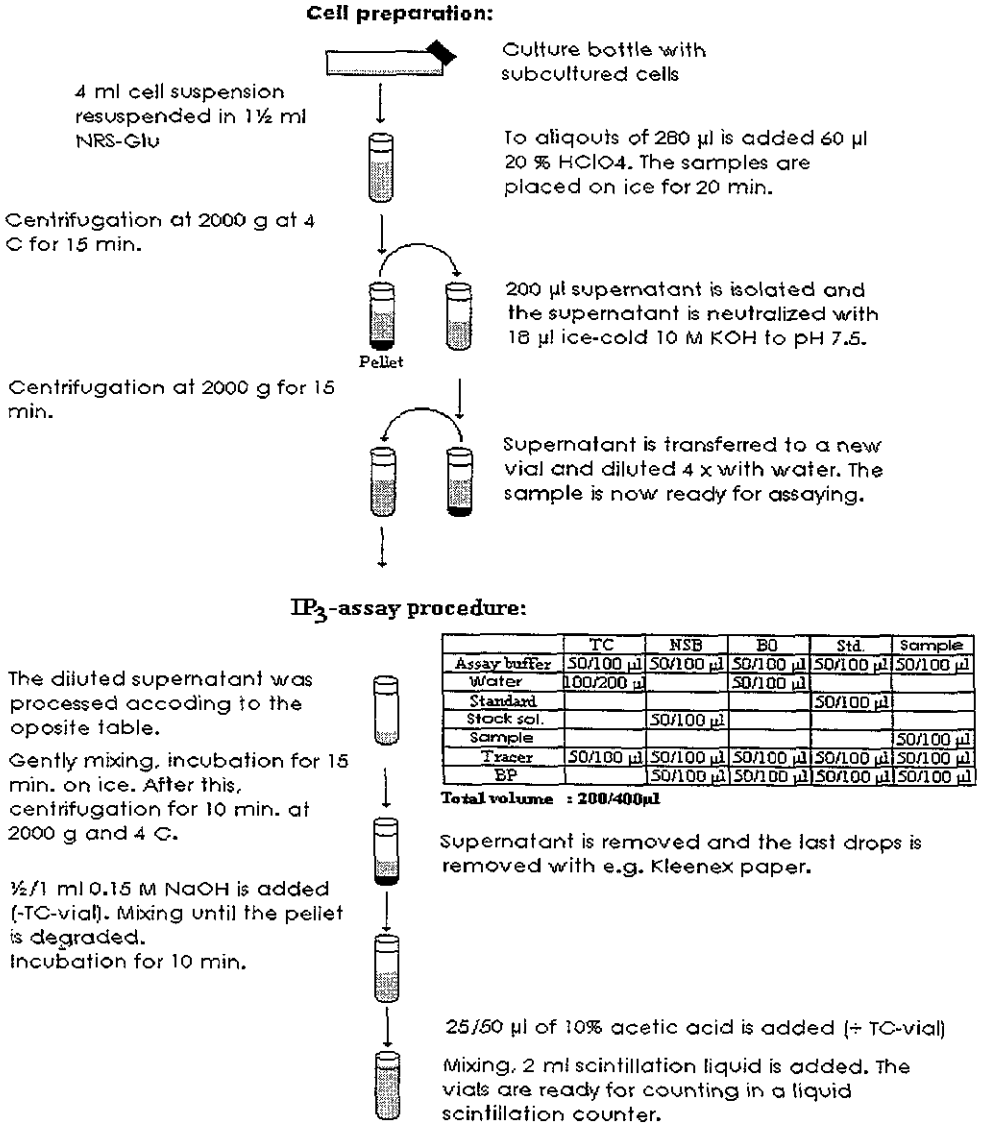

	TC	NSB	B0	Std.	Sample
Assay buffer	50/100 µl	50/100 µl	50/100 µl	50/100 µl	50/100 µl
Water	100/200 µl		50/100 µl		
Standard				50/100 µl	
Stock sol.		50/100 µl			
Sample					50/100 µl
Tracer	50/100 µl	50/100 µl	50/100 µl	50/100 µl	50/100 µl
BP		50/100 µl	50/100 µl	50/100 µl	50/100 µl

Total volume : 200/400µl

Flow-diagram 4.1. A schematic overview of cell preparation and assaying for determination of IP_3 in A6 cell suspension. The cell preparation and assay procedure have been optimized to halves the volumes of what recommended in the commercial kit (Amersham, Kit: TRK 1000). Abbreviations: TC, total count; NSB, nonspecific binding; BP, binding protein B0; B_0 - maximum $^3IP_3$-binding to BP.

The principle behind the assay is that unlabelled IP_3 competes with a fixed amount of [^{3}H]-labelled IP_3 for a limited number of bovine adrenal IP_3 binding proteins. The bound IP_3 is then separated from the free IP_3 by centrifugation. The free IP_3 in the supernatant is discarded by simple decantation, leaving the bound fraction adhering to the tube. The amount of unlabelled IP_3 in the sample is calculated from a standard curve using the ^{3}H counts. Nonspecific binding measured in the presence of 1 nM IP_3 was typically 10% of the total count. Specific binding was typically 30 % of the total count. Moreover, the used concentration of $CdCl_2$ did not affect the binding capacity of the binding protein.

Data handling: Data were analysed by computer assisted curve-fitting to a logistic equation, which together with the protein content allowed calculation of the specific IP_3-content as pmol IP_3/mg protein. Pilot experiments indicated that the IP_3-content of control cells did not change significantly during a typical time course of experiment, i.e. 60 sec of exposure.

4.11. Measurements of chloride transport

Optical measurements

A method for determination of Cl^- secretion in single cells using a laser confocal microscope was developed during a four months stay at Giessen Universität, Germany. Due to lack of time the method was never validated and as such results are not presented in the current thesis. In the following the method is described shortly: A6 cells with a final density of 20.000 - 30.000/cm^2 were grown on filters with low autofluorescence (Costar, 0.4 µM). 7-8 days later, a small piece of the filter containing subconfluent cells was isolated and then glued with silicone around a ½ cm^2 opening in a 4-ml plastic chamber with the basolateral side facing the chamber volume and the apical side facing an inverted microscope attached to a confocal laser device (MRC 1024, Biorad, Hemel Hempstaed, UK). NaCl-Ringer in the bathing solution was substituted by Na_2SO_4 -Ringer. A 20 µl drop of Cl-free Ringer was placed on the apical side where upon a normal objective cover glass was fixed (figure 4.2). The basolateral chamber contained 3 ml Cl-free Ringer. During experiments test agents in adequate amounts were added. Settings of laser power and emission filters were 3% and 455/30 nm (filter blocks; UBHS and E2), respectively. The fluorescence Cl^--sensitive dye 6-methoxy-N-(sulfopropyl)quinolinium (SPQ[2], Molecular Probes) at 10 mM was added to the solution on both sides of the monolayer to detect Cl^--transport. Because SPQ is highly polar and membrane impermeable, measurements were limited to the extracellular face. Area around the cells where pointed out by the software and Cl^--transport was measured as the decline in fluorescence intensity at 450 nm emission caused by the quenching effects of Cl^- on SPQ. Cells were also pointed out but because of SPQ's impermeable features no quenching should occur. The kinetics were evaluated by software provided by Biorad. Figure 4.3 illustrates a typical photo of cell clusters achieved with the confocal laser microscope

[2]SPQ is a hydrophilic single-wave indicator that is quenched by halides resulting in an ion concentration-dependent fluorescence decrease without a shift in wavelength (emission = 443 nm and excitation = 344 nm). The efficiency of the quenching process is represented by the Stern-Volmer quenching constant (K_{sv}), which is reciprocal to the ion concentration that produces 50 % of maximum quenching.

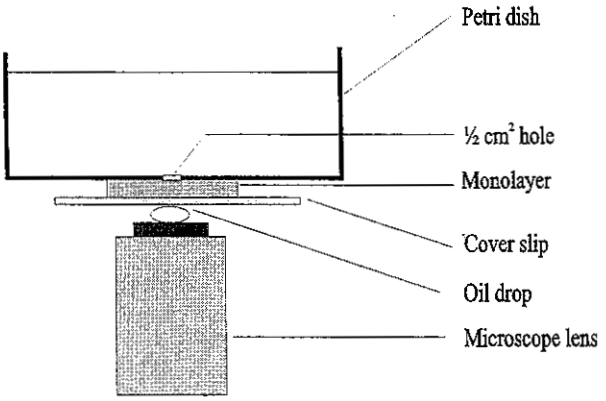

Figure 4.2. *Arrangement of optical experiments (see text for further details). The Apical side is facing the microscope lens attached to a laser device.*

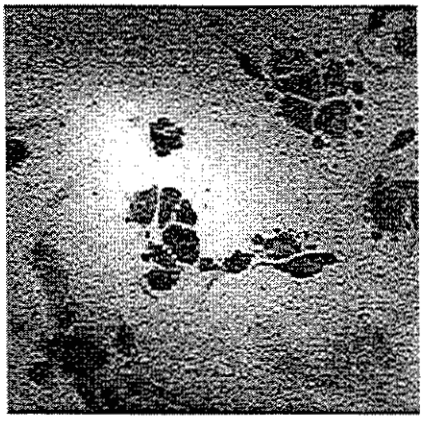

Figure 4.3. *A photo of a typical SPQ-experiment achieved with the confocal laser microscopy at 3 % laser power and 400 x magnification. SPQ was added to the apical and basolateral solution at 10 mM to detect Cl^--transport across the cell membrane. Cl^--transport was measured as the decline in fluorescence intensity at 450 nm emission caused by the Cl^- mediated quenching effects of SPQ. Cell clusters are dark and the bright area is caused by the laser beam itself.*

Fluorescence measurements

In some experiments (VI) the fluorescent probe SPQ was used to monitor intracellular chloride concentrations. About $2 \cdot 10^6$ cells 4-8 days of age suspended in growth medium were centrifuged for two minutes at 180 g. The growth medium was removed and the cells were resuspended in serum free DMEM. The cell suspension was incubated 30 minutes at room temperature with 10 mM SPQ in a hypotonic solution (Cl^--containing Ringer/H_2O 1:1) as described by Pilas & Durack (1997). After loading, the cell suspension was centrifuged for 2 minutes at 180 g and resuspended for 15 minutes at room temperature in serum free DMEM to allow recovery from hypotonic shock. Just before being analysed the cells were washed once in Cl^--free Ringer and then placed in a quartz cuvette (for further details see flow diagram 4.2).

The emission spectra and chloride-specific quenching characteristics of SPQ in Cl^--free Ringer were measured at 344 nm excitation wavelengths (slit width 2.5 nm) as shown in figure 4.4A. The final concentration of SPQ used was 1 μM. The chloride concentration varied from 0 to 200 mM. The emission wavelength was set at 443 nm (slit width 2.5 nm) during all SPQ-experiments. A maximal intensity of fluorescence (F_0) was determined at the end of each experiment by adding 1 % (v/v) triton X-100 to the cuvette. The flourescent intensity was measured at 20 ms intervals. Autofluorescence of the chemicals used and cells not loaded with SPQ were also measured and subtracted from all test-values. To calculate intracellular [Cl^-], a

calibration curve was established by increasing the Cl^- concentration in Cl-free Ringer containing 10 µM SPQ (figure 4.4B). From the slope of the linear plot, the Stern-Volmer quenching constant (Biwersi *et al.*, 1992), K_{sv}, was determined to be 125.4 ± 7.1 M^{-1} (n = 5 and R = 1.00). Experiments with the same protocol were conducted on different cell passages to take into account the effect of biological variation.

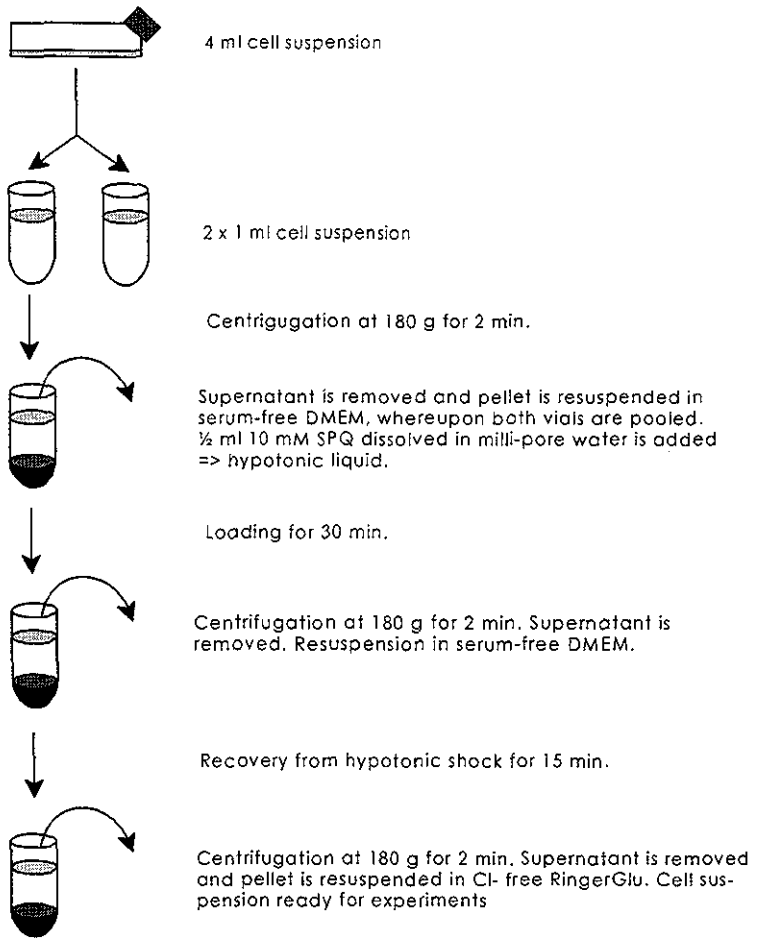

Flow diagram 4.2. *An overview of cell preparation and loading of SPQ to detect Cl^--secretion in A6 cells.*

Data handling: Relative rates of Cl^--transport computed from the time course of intracellular fluorescence were expressed as relative fluorescence variation using $(\Delta F/dt)/F_0$, where $(\Delta F/dt)$ represents the change in intensity upon addition of an agent and F_0 the maximal intensity in presence of triton X-100. Data were also expressed as the change in Cl^- concentration pr. minute ($[\Delta Cl^-]$). Calculations of chloride concentration were performed according to equation 4.1. (Biwersi *et al.*, 1992):

Eq. 4.1.

$$K_{sv} \cdot [Cl^-] = \left(\frac{F_0}{F}\right) - 1$$

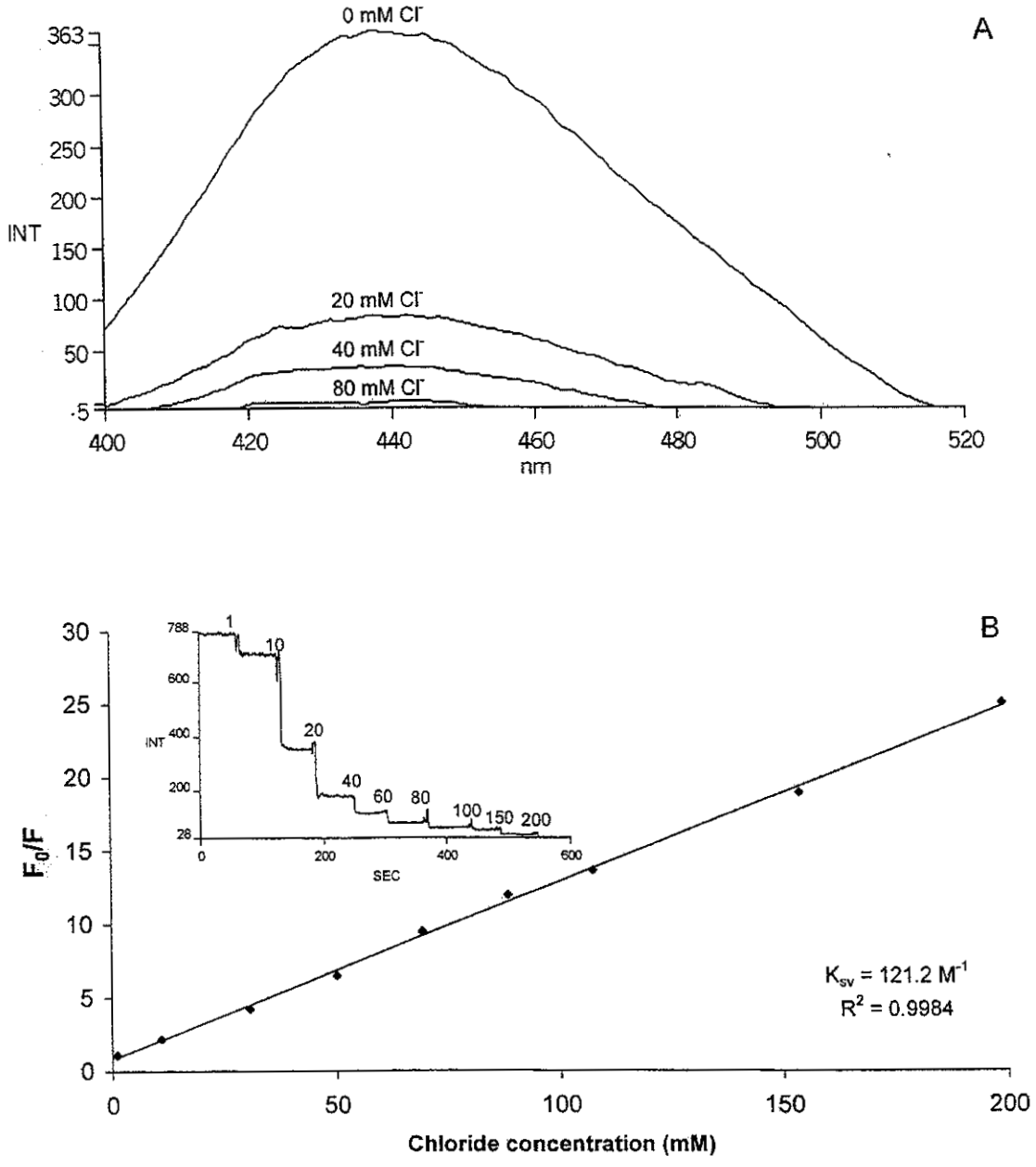

Figure 4.4. *A; shows the quenching of SPQ fluorescence emission by increasing concentrations of Cl⁻. SPQ (1 μM) was dissolved in Cl-free Ringer and scans between 400 and 600 nm were performed on a luminescence spectrophotometer exciting at 344 nm. B; shows the Stern-Volmer plot for fluorescence quenching of SPQ (10 μM) by increasing concentrations of Cl⁻ in chloride free Ringer. The results are expressed as fluorescence ratio F_0/F where F_0 represents the maximal intensity and F the change in intensity upon addition of an increasing concentration of Cl⁻. The slope of the linear plot is the Stern-Volmer quenching constant, K_{sv} (see materials for further details). Inserted: a time course of SPQ-quenching by chloride (number above curve indicate Cl⁻ concentration given in mM).*

4.12. Measurements of intracellular calcium

All experiments (VII) were performed with A6 cells isolated after 4-8 days of growth. To monitor intracellular calcium concentrations, the fluorescent probe Fura-2/AM[3] (Molecular Probes, Leiden, NL) was used. Prior to the loading of cells the dye was mixed 1:1 with pluronic acid to increase the dye-uptake (see above). Isolated cells suspended in DMEM were loaded with 500 μM Fura-2/AM on a rocking device at room temperature for 30 minutes covered in aluminium foil. Ten minutes before end of loading, 50 μM TPEN (tetrakis-(2-pyridylmethyl) ethylenediamine) and 5 mM probenecide were added to the cell suspension. TPEN is known as a membrane permeant chelator with extremely high affinity for heavy metals (Hinkle, 1992; Richardson & Taylor, 1993) and 5 mM probenecide is capable of inhibiting the organic anion-transporter responsible for the efflux of the dye (Di Virgilio *et al.*, 1988; Di Virgilio *et al.*, 1990; McDonough & Button, 1989; Mitsui *et al.*, 1993). For further details about this topic please refer to manuscript VII. After the loading, a small volume of isolated cells (about $\frac{1}{2}\cdot 10^6$ cells per experimental datum) was washed and resuspended three times (two minutes at 180 g) in NRS under gentle stirring in a plastic tube (see flow diagram 4.3). Ca^{2+}-free experiments were performed by replacing NRS with Ca^{2+}-free Ringer solution during the last washing of the cells. All experiments were executed in a quartz cuvette with a total sample volume of 500 μl containing 5 mM probenecide. Preliminary studies revealed that probenecid at the used concentration did not damage the cells during the time course of the experiments. Also, probenecid did not influence the basal level of Ca^{2+}_i. The excitation wavelength was set to alternate between 340 and 380 nm (10 nm slit width) every 20 ms and the emission wavelength was monitored at 540 nm (10 nm slit width).

A small fura-2 leak occurred through the cell membranes into the extracellular space. Using Mn^{2+} to quench this leak fluorescence, the leak was estimated to be 0.63 ± 0.05 % pr. min (n = 3) (for further details see manuscript VII). As most of the experiments showed effects instantaneously greater than 100%, the small leak of fura-2 could not explain the changes in the fluorescent Ca^{2+}_i. Furthermore, the extend of fura-2 compartmentalization was estimated by adding 50 μM digitonin, which is known to permeabilize the plasma membrane. Subsequently, 1% Triton X-100 was added to permeabilize and release dye from subcellular organelles at the end of an experimental session. The fraction of total intracellular dye compartmentalized was calculated according to Kao (1994) and was 8.5 ± 0.6 % (n = 4).

Data handling: To calculate the intracellular Ca^{2+} concentration, Grynkiewicz' equation was used, with a K_d-value of 224 nM as reported by Grynkiewicz *et al.* (1985). Routinely, a calibration program was done on the same cell batch as the one used during experiments to determine the limiting values of the ratio I_{340}/I_{380} when the probe is in the is Ca^{2+}-saturated form (R_{max}) and in the Ca^{2+}-free form (R_{min}) by adding the detergent triton X-100 and excess of EGTA (50 mM) to the cell suspension, respectively. The calcium concentration used to obtain R_{max} was 1 mM. During calibration, cells not loaded with fura-2 as well as chemicals used were tested for autofluorescence.

The I_{340}/I_{380}-ratio was used to calculate the intracellular Ca^{2+} concentration, $[Ca^{2+}]_i$ according to Grynkiewicz' equation as indicated below. Results will often be presented as the difference in

---

[3]Fura-2 is lipophilic in its AM-form and become hydrophilic when the AM-binding is hydrolysed by intracellular esterases. Fura-2 is a dual-wave indicator that upon binding Ca^{2+} exhibits an absorption shift that can be detected by luminescence at excitation wavelengths 340/380 nm and emission wavelength 510 nm. K_d for Ca^{2+} = 145 nM at pH 7.0 and 22 °C.

I_{340}/I_{380}-ratio before and after addition of an agent and expressed as relative fluorescence ΔF_{agent}. Calculations of $[Ca^{2+}]_i$ were performed according to equation 4.2.:

Eq. 4.2.

$$[Ca^{2+}]_i = K_d \cdot \left(\frac{R - R_{min}}{R_{max} - R}\right) \cdot \left(\frac{s_{f2}}{s_{b2}}\right)$$

The factor s_{f2}/s_{b2} represents the ratio of the measured fluorescence intensity when all dye is Ca^{2+} free and the intensity measured when all the dye is saturated with Ca^{2+}, both measurements taken at 380 nm.

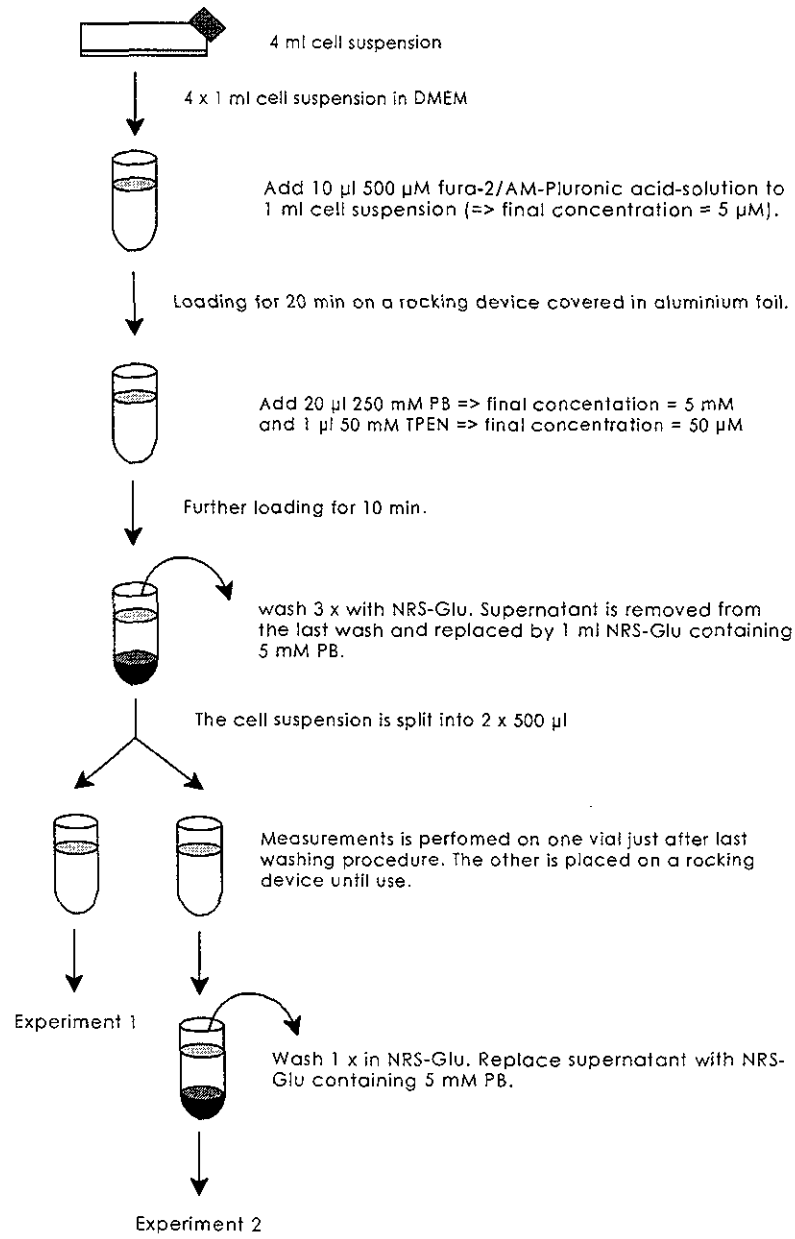

Flow diagram 4.3. *Schematic overview showing cell preparation and loading of A6 cells with fura-2/AM for determination of intracellular Ca^{2+}. PB = probenecid, NRS-Glu = normal Ringer solution containing 5 mM glucose.*

4.13. Chemicals & solutions

If the chemicals were dissolved in dimethylsulphoxide (DMSO) or N, N-dimethylformamide (DMF) a final maximum concentration of 1% (v/v) of the solvents were allowed. The effect of the solvents on the I_{sc}- and fluorescence baseline as well as the autofluorescence was checked before doing experiments.

Composition of the used Ringer-solutions:

Normal-Ringer solution (in mM):	Na^+, 115; K^+, 2.5; Cl^-, 117; Ca^{2+} 1; CO_3^{2-}, 2.5.
Ca^{2+}-free Ringer (in mM):	Na^+, 115; K^+, 2.5; Cl^-, 115; CO_3^{2-}, 2.5; EGTA, 0.1.
Cl^--free Ringer (in mM):	Na^+, 110; K^+, 2; Ca^{2+}, 1; SO_4^{2-}, 57; sucrose, 73.

In case of Cl^--depletion in electrochemical experiments, only the chamber on the basolateral side was supplemented with Cl^--free Ringer. The pH was in all cases 7.4. A final concentration of 5 mM glucose was used during all experiments.

4.14. Statistics

Results are expressed as means ± SE, where n indicates the number of independent experiments. Simple two-way comparisons were evaluated by Student's t-test. Comparisons between control and multiple treatment groups were evaluated by one-way ANOVA followed by *post-hoc* analysis of means using the least-significance-difference (LSD) method (Statistica, ver 5.1). Results that had non-parametric distribution were analysed statistically using the non-parametric Kruskal-Wallis ANOVA test and then further tested in groups by Mann-Whitney U test. Statistics of data presented in the form of a percentile score were evaluated on raw data and then expressed as % of control ± SE (%). P-values of less than 5% were considered significant.

5. MAIN RESULTS

The current section describe Cd^{2+}-related effects mainly. Separate subsections briefly summarize cisplatin results (IV) and results not presented in articles or manuscripts. As mentioned in the preface I went to prof. Clauss' laboratory among other things to study noise spectra. Unfortunately, it was not possible to obtain noise-spectra of Cd^{2+}-exposed A6 cells why this topic will not be covered in the present thesis.

5.1. Basal I_{sc}-response and dose-response (II & VII)

Addition of 1 mM $CdCl_2$ to the basolateral surface of A6-monolayers induced prompt and transient increases in I_{sc} ($\Delta I_{sc(Cd)}$) from 2.3 ± 0.3 to 10.6 ± 0.8 μA/cm^2 (n=25, p<0.001). The activation sustained for less than five minutes before returning to basal level (figure 5.1). However, when 1 mM Cd^{2+} was added to the apical side the response differed completely from that observed when Cd^{2+} was applied to the basolateral side as apical Cd^{2+} exposure caused a $\Delta I_{sc(Cd)}$ of -1.5 ± 0.1 (n = 3) and basolateral exposure a $\Delta I_{sc(Cd)}$ of 8.3 ± 0.6 (n = 25). This suggests that the action of Cd^{2+} is highly side-specific, justifying further examination of both apical and basolateral Cd^{2+}-exposure. However, because of the prompt and transient nature of $\Delta I_{sc(Cd)}$ during basolateral treatment and for reasons debated in the Discussion further studies in this thesis focussed on basolateral Cd^{2+}-treatment only.

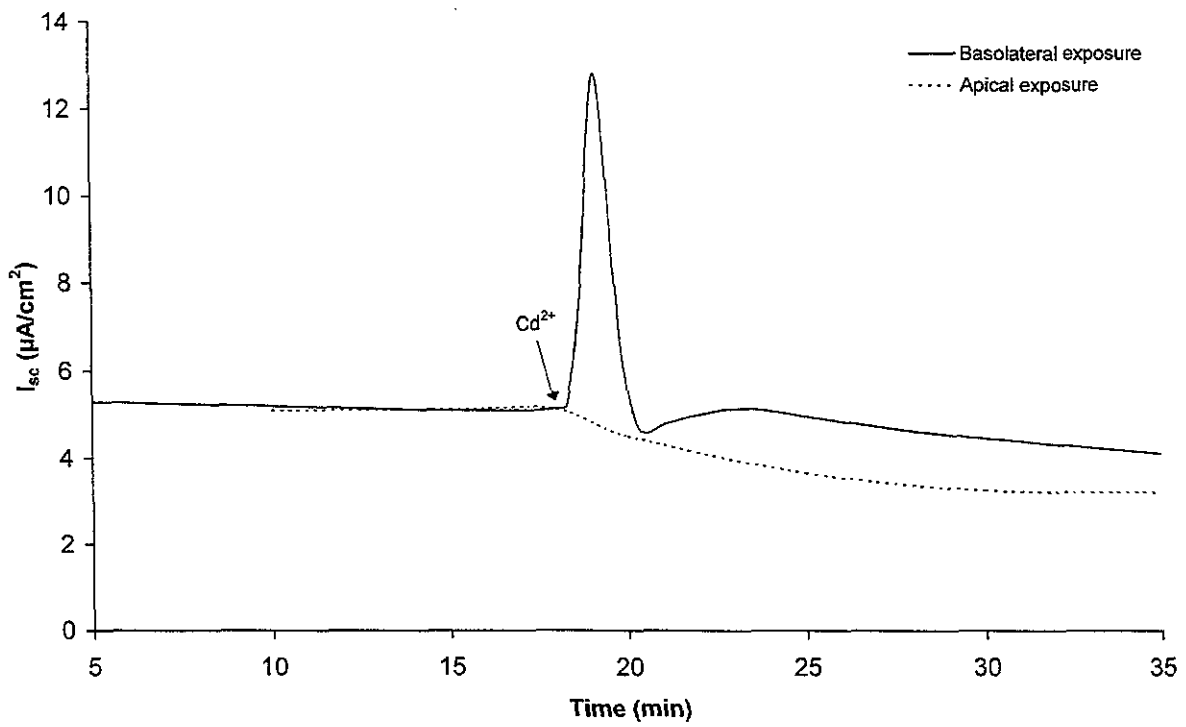

Figure 5.1. Time course of short-circuit-current (I_{sc}) experiment on confluent A6 cell monolayers. Cadmium exposure of the apical or basolateral side had completely different effects as 1 mM Cd^{2+} added to the basolateral side caused I_{sc} to increase in a prompt and transient manner whereas 1 mM Cd^{2+} added to the apical side caused I_{sc} to drop slowly until a base level was reached (dotted line). Data reproduced from paper VII.

The accumulated dose-response was measured to examine the sensitivity of active ion transport to Cd^{2+} by adding increasing concentrations of $CdCl_2$ to the basolateral solution and measuring ΔI_{sc}. Dose-response relationships were measured in a modified Ussing chamber allowing washing between each addition of Cd^{2+}. The results showed that below 100 μM $CdCl_2$ A6 cells respond marginally, however, response was detectable at 1 μM (figure 5.2). From 100 μM to 1000 μM $CdCl_2$ ΔI_{sc} increased from 2.2 ± 0.4 to 11.4 ± 1.5 μA/cm^2 (n = 6, figure 5.2, inserted figure). The half maximal stimulation concentration ($H_{0.5}$) determined as mean of six experiments was 365.3 ± 19.6 μM with a maximal response at 1 mM.

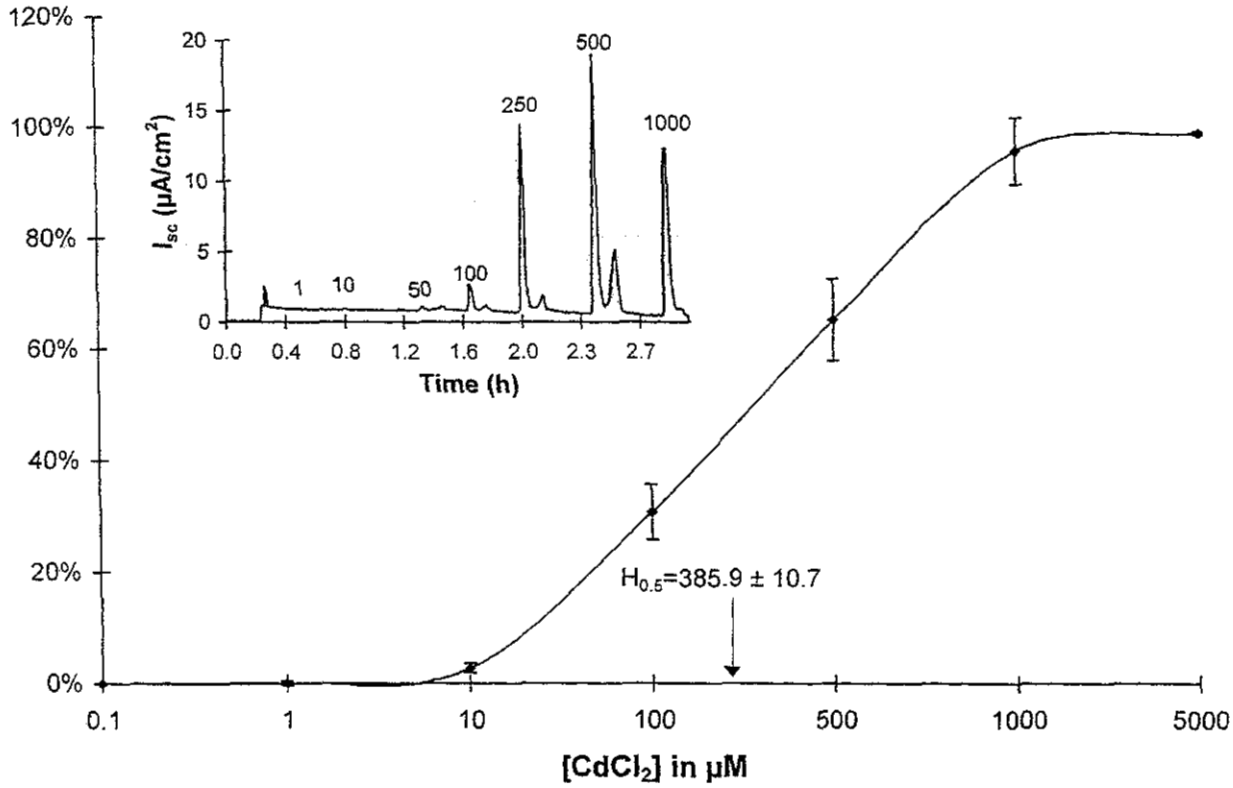

Figure 5.2. *Dose-response relationship between short-circuit-current (I_{sc}), expressed as % of control, and increasing concentrations of cadmium administered to the basolateral surface of A6 cells. The half maximal stimulation concentration ($H_{0.5}$) was calculated as the 50%-level of maximal Cd^{2+}-induced stimulation of I_{sc}. By intrapolation $H_{0.5}$ was estimated to 365.3 ± 19.6 μM (n = 6). The monolayer was washed with normal Ringer solution between each addition of Cd^{2+}. Inserted picture; time course of I_{sc} stimulated by increasing concentrations of Cd^{2+} (figures on top of each peak). Data are expressed as mean ± SE. Data reproduced from paper VI.*

5.2. Cytotoxicity (I & II)

The effect of Cd^{2+} on cell integrity was determined using two different approaches, namely by successive determinations of R_{te} and by determination of the IC_{50}-value (see Methods for further details). Successive determinations of R_{te} on A6 cells mounted in modified Ussing chambers indicated that the time from basolateral addition of 1 mM $CdCl_2$ to the time when R_{te} started to decrease markedly was 39.8 ± 5.7 minutes and that R_{te} reached nearly zero Ω in 109.2 ± 29.3 minutes (n=5 in both cases). Consequently, all I_{sc}-experiments were terminated within 40 minutes

after addition of Cd^{2+} to assure that cell integrity was intact. When R_{te} was used as an endpoint, apical and basolateral additions of $CdCl_2$ for 24 hours resulted in IC_{50}-values of 173.9 and 147.8 µM, respectively (figure 5.3). Extension of the incubation period for another 24 hours increased the IC_{50} value for apical $CdCl_2$ addition to 247.0 µM, whereas the IC_{50} value for basolateral exposure was unchanged. The monolayer reacted differently depending on which surface was exposed to cadmium. Thus, after 24 hours of exposure with 200 µM Cd^{2+}, R_{te} was 1.2 % and 32.9 % of control values when Cd^{2+} was applied to the basolateral and apical side, respectively. The apical/basolateral R_{te}-values became even more pronounced at concentrations higher than 200 µM. Above 200 µM the basolateral R_{te} dropped further to 0% and the apical curve levelled off and never decreased below 20.3 % at concentrations as high as 1000 µM. Like in the I_{sc}-experiments, cell integrity studies also demonstrated side-specific effects, where the cytotoxic action of Cd^{2+} was far more pronounced at the basolateral side than at the apical side of A6 monolayers.

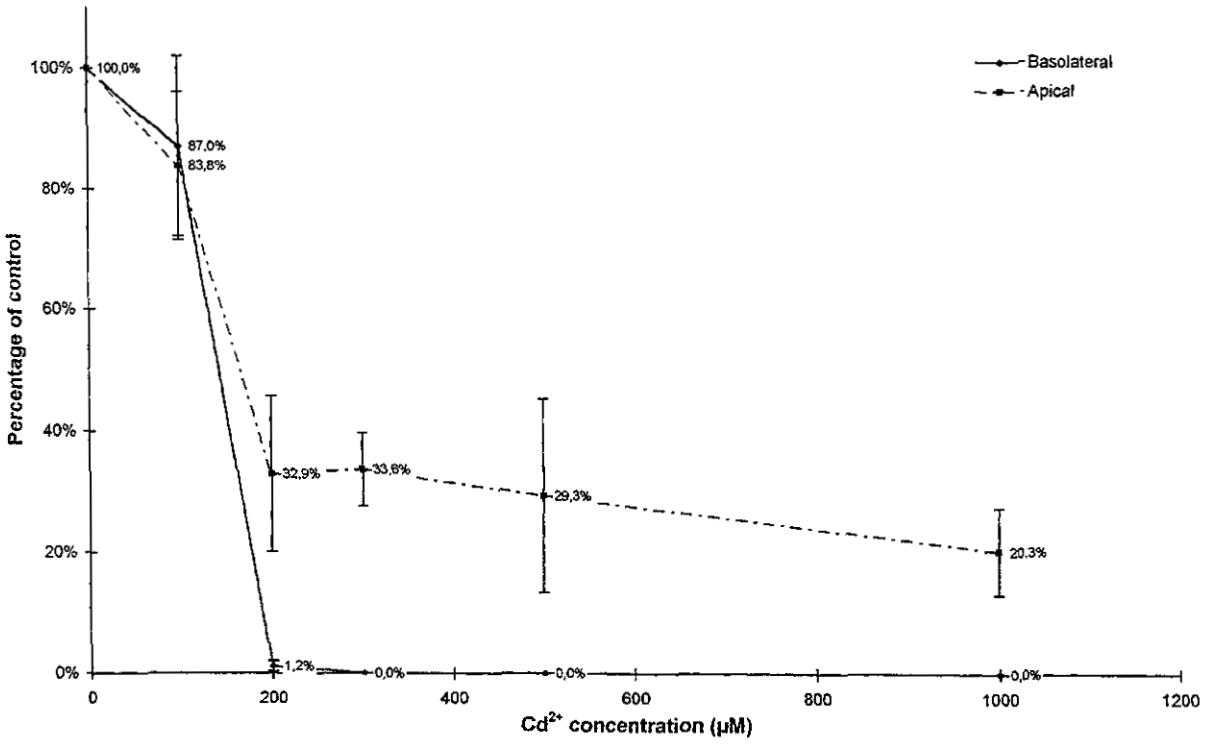

Figure 5.3. Effect of apical and basolateral Cd^{2+} exposure on transepithelial resistance (expressed as % of control values). $CdCl_2$ was applied basolaterally (full line) or apically (dotted line). A6 cells were exposed for 24 hours at the concentrations shown in the figure. Values are means ± SE of two experiments. Modified and reproduced from article II.

5.3. Ionic nature behind $\Delta I_{sc(Cd)}$ (I, II & VI)

To investigate the ionic nature behind the increase in $\Delta I_{sc(Cd)}$, inhibitors of Na^+ and Cl^- transport were used. Addition of 100 µM of the sodium channel blocker Amiloride (Garty, 1988) to the apical solution immediately inhibited I_{sc}. However, the characteristic I_{sc}-peak evoked by 1 mM $CdCl_2$ was still evident and undiminished as $\Delta I_{sc(Cd)}$ of amiloride pretreated monolayers was 104.3 ± 8.5 % (n = 5, p = NS) of control monolayers (n is raised since the publication of paper II). This

indirectly suggests that Na^+ is not involved in $\Delta I_{sc(Cd)}$. Since Cd^{2+} applied basolaterally increases I_{sc} in a Na^+-independent way, it is most likely that chloride secretion is involved in the transient nature of $\Delta I_{sc(Cd)}$. As shown in table 5.1 substitution of basolateral chloride by SO_4^{2-} for at least 25 minutes reduced $\Delta I_{sc(Cd)}$ to 11.5 ± 3.5 % (n = 4, $p < 0.001$) compared with control monolayers showing that Cl^- transport plays a crucial role in Cd^{2+}-activated I_{sc}. Various Cl^--transport blockers were employed to further characterize the possible Cl^- current induced by Cd^{2+}. The blockers were applied to the apical solution with exception of furosemide, which was applied to the basolateral solution. Table 5.1 shows that both non-selective anion blockers DPC (Di Stefano, *et al.*, 1985) and NPPB (Wangemann *et al.*, 1986) reduced $\Delta I_{sc(Cd)}$ significantly to 64.4 ± 14.0 % ($p < 0.05$) and 37.8 ± 3.5 % ($p < 0.01$) of control level, respectively. Among the two Cl^-exchange blockers, furosemide and DIDS (Cabantchik & Greger, 1992), only furosemide reduced $\Delta I_{sc(Cd)}$ significantly to 56.5 ± 20.8 % of control level ($p < 0.05$). The fenemates, niflumic acid (NFA) and flufenamic acid (FFA), both blockers of Ca^{2+}-activated Cl^- currents ($I_{Cl(Ca)}$) (White, 1990) had significant blocking effects with FFA being most potent. Accordingly, NFA reduced $\Delta I_{sc(Cd)}$ to 46.6 ± 15.8 % ($p < 0.01$) and FFA to 5.0 ± 0.6 % ($p < 0.001$) of control levels, which for FFA corresponds to 0.6 ± 0.1 $\mu A/cm^2$ (n = 5) compared with the control of 8.8 ± 0.8 $\mu A/cm^2$ (n = 24). Overall, the cotransporter-inhibitors had only marginal effects on $\Delta I_{sc(Cd)}$, the fenemates having the greatest effect on $\Delta I_{sc(Cd)}$. This suggests that the observed Cd^{2+}-activated I_{sc} involves Cl^--secretion that possibly depends on calcium mobilization, likely through activation of $I_{Cl(Ca)}$.

Table 5.1. *The effect of various chloride channel inhibitors on Cd^{2+}-activated short-circuit-current (1 mM $CdCl_2$, basolaterally). The results are expressed as absolute values and as percent of control levels. Data are given as means ± SE in %; p, significance level by comparison with control; n, number of experiments. All blockers with exception of furosemide (500 μM) were added to the apical side in concentrations as follows (in μM); 100: DIDS, FFA, NFA, NPPB; 350: DPC. Reproduced from manuscript VI.*

Treatment	$\Delta I_{sc(Cd)}$ ($\mu A/cm^2$)	% of control	p	n
Control	8.8 ± 0.8	100		25
Chloride depletion	1.0 ± 0.3	11.5 ± 3.5	<0.001	4
DPC	5.7 ● 1.2	64.4 ± 14.0	<0.05	7
NPPB	3.3 ± 0.3	37.8 ± 3.5	<0.01	4
FFA	0.6 ± 0.1	5.0 ± 0.6	<0.001	5
NFA	3.8 ± 1.4	46.6 ± 15.8	<0.01	6
DIDS	9.5 ± 2.5	107.7 ± 28.8	NS	4
Furosemide	5.0 ± 1.8	56.5 ± 20.8	<0.05	6

5.4. Direct measurements of Cd^{2+}-mediated Cl^- transport using SPQ-fluorescence (VI)

Results from I_{sc}-experiments showed that Cd^{2+} transiently activates the transepithelial ion transport in A6 monolayers, apparently including Cl^--secretion only. To address this topic further the Cd^{2+}-activated ion-transport was measured directly using the Cl^--specific probe, SPQ (Verkman, 1990). The cells were loaded with SPQ as this is the most appropriate methods for detecting small changes in chloride transport (Biwersi, *et al.*, 1994). The optimal way to detect chloride transport is to have chloride concentrations that resemble the physiological conditions, i.e. high [Cl^-] outside the cells. However, to increase the driving force for Cl^- the SPQ-loaded

cells were bathed in Cl^--free Ringer (for further discussion please refer to manuscript VI). Because of the driving force Cl^- started to efflux from the cells immediately after replacement of Cl^--containing Ringer with Cl^--free Ringer. To minimize the influence of Cl^--free conditions on the calculation of intracellular Cl^- content, the mean chloride content was calculated from data obtained just after the start of experiment and was 14.1 ± 0.6 mM (n = 30). The average basal Cl^--secretion, expressed as the change in Cl^--concentration per min and abbreviated as [ΔCl^-], during Cl^--free condition, was -523.3 ± 42.7 μM · min^{-1} (n = 32). The value is negative due to the loss of Cl^- in the SPQ-loaded intracellular environment. As shown in figure 5.4, a cell suspension exposed to 1 mM $CdSO_4$ increased the arbitrary slope, expressed as $\Delta F/F_0 \cdot min^{-1}$ (× 10^3), from the basal level of 9.67 ± 1.67 to 24.48 ± 3.97 ($p < 0.001$, n = 10). Accordingly, [ΔCl^-] increased from -566.9 ± 115.0 to -1050.0 ± 154.5 μM · min^{-1} ($p < 0.001$, n= 10) in Cd^{2+}-exposed cells compared with control cells. This occurred within 122.4 ± 14.9 seconds before returning to the basal slope value (plateau level).

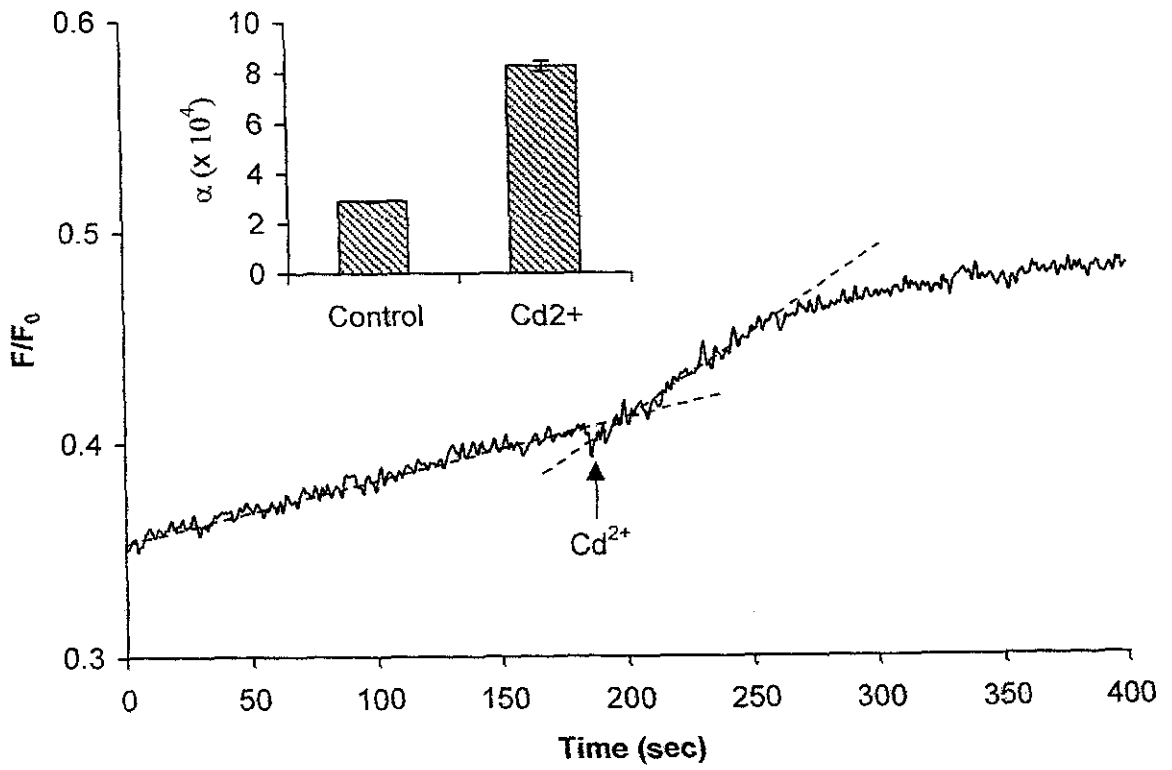

Figure 5.4. Typical recording showing changes in intracellular Cl^- concentration (expressed as F/F_0-ratio) following exposure to 1 mM $CdSO_4$. Please note that increased fluorescence means lower intracellular Cl^- concentration. The average slope of fluorescence before and after addition of cadmium is indicated by the dotted lines. The fluorescence at time zero represents the basal chloride content. The inserted figure shows the mean value ± SE of the slopes, α, (× 10^4 s^{-1}) before and after Cd^{2+} exposure. Cells were loaded with 5 mM SPQ according to the descriptions in Methods. Reproduced from article VI.

The fenemates, NFA and FFA, were the most effective inhibitors of $\Delta I_{sc(Cd)}$ as indicated in table 5.1. The two fenemates were therefore applied to the SPQ-loaded cell suspension at final concentrations of 100 μM. As demonstrated in figure 5.5 both agents almost completely abolished

the Cd^{2+}-activated Cl^--secretion. Thus, $\Delta F_{Cd}/F_0 \cdot min^{-1}$ ($\times 10^3$) went from 24.48 ± 3.97 (n = 10) in control cells to 4.29 ± 1.35 ($p < 0.001$, n = 5) and to 3.15 ± 0.58 ($p < 0.001$, n = 3) in FFA and NFA-treated cells, respectively. Not only did the fenemates lower the Cd^{2+}-activated secretion ($[\Delta Cl^-]_{Cd}$) compared with control conditions, but secretion was also lower than the basal secretion of -523.3 ± 42.7 μM · min^{-1}. Hence, $[\Delta Cl^-]_{Cd}$ was significantly lowered in the presence of FFA and NFA to -185.7 ± 55.9 μM · min^{-1} ($p < 0.01$) and -102.9 ± 19.6 μM · min^{-1} ($p < 0.05$), respectively compared with control conditions. As illustrated in figure 5.5, the use of the detergent, Triton X-100 caused the fluorescence to increase promptly, which could be reversed by adding excess Cl^- to the cell suspension (see figure legend for details).

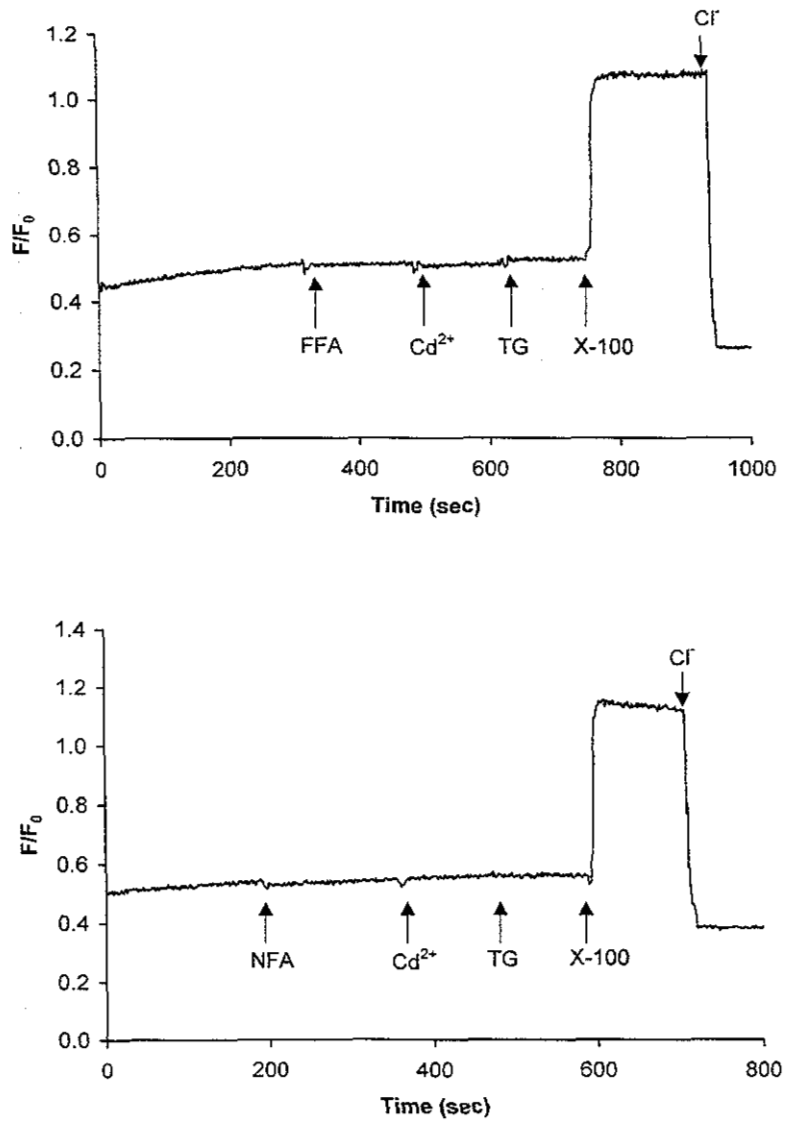

Figure 5.5. *Typical time courses showing the effects of chloride channel blockers on Cd^{2+}-stimulated Cl^--secretion measured as F/F_0. Both FFA (top figure) and NFA (bottom figure) completely abolished Cd^{2+}-stimulated fluorescence. Thapsigargin (TG)-mediated release of intracellular Ca^{2+} had no effect on fluorescence in cells preexposed to Cd^{2+} and Cl^--channel blockers. Addition of the detergent, Triton X-100 (1 % v/v) caused the fluorescence to increase promptly. This proves that Cl^- is driven out of the cells towards the Cl^--free medium causing less quenching of SPQ. Excess addition of Cl^- rapidly quenches SPQ to levels lower than basal. Concentrations used: FFA and NFA; 100 μM; Cd^{2+}, 1 mM; TG, 0.8 μM; Cl^-, 100 mM.*

5.5. Calcium involvement in Cd^{2+}-mediated Cl^- secretion (I, II, VI & VII)

The fast kinetics of $\Delta I_{sc(Cd)}$ and the fact that particularly the fenemates, known to block Ca^{2+}-dependent chloride channels, displayed the most prominent inhibitory effects on $\Delta I_{sc(Cd)}$ and SPQ-sensitive Cl^--secretion give strong evidence of the involvement of Ca^{2+}. Therefore, to study this further some preliminary experiments were performed with TG, a well-characterized blocker known to inhibit the Ca^{2+}-ATPase in endoplasmic reticulum (Thastrup, 1989). Consequently, depletion of Ca^{2+} revealed that $\Delta I_{sc(Cd)}$ decreased significantly from control conditions of 8.8 ± 0.8 $\mu A/cm^2$ (n=24) to 3.9 ± 1.1 (n=3, $p<0.05$) (figure 5.6). Preexposure with TG and A23187 both known to provoke a massive increase in intracellular Ca^{2+}, the latter by acting as a Ca^{2+}-ionophore (Reed & Lardy, 1972), almost removed $\Delta I_{sc(Cd)}$, as $\Delta I_{sc(Cd)}$ decreased to 0.3 ± 0.1 $\mu A/cm^2$ (n=4, $p<0.001$) and to 0.2 ± 0.1 $\mu A/cm^2$ (n=3, $p<0.001$), respectively. Furthermore, Cd^{2+} and TG could neutralize each other since neither Cd^{2+} nor TG could stimulate the I_{sc} further when preexposed to the counterpart (figure 5.6, inserted). Similar responses were obtained in SPQ-loaded cells as TG and Cd^{2+} also could neutralise the response of the counterpart (please refer to manuscript VI). Overall, the results suggest that Ca^{2+} may play an important role in Cd^{2+}-mediated Cl^- secretion as indicated both in I_{sc} and SPQ-experiments.

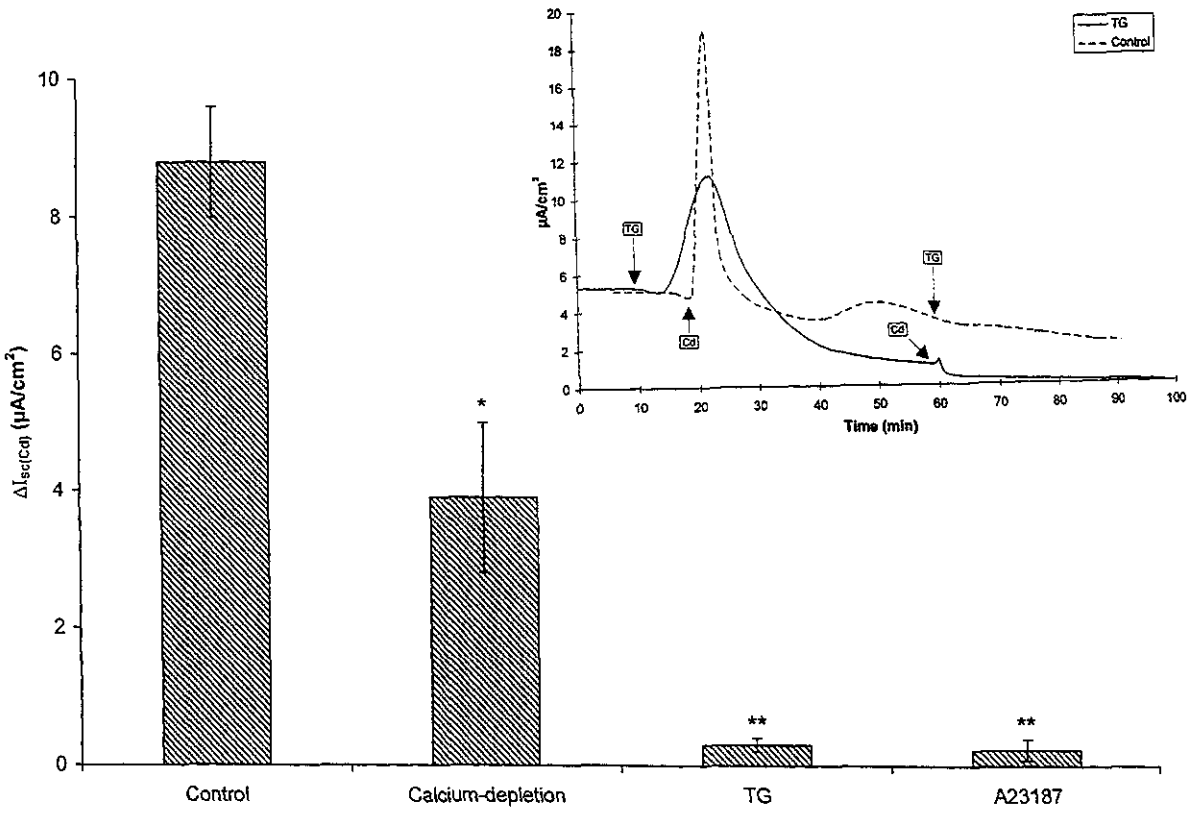

*Figure 5.6. Effect of calcium-depletion, TG and A23187 on Cd^{2+} (1 mM)-stimulated short-circuit-current ($\Delta I_{sc(Cd)}$). TG (0.4 μM) and A23187 (4 μM), both known to cause massive increases in intracellular Ca^{2+}, almost completely cancelled $\Delta I_{sc(Cd)}$. Inserted: time course showing the effect of TG and Cd^{2+} on $\Delta I_{sc(Cd)}$. TG and A23187 were added to the basolateral side of monolayers. * $p < 0.05$ and ** $p < 0.01$ compared with control. Modified and reproduced from article II & manuscript VI.*

5.6. Direct measurement of intracellular Ca^{2+} using fura-2 (VII)

Indirect evidence suggests that Ca^{2+}-mobilization is involved in $\Delta I_{sc(Cd)}$ why direct measurements of intracellular Ca^{2+} were needed. The well-characterized Ca^{2+}-probe, fura-2, was used to further characterize Cd^{2+}-mediated intracellular events.

Studies of the effects of Cd^{2+} on intracellular Ca^{2+} homoeostasis using fura-2 is hampered by the fact that divalent metal ions like Cd^{2+} also binds to the probe and cause fluorescence often more intense than that of the fura-2-Ca^{2+} complex. However, this depends on the fact that Cd^{2+} enters the cells in its free form. As described in Methods the cells were incubated with TPEN, before carrying out the experiments to prevent interactions with Ca^{2+}-fura-complex. TPEN chelates heavy metals and not Ca^{2+} allowing minimum disturbance of the fluorescence signal achieved from the Ca^{2+}-dye-complex (Hinkle, 1992; Snitsarev *et al.*, 1996). Therefore, the contribution from Cd^{2+}-fura-complex can be ignored if TPEN behaves as expected. In a pilot study, the cell membrane of A6 cells was permeabilized with 10 μM of the calcium ionophore ionomycin to permit Cd^{2+} entry to the cells and then chelated with TPEN (figure 5.7). Addition of 50 μM TPEN completely cancelled the increase in fluorescence evoked by 400 μM Cd^{2+}. Furthermore, addition of 5 mM EGTA did not affect the fluorescence supporting that fura-2 was only located intracellularly. Again, please refer to the discussion of manuscript VII regarding the comprehensive discussion of Cd^{2+} interactions with the fura-2 probe.

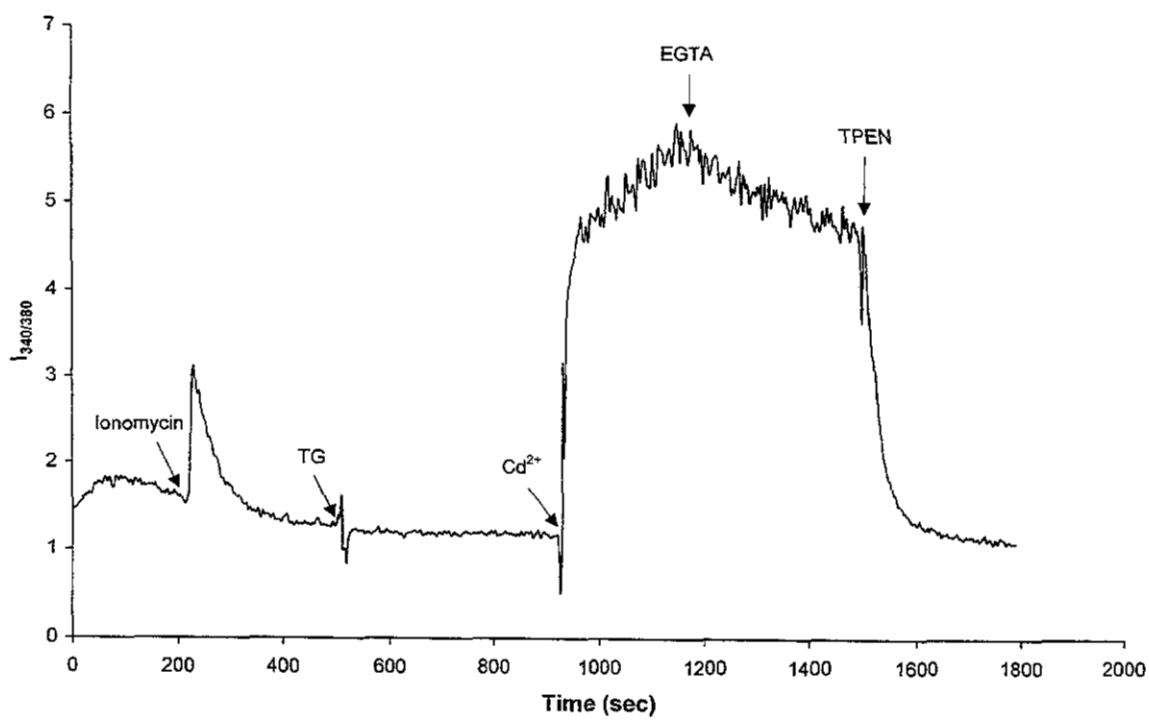

Figure 5.7. *Cells were permeabilized by 10 μM Ionomycin and depleted for intracellular Ca^{2+} using 800 μM TG. Subsequently, the permeable membrane allowed Cd^{2+} (400 μM) to enter the intracellular environment resulting in a prompt increase in fluorescence expressed as I_{340}/I_{380}, which was unaffected by 5 mM EGTA, but could be reversed by 50 μM TPEN.*

The test concentration of Cd^{2+} was set at $H_{0.5}$-level, i.e. 400 μM in the subsequent experiments. The basal concentration of$[Ca^{2+}]_i$ of isolated, fura-2-loaded A6 cells were 111 ± 7 nM determined in 73 experiments. $[Ca^{2+}]_i$ rose steeply to peak-values of 579 ± 61 nM (n = 23) within 15 ± 1

seconds when stimulated with 400 μM Cd^{2+} ($[\Delta Ca^{2+}]_{Cd}$), and declined afterwards to control level or slightly above control level within 3 minutes (figure 5.8). When the fluorescence intensity at peak height was compared with the basal level, Cd^{2+} displayed a peak/basal-ratio of 6.1 ± 0.6 (n = 23) consistently with the previously obtained I_{sc}-results. Dose-response studies showed that below 10 μM Cd^{2+} fura-2 loaded A6-cells responded marginally whereas above this threshold the response was dose-dependent (figure 5.8, inserted).

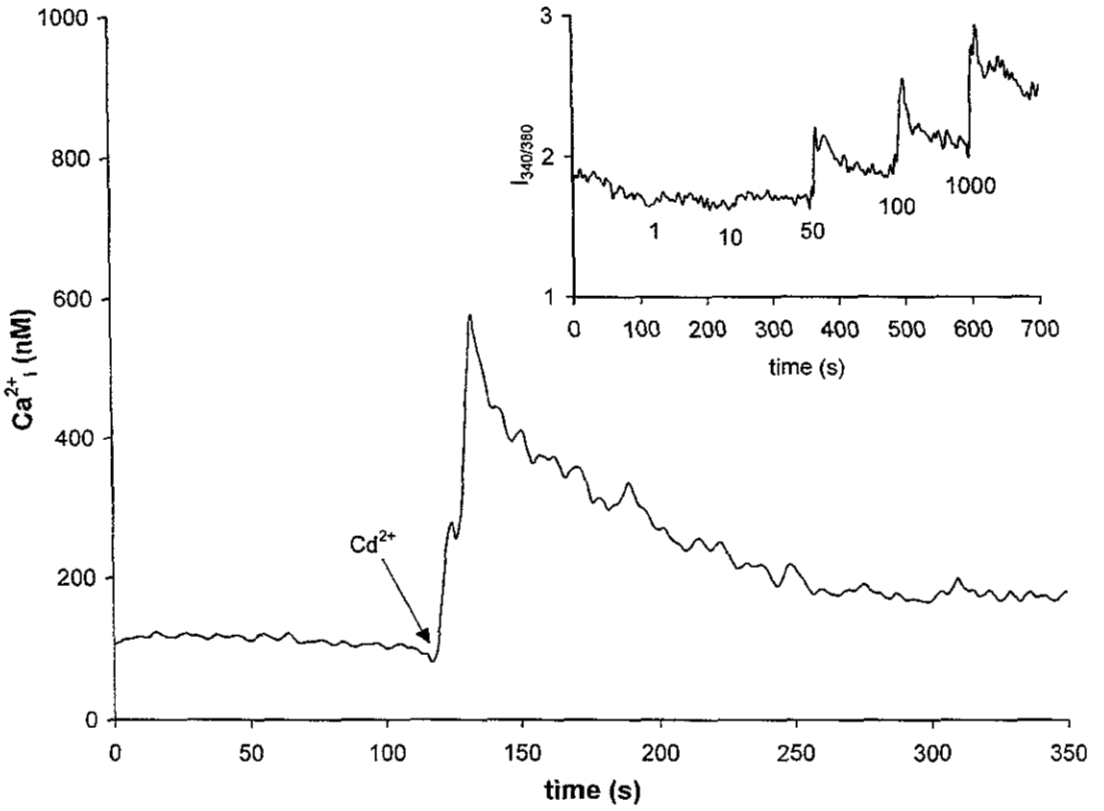

Figure 5.8. $[Ca^{2+}]_i$ measurements in suspensions of fura-2 loaded A6 cells at rest and after application of 400 μM Cd^{2+}. Cd^{2+} evokes a fast and transient increase in $[Ca^{2+}]_i$, which within 3 minutes declines to or slightly above basal level. Furthermore, the transient increase is dose dependent as showed in the inserted figure and responds at concentrations of Cd^{2+} above 10 μM which is consistent with the I_{sc}-results. Reproduced from manuscript VII.

5.7. Origin of Cd^{2+}-induced Ca^{2+} increase (II & VII)

To investigate the origin of the $[\Delta Ca^{2+}]_{Cd}$, TG and TMB-8, a benzoic acid derivative reported to abolish the Ca^{2+}-mobilization from IP_3-sensitive stores in rat kidney (Salomonsson & Arendshorst, 1999), were used. However, only results from TG-experiments are showed here. As for TMB-8 results and discussion see manuscript VII. 0.8 μM TG induced, as expected, an increase in Ca^{2+}_i which remained at a plateau level of 337 ± 59 nM (n = 8)(figure 5.9). Interestingly, TG (and TMB-8) abolished $[\Delta Ca^{2+}]_{Cd}$ as the peak/basal-ratio was 0.4 ± 0.1 (n = 4) compared with a control level of 6.1 ± 0.6 (n = 23). Preexposure with Cd^{2+} and subsequent addition of TG increased $[\Delta Ca^{2+}]_{Cd}$ to 383 ± 67 nM (n = 7), which was insignificantly different from the control levels mentioned above (figure 5.9). This proves that the intracellular pools are the main source of $[\Delta Ca^{2+}]_{Cd}$, and that they are not emptied by Cd^{2+}.

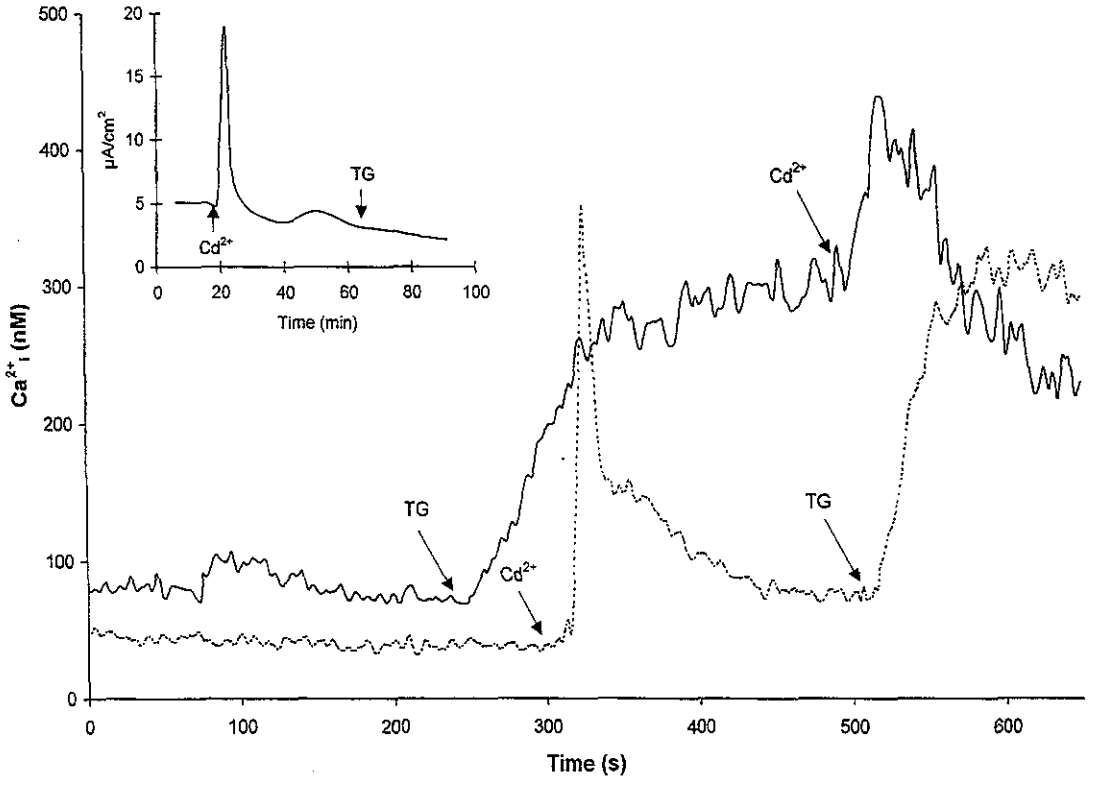

Figure 5.9. Time course showing $[Ca^{2+}]_i$ when cells are exposed to Cd^{2+} (400 μM) and subsequently to TG (0.8 μM, dotted line) or conversely (full line). See legend belonging to figure 5.6 for additional information. Inserted figure shows a typical time course of an I_{sc}-experiment when TG is added to Cd^{2+}-preexposed A6 cells (data obtained from article II). Note that TG is able to increase Ca^{2+}_i further following Cd^{2+} treatment (dotted line). Reproduced from article II & manuscript VII.

5.8. Interaction studies

In a pilot study it was found that in cells preexposed to Cd^{2+}-related metal Zn^{2+}, $\Delta I_{sc(Cd)}$ was completely abolished (figure 5.10). Therefore, interaction studies between Cd^{2+} and Ni^{2+} and Zn^{2+} were performed in SPQ and fura-2 experiments to explore if the effects of these three metals are by similar mechanisms. In fact, Zn^{2+} and Ni^{2+}, could also activate the SPQ-sensitive Cl^--transport in a Cd^{2+}-like manner and Zn^{2+} was an even more potent activator than Cd^{2+} (table 5.2). Regarding the Cd^{2+}-metal interactions, preexposure with Zn^{2+} and Ni^{2+} significantly inhibited the Cd^{2+}-stimulated ratio $\Delta F_{Cd}/F_0 \cdot min^{-1}$ ($\times 10^3$) from 24.48 ± 3.97 to 3.28 ± 1.22 ($p < 0.001$) and to 6.54 ± 0.96 ($p < 0.01$), respectively (table 5.3). Accordingly, preexposure with Zn^{2+} and Ni^{2+} (and TG) all inhibited the Cd^{2+}-activated Cl^--secretion comparable to the results obtained with the fenemate-blockers (table 5.3). Overall, the ratio between stimulator and basal fluorescence ($\Delta F_{stimulator}/\Delta F_{basal}$) was calculated as 2.9 ± 0.5, 3.8 ± 0.5, 2.6 ± 0.3 and 1.7 ± 0.2 for Cd^{2+}, Zn^{2+}, Ni^{2+} and TG, respectively. ANOVA did not reveal any statistical differences between the stimulators.

Table 5.2. Effects of Cd^{2+}, Zn^{2+}, Ni^{2+} and TG on chloride transport in SPQ-loaded A6-cells. The concentrations used were 1 mM for the metals and 0.8 μM for thapsigargin added to a chloride free extracellular solution. The results are expressed either as relative fluorescence variation, $\Delta F/F_0$ where ΔF represents the change in intensity upon addition of an agent and F_0 the maximal intensity, or as μM/min calculated from the linear plot given in figure 4.4. Results are expressed as mean ± SE. ANOVA did not bring out any differences between the stimulators. In general, the potency of stimulators was in decreasing order; $Zn^{2+} > Cd^{2+} > Ni^{2+} > TG$. Reproduced from manuscript VI.

	Effects of stimulators on Cl^- secretion			
	$\Delta F/F_0 \cdot min^{-1}(\times 10^3)$		$\mu M \cdot min^{-1}$	
	Control	Stimulator	Control	Stimulator
Cd^{2+} (n = 10)	9.67 ± 1.67	24.48 ± 3.97***	-583.1 ± 114.2	-1050.0 ± 154.5***
Zn^{2+} (n = 5)	7.09 ± 1.32	31.94 ± 4.50***	-512.0 ± 114.7	-1234.2 ± 80.3***
Ni^{2+} (n = 3)	7.26 ± 1.14	18.07 ± 0.76*	-371.8 ± 47.7	-774.1 ± 104.4
TG (n = 5)	10.00 ± 1.27	16.30 ± 2.62	-617.2 ± 64.1	-729.2 ± 150.3

* $p < 0.05$, ** $p < 0.01$, *** $p < 0.001$ compared with control.

*Table 5.3. Effects of various compounds on Cd^{2+}-stimulated Cl^--secretion expressed as $\Delta F_{Cd}/F_0 \cdot min^{-1}$ (× 10^3) and change in Cl^--concentration pr. min, $[\Delta Cl^-]_{Cd}$ compared with cells only exposed to Cd^{2+} ($\Delta F_{control}$) or untreated cells (ΔF_{basal}). Cells were loaded with 5 mM SPQ as specified in Materials and fluorescence was measured under chloride-free extracellular conditions on a spectrophotometer. Zn^{2+}, Ni^{2+} and TG were used to define interactions with Cd^{2+}. Test agents were compared either with $\Delta F_{control}$ (statistic significance marked as *) or with ΔF_{basal} (statistic significance marked as ‡). Data shown are mean values ± SE. Reproduced from manuscript VI.*

		Test agents					
	$\Delta F_{control}$ (n = 10)	Zn^{2+} (n = 3)	Ni^{2+} (n = 3)	TG (n = 4)	FFA (n = 5)	NFA (n = 3)	ΔF_{basal} (n = 32)
$\Delta F_{Cd}/F_0 \cdot min^{-1}(\times 10^3)$	24.48 ± 3.97	3.28 ± 1.22 ***	6.54 ± 0.96 ***	2.66 ± 1.24 ***/‡	4.29 ± 1.35 ***/‡	3.15 ± 0.58 ***	10.49 ± 0.84
$[\Delta Cl^-]_{Cd}$ ($\mu M \cdot min^{-1}$)	-1050.0 ± 154.5	-163.7 ± 68.5 */‡	-225.7 ± 38.6 ***/‡	-108.3 ± 48.2	-185.7 ± 55.9 **/‡‡	-102.9 ± 19.6 */‡	-523.3 ± 42.7

* $p < 0.05$, ** $p < 0.01$, *** $p < 0.001$ compared with $\Delta F_{control}$. ‡ $p < 0.05$, ‡‡ $p < 0.01$ compared with ΔF_{basal}.

Thus, the interaction study revealed that Zn^{2+}, Ni^{2+} and Cd^{2+} most likely induce Cl^- secretions in A6 cells by similar mechanisms as the responses were very similar to those observed for Cd^{2+}. Therefore, parallel experiments, where the endpoint is intracellular Ca^{2+} were performed, as Ca^{2+} mobilization is likely to play an important role in Cd^{2+}-mediated Cl^- secretion. Hence, both metals induced Ca^{2+}-mobilization in a Cd^{2+}-like fashion, i.e. they too displayed transient characteristics with a very fast kinetic (figure 5.10). In fact, both metals (400 μM) were more potent inducers than Cd^{2+}; peak-levels for Zn^{2+} and Ni^{2+} were 1116 ± 210 nM (n = 7) within 14 ± 1 seconds and 868 ± 119 nM (n = 5) within 16 ± 2 seconds, respectively. This corresponds to peak/basal-ratios of 14.0 ± 2.7 and 11.0 ± 1.8, respectively and was about twofold higher than the corresponding Cd^{2+}-level of 6.1 ± 0.6 (n = 23). Pretreatment with either Zn^{2+} or Ni^{2+} prevented the Cd^{2+}-inducible Ca^{2+}-increases normally observed with Zn^{2+} being the most potent cancelling metal. Hence, Zn^{2+} and Ni^{2+} reduced the peak/basal-ratio of Cd^{2+} to 0.3 ± 0.1 and 0.8 ± 0.1 (n = 4 in both cases), respectively. These data confirm and extend the previous findings in the sense that the similar metals Cd^{2+}, Zn^{2+} and Ni^{2+} evoke Ca^{2+} transients and Cl^--secretion in A6 cells by similar mechanisms.

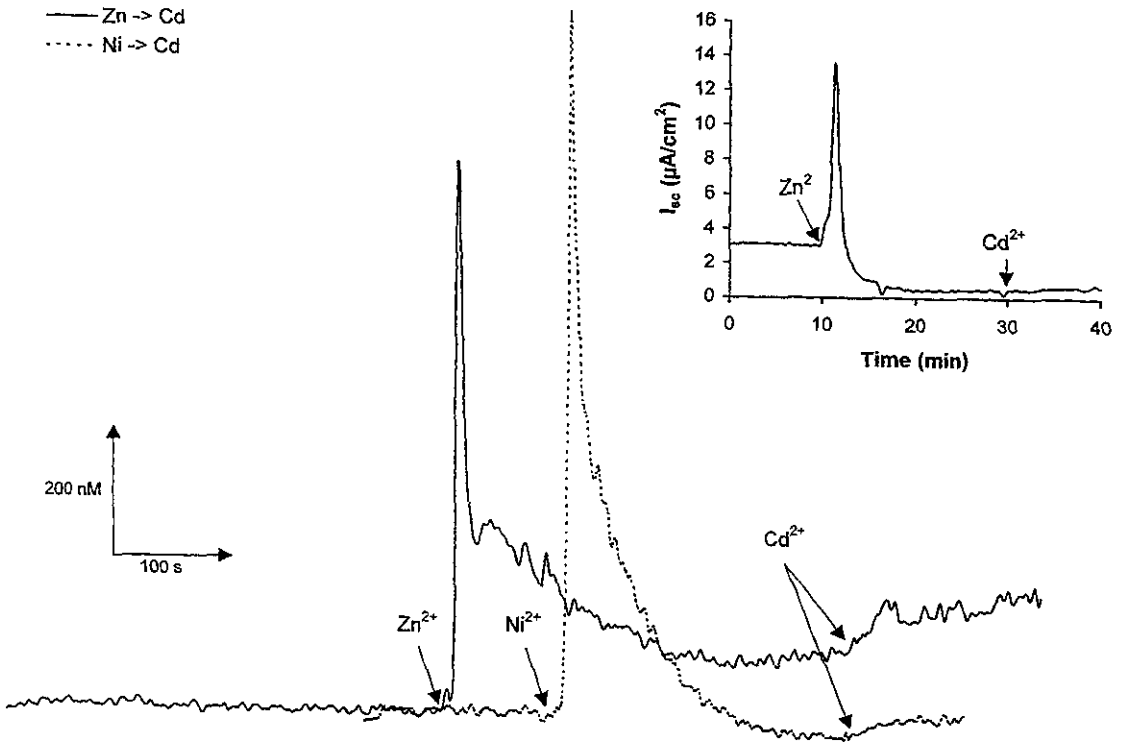

Figure 5.10. Interactions between Cd^{2+} and the two related metals, Zn^{2+} and Ni^{2+}. Both Zn^{2+} and Ni^{2+} (both 400 µM) displayed time-courses very alike those observed when A6 cells are exposed to 400 µM Cd^{2+} (see figure 5.9 for comparisons). Pretreatment with either Zn^{2+} or Ni^{2+} prevented the Cd^{2+}-induced Ca^{2+}-increases normally observed suggesting that both metals evoke Ca^{2+} transients and Cl^--secretion in A6 cells by similar mechanisms. Inserted: typical time-course of an I_{sc}-experiment when Cd^{2+} was added to preexposed Zn^{2+}-treated cells. Note that Zn^{2+} induced I_{sc} increases very similar to what was observed for Cd^{2+} and the similarity with Ca^{2+}-measurements (see results and discussion for further details). Modified and reproduced from manuscript VII.

5.9. CaR-involvement (V & VII)

To examine how Cd^{2+} may cause Ca^{2+}-mobilization, the possible activation of CaR was studied. CaR belongs to the seven-pass type of receptor, which upon ligand-binding (through the G-protein cascade) activates PLC leading to increased levels of IP_3 (see Introduction for further details about the CaR). Therefore, if Cd^{2+} (and Zn^{2+} and Ni^{2+}) serves as a CaR-ligand, modulation of PLC-mediated activation and increased IP_3-levels are to be expected.

PLC-inhibitors

The involvement of PLC-dependent activation of $\Delta I_{sc(Cd)}$ was examined by using U73122, a membrane permeable aminosteroid that blocks the phosphatidylinositol-specific PLC (Hildebrandt *et al.*, 1997). As shown in figure 5.11, preexposure of confluent A6 cell monolayers to 10 µM U73122 at the basolateral side resulted in almost total cancellation of $\Delta I_{sc(Cd)}$ at both 100 µM Cd^{2+} and 1 mM Cd^{2+} as $\Delta I_{sc(Cd)}$ was diminished to 17.4 ± 9.0 % and 9.3 ± 3.5 % of control level, respectively ($n = 4$ and $p < 0.01$ in both cases). Further experiments were carried out with

neomycin, an aminoglycoside antibiotic that has often been used as an inhibitor of PLC-mediated signalling processes (Hildebrandt *et al.*, 1997; Sipma *et al.*, 1996). Pretreatment with 500 µM neomycin completely abolished $\Delta I_{sc(Cd)}$ at 100 µM of Cd^{2+}-exposure as $\Delta I_{sc(Cd)}$ was diminished to 6.3 ± 4.1 % (n = 3, $p < 0.01$). However, at 1000 µM Cd^{2+} neomycin did not affect $\Delta I_{sc(Cd)}$ compared with cells not pretreated with neomycin (figure 5.11) suggesting that neomycin is not as potent or specific a PLC-inhibitor as U73122.

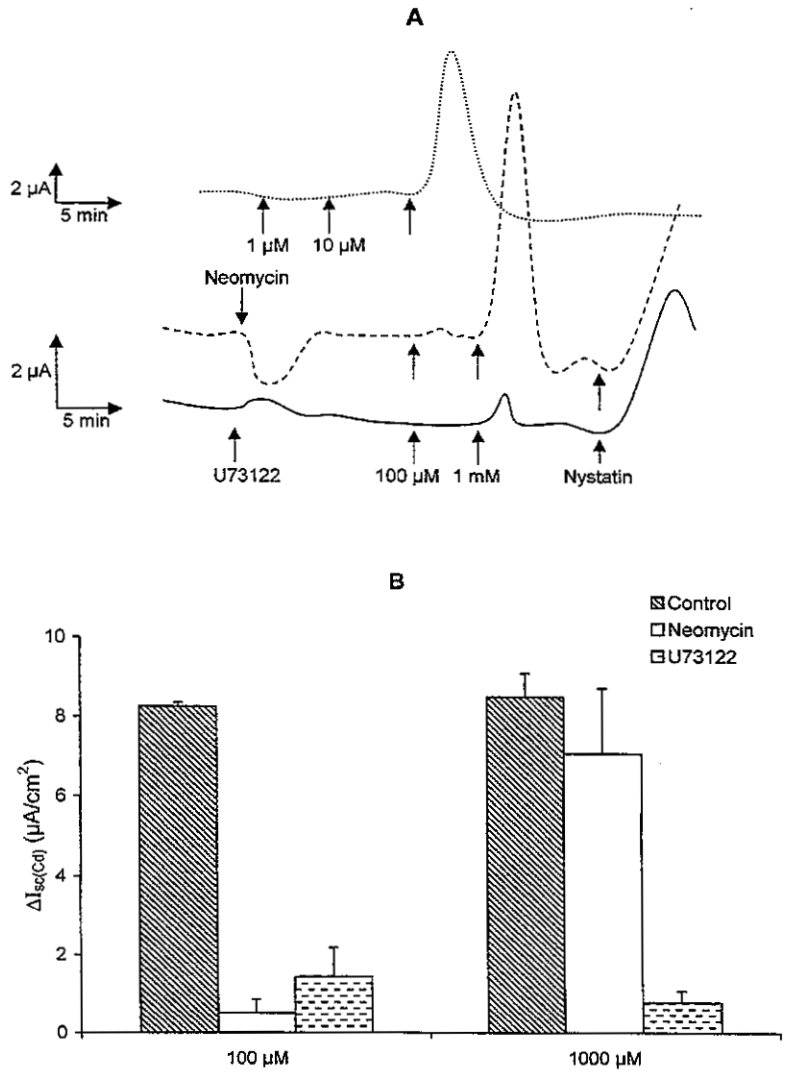

Figure 5.11. *(A). Typical time course showing the effects of the PLC-inhibitors, U73122 (full line) and neomycin (punctuated line) on basolateral Cd^{2+}-induced I_{sc} ($I_{sc(Cd)}$). The control response at 0 to 100 µM Cd^{2+} is illustrated as the upper dotted line. U73122 and neomycin were added to the basolateral side of the A6 cell monolayers at 10 µM and 500 µM, respectively. The apical membrane was permeabilized by nystatin (300 U/ml) to illustrate that the basolateral membrane transport still was intact. (B). Bar diagram displaying the effect of U73122 (10 µM) and neomycin (500 µM) on $\Delta I_{sc(Cd)}$ at concentrations of 100 µM and 1000 µM Cd^{2+}, respectively. U73122 suppresses $\Delta I_{sc(Cd)}$ both at 100 µM and 1000 µM whereas neomycin only suppresses $\Delta I_{sc(Cd)}$ at 100 µM Cd^{2+}. n-values are as follows for control, neomycin and U73122 at 100 µM; 4, 3, 4 and at 1000 µM; 24, 4, 4. Reproduced from manuscript VII.*

Using U73122 and neomycin in Ca^{2+}-measurements demonstrated that 10 μM U73122 partially suppressed $[\Delta Ca^{2+}]_{Cd}$ at 400 μM and totally at 100 μM. Thus, pretreatment with U73122 and subsequent addition of 100 μM Cd^{2+} caused $[Ca^{2+}]_i$ to fall from 503 ± 106 nM (n = 4) in control cells to 69 ± 16 nM (n = 3, $p < 0.05$). Even at a concentration of 400 μM Cd^{2+} the peak/basal-ratio was significantly higher in control cells than in U73122-treated cells as the ratio fall from 6.1 ± 0.6 (n = 23) to 2.1 ± 0.9 (n = 3, $p < 0.05$), respectively. Neomycin was an even more potent inhibitor of $[\Delta Ca^{2+}]_{Cd}$ than U73122 as 250 μM neomycin almost cancelled the control response at 400 μM Cd^{2+}. Hence, $[\Delta Ca^{2+}]_{Cd}$ dropped from 579 ± 61 nM (n = 23) in control cells to 50 ± 13 nM (n = 5) in neomycin preexposed cells ($p < 0.001$) corresponding to peak/basal-ratios of 6.1 ± 0.6 and 0.4 ± 0.1, respectively. These data suggest that $[\Delta Ca^{2+}]_{Cd}$ is dependent upon PLC-sensitive pools with neomycin being the most potent inhibitor of $[\Delta Ca^{2+}]_{Cd}$ at the given concentrations used. Please refer to manuscript VII for graphics.

IP_3-generation

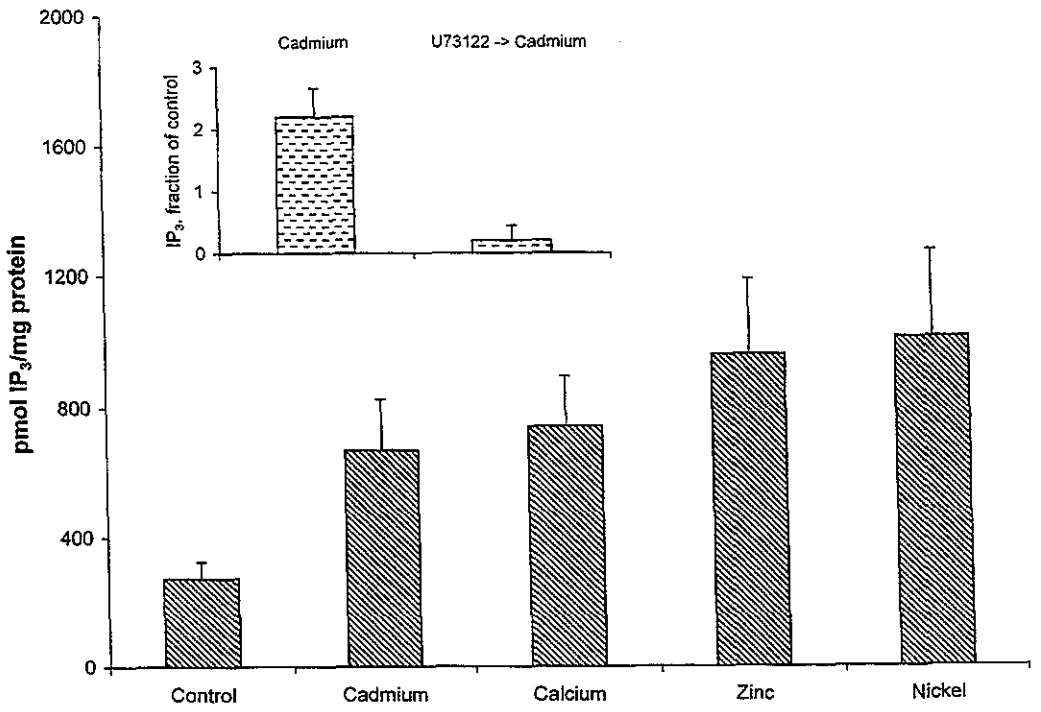

Figure 5.12. *IP_3-accumulation in A6 cells when exposed for 60 seconds to 1.4 mM Ca^{2+} (1 mM Ca^{2+} present in the medium) and 400 μM Cd^{2+}, Zn^{2+} and Ni^{2+} obtained from 4, 18, 8 and 8 experiments, respectively. All cations increased the IP_3-content significantly compared with the non-treated control cells. Inserted: when cells were preexposed to 5 μM of the PLC-inhibitor, U73122 for 2 min the Cd^{2+}/control-ratio of IP_3-accumulation was 0.2 ● 0.2 (n= 4) showing that U73122 did not influence the resting level but also that U73122 could completely suppress the Cd^{2+}-induced IP_3-generation as Cd^{2+}/control-ratio in non-treated cells increased to 2.2 ± 0.5 (n = 3). Data are expressed as mean ± SE. Modified and reproduced from manuscript VII.*

Resting IP_3-levels, measured with the receptor binding assay, were 272.2 ± 51.7 pmol · mg protein in A6 cell suspension. All the tested cations could increase the IP_3-content significantly above control level (figure 5.12). Hence, activation of the cells for 60 sec with 400 μM Ca^{2+},

Cd^{2+}, Zn^{2+}, Ni^{2+} increased the IP_3-content significantly to 740.1 ± 153.2 (n = 4, p< 0.05), 668.2 ± 156.6 (n = 18, p < 0.02), 957.6 ± 229.0 (n = 8, p < 0.01) and 1008.9 ± 263.3 pmol · mg^{-1} (n = 8, p < 0.001) in comparison with the resting level. Preincubation of cells with the U73122 (5 μM) for 2 min completely suppressed Cd^{2+}-induced IP_3-generation (figure 5.12, inserted). Thus, the Cd^{2+}/control-ratio of IP_3-accumulation increased to 2.2 ± 0.5 (n = 4) whereas U73122 pretreated cells demonstrated a Cd^{2+}/control-ratio of 0.2 ± 0.2 (n = 3). This suggests that U73122 function as an effective inhibitor of PLC since the IP_3-level was not different from the resting level. Moreover, these data show that U73122 is a potent inhibitor of Cd^{2+}-inducible IP_3-generation.

5.10. Cd^{2+}-AVT interactions (III)

The amphibian antidiuretic hormone AVT stimulates I_{sc} in A6-epithelia by evoking a bi-phasic response (see figure 5.13, left figures), where the first I_{sc}-stimulation consists of Cl^- secretion entirely (AVT_1) and the second I_{sc}-stimulation consists of both Cl^- secretion and Na^+ absorption (AVT_2) (Bjerregaard, 1995; Chalfant, 1993).

Addition of 1 mM Cd^{2+} to the basolateral surface markedly inhibited AVT-induced (50 nM) increase in I_{sc} (figure 5.13, right figure). In four experiments, Cd^{2+} inhibited AVT_1 from 6.5 ± 1.3 to 1.2 ± 0.3 μA/cm^2 (p < 0.01) and AVT_2 from 5.0 ± 0.5 to 0.6 ± 0.1 μA/cm^2 (p < 0.001). It is generally accepted that cAMP, a product of AC activity, serves as an intracellular second messenger for AVT (and ADH) by inducing an increase in the ion permeability of the apical membrane in distal epithelial cells (see introduction for further details) (Hays, 1996; Verrey, 1994; Zeiske *et al.*, 1998). Activation of phosphodiesterase (PDE) assures restoration of the intracellular concentration of cAMP (Taylor & Palmer, 1982). To decide if the Cd^{2+}-induced inhibition of AVT-stimulated I_{sc} was related to an inhibition of enzymes involved in cAMP metabolism, the activity of AC and PDE were measured. The overall results were that Cd^{2+} inhibited the AC-activity whereas the PDE-activity was unaffected, which accordingly suggests that the mechanism by which Cd^{2+} inhibits AVT-induced I_{sc} could be through deprivation of AC-activity.

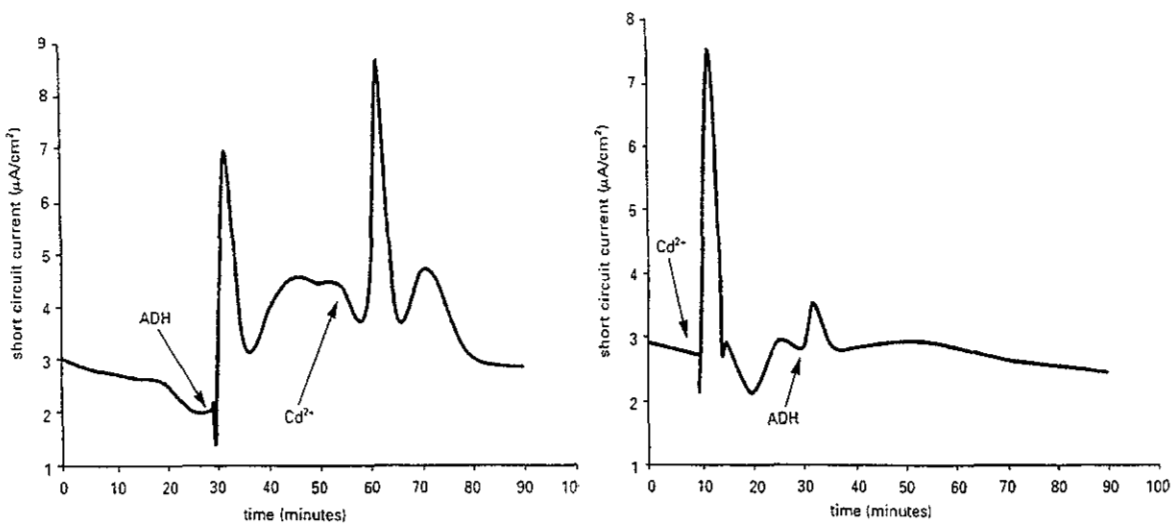

Figure 5.13. Left: Control response of AVT (50 nM) and subsequent addition of 1 mM Cd^{2+}. Note the AVT_1 and AVT_2 top. Right: Control response of 1 mM Cd^{2+} and subsequent addition of 50 nM AVT. Cadmium and AVT were added to the basolateral surface of A6 monolayers. Reproduced form article III.

5.11. Additional results

Effect of Cd^{2+} on Na^+-K^+-ATPase activity (unpublished data)

In a pilot study nystatin was used as indicator of *in vitro* Na^+-K^+-ATPase activity. Because nystatin-mediated apical permeabilization causes an influx of ions (primary Na^+), the measured active ion transport corresponds to the activity of Na^+-K^+-ATPase. Hence, $\Delta I_{sc(Nys)}$ (ΔI_{sc} when nystatin was added) is proportional to Na^+-K^+-ATPase activity (see Methods for further details and article IV for examples of nystatin-induced I_{sc}). Ouabain pretreated monolayers were used to determine the lowest ΔI_{sc} ($\Delta I_{sc(Oua)}$) obtainable activity due to the specific inhibition of Na^+-K^+-ATPase. When 1 mM Cd^{2+} was added to the basolateral surface of A6 monolayers, $\Delta I_{sc(Nys)}$ was 10.4 ± 0.9 µA/cm^2, which was insignificantly different from the control value of 9.2 ± 1.9 µA/cm^2 where nystatin was added to the apical surface after 30 min. (table 5.4). Thus, the results show that *in vitro* measurements of Na^+-K^+-ATPase activity is unaffected by 1 mM Cd^{2+} added to the basolateral surface.

Table 5.4. *Effect of Cd^{2+} on Na^+-K^+-ATPase activity using nystatin-induced I_{sc}. The monolayers were exposed to 1 mM Cd^{2+} for 30 min and then permeabilized by nystatin (300 U/ml) added to the apical surface. The change I_{sc} ($\Delta I_{sc(nys)}$) followed by the addition of nystatin was corrected for the lowest obtainable Na^+-K^+-ATPase activity ($\Delta I_{sc(Oua)}$) achieved by the addition of 100 µM ouabain before measuring $\Delta I_{sc(nys)}$. Data are expressed as mean ±SE.*

	Effect of Cd^{2+} on nystatin-induced I_{sc}		
Treatment	$\Delta I_{sc(Nys)}$ in µA/cm^2	% of control*	n
Control	9.2 ± 1.9	100	4
Cadmium	10.4 ± 0.9	113.0 ± 9.8	6

*All values were corrected for ouabain $\Delta I_{sc(Oua)}$ of 5.4 ± 0.9 (n = 7) before calculation of % of control.

$^{109}Cd^{2+}$ isotope studies (unpublished data)

In a pilot study the compartmentalization of Cd^{2+} in A6 cells was analysed using $^{109}Cd^{2+}$-isotope. $^{109}Cd^{2+}$ of known specific activity was added to A6 cell suspensions at predefined intervals. At a given time surplus of the Cd^{2+}-chelator EGTA was added and the cells washed to stop the flux of $^{109}Cd^{2+}$ (see Methods for further details). The cell suspension was then homogenized and fractionated into a pellet and supernatant fraction. Results of γ-counting the samples are shown in figure 5.14. In the supernatant fraction, the mean of three experiments were 3.3 ± 0.3, 9.7 ± 3.9, 8.8 ± 1.7, 12.6 ± 5.0 and 27.1 ± 17.2 pmol/mg protein for ½, 5, 15, 30 and 60 minutes of exposure, respectively. The corresponding results for the pellet fraction were 3.2 ± 0.4, 11.0 ± 5.1, 8.7 ± 2.7, 15.8 ± 6.3 and 36.5 ± 19.0 pmol/mg protein for ½, 5, 15, 30 and 60 minutes of exposure, respectively. Statistic LSD-test revealed significant difference between ½ and 60 minutes of exposure in the pellet fraction ($p < 0.05$) suggesting that Cd^{2+} primarily accumulates in the plasma membrane within measuring time.

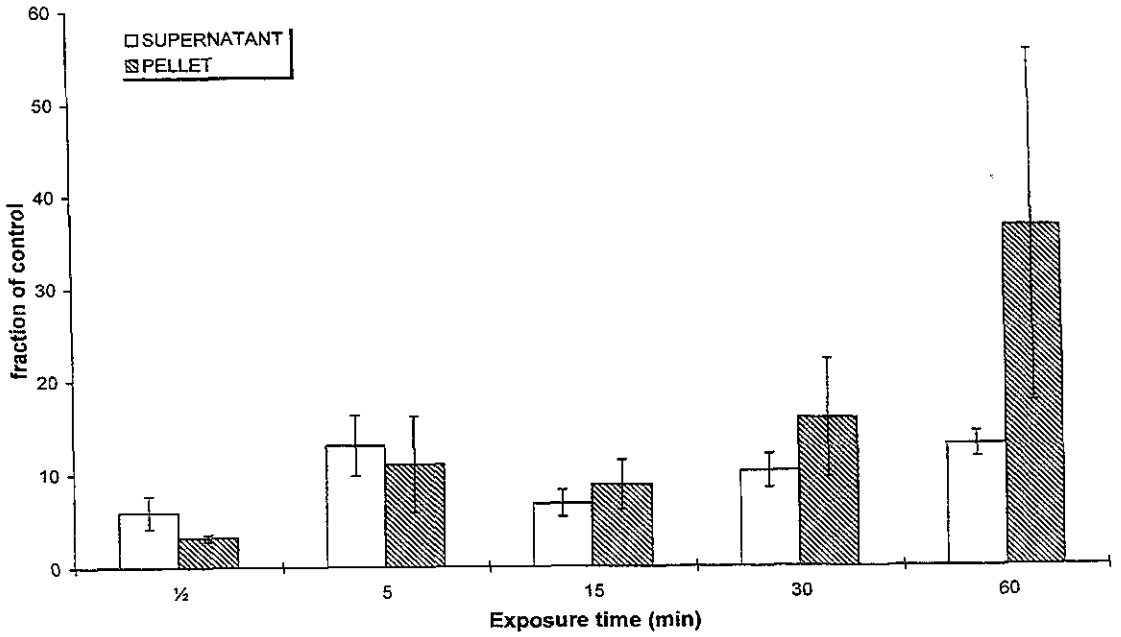

Figure 5.14. *Cd^{2+} accumulation in supernatant and pellet fraction in A6 cell suspensions. Cells were exposed with 400 μM $^{109}Cd^{2+}$ for time periods indicated in the figure. The accumulation is given as pmol Cd^{2+} · mg^{-1} protein and then compared with control level, i.e. no Cd^{2+} exposure (n = 3). Data are expressed as mean ± SE. There was significant difference between ½ and 60 minutes of exposure in the pellet fraction ($p < 0.05$).*

Multi-drug activity in A6 cells (unpublished data)

I a pilot study the Cd^{2+}-specific fluorescence probe, APTRA-BTC/AM, was used to determine transport of Cd^{2+} across A6 epithelial membranes (the loading technique is presented in Methods). Figure 5.15 illustrates a typical response, when APTRA-BTC/AM-loaded A6 cells were exposed to 400 μM Cd^{2+}. Cd^{2+} evoked a prompt increase in fluorescence as expected if Cd^{2+} binds to APTRA-BTC, however, 4.5 mM EGTA could reverse the increase. This indicates that all the dye has been processed (the AM-form does not bind Cd^{2+} - see figure 5.15, inserted) and then transported to the extracellular face, where EGTA, which is membrane impermeable, chelated Cd^{2+} bound to the probe. Multi-drug-resistance proteins (MDR) are known transporters of a variety of agents, including fluorescence dye (Draper *et al.*, 1997; Essodaïgui *et al.*, 1998; Mitsui *et al.*, 1993). Therefore, to decide if MDR-activity was involved in the possible dye extrusion, probenecide and sulfinpyrazone, both known as MDR-inhibitors, were used (Di Virgilio *et al.*, 1990; Gollapudi *et al.*, 1997).When APTRA-BTC/AM and Cd^{2+} were added to cell suspensions a distinct and steady increase in fluorescence was observed (figure 5.16), which was blockable by both probenecide and sulfinpyrazone. Only the time course of probenecide is illustrated in figure 5.16, but the time course for sulfinpyrazone is similar. Moreover, the blocking effect was dose-dependent and IC_{50}-values could be calculated. Thus, the IC_{50}-values corresponded to 685 ± 206 μM (n = 5) and 3.3 ± 0.2 mM (n = 6) for sulfinpyrazone and probenecide, respectively. Overall, this may suggest that the MDR-activity is responsible for the extrusion of APTRA-BTC as will be discussed in a restricted manner in the Discussion due to ongoing patent considerations.

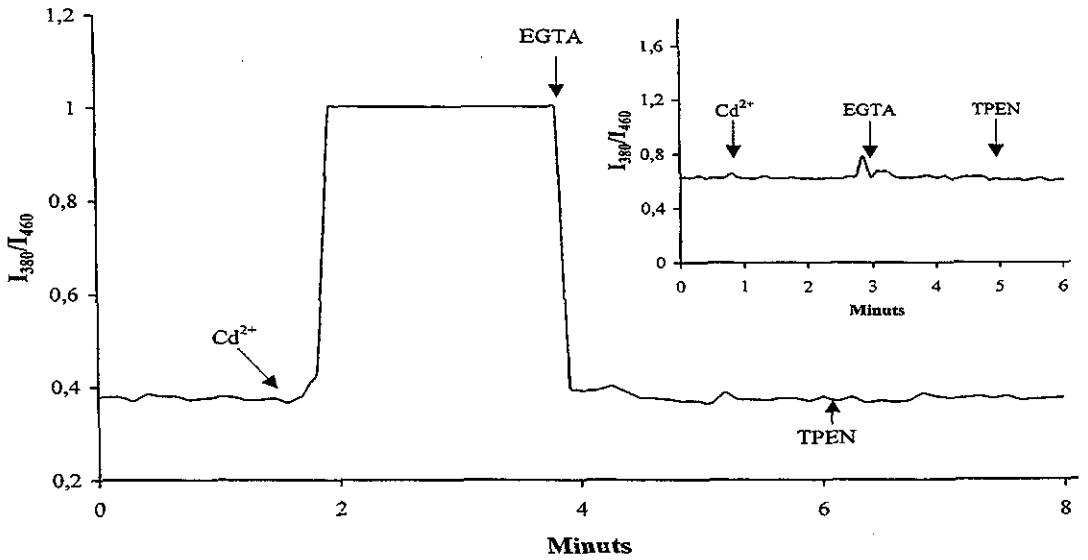

Figure 5.15. Typical recording of fluorescence of APTRA-BTC/AM-loaded cell suspensions. ½ ml cell suspension was incubated for 60 min with 5 µM APTRA-BTC/AM. Fluorescence measured at I_{380}/I_{460} increased promptly when 400 µM Cd^{2+} was added, and was restored by 4.5 mM EGTA. Subsequent addition of the chelator, TPEN (50 µM), did not affect fluorescence indicating that the dye was present in the extracellular phase. Inserted figure: same conditions as described for the main figure but cells were replaced by water. Thus, when cells are absent APTRA-BTC/AM is not cleaved to its active form, APTRA-BTC why addition of Cd^{2+} do not affect fluorescence.

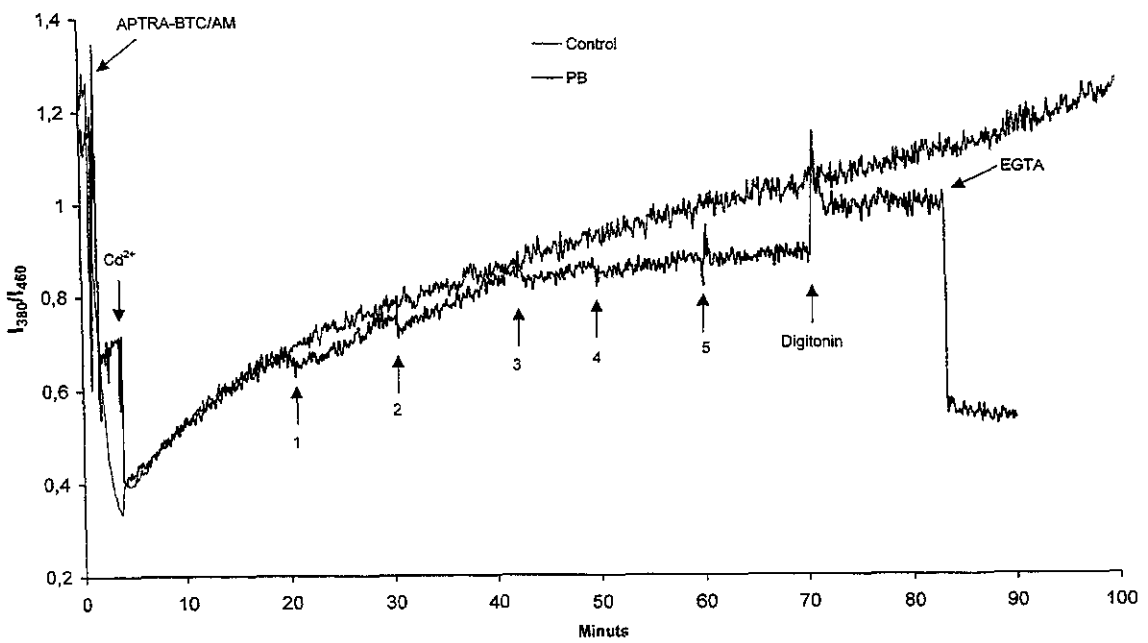

Figure 5.16. Bottom curve: A typical dose-response experiment, where increasing concentrations of the MDR-inhibitor probenecid (PB) is accompanied by decreasing slopes. APTRA-BTC/AM(170 nM) was added to the cell suspension at time zero. Two minutes later 400 µM Cd^{2+} was added, upon which the fluorescence dropped promptly and then increased in intensity, which was blockable by PB. Figures on top of curve correspond to concentrations of PB added in mM. Concentrations of digitonin = 12.5 µM and EGTA = 3.6 mM. Top curve: control experiment. APTRA-BTC/AM and Cd^{2+} were added as indicated but PB was not used.

Cisplatin experiments (IV)

The present results, which are based on collaboration with master students during autumn 1996, will be presented and discussed only shortly. For detailed information please refer to the specific article in the appendix.

Cisplatin is an antitumour agent with extensive nephrotoxicity. Accordingly, the goal of the present study in A6 cells was to clarify the mechanism behind cisplatin induced nephrotoxicity in the distal nephron. I_{50}-measurement revealed that the effects were extremely side-specific, as I_{50}-values were 49 and 540 μM for basolateral or apical 24 h-exposure, respectively. Moreover, I_{sc} declined in a dose-dependent way that for the highest concentration (800 μM) resembled the one observed for ouabain suggesting that cisplatin interferes with the Na^+-K^+-ATPase. Hence, studies of Na^+-K^+-ATPase activity using nystatin (see above for details about the technique) demonstrated that 800 μM cisplatin inhibited the pump by 50% after 60 minutes of exposure.

6. OVERALL DISCUSSION

The present thesis deals with the basolateral effects of cadmium on cellular and cytotoxic mechanisms when administered to renal distal epithelial A6 culture cells. The subject is untraditional in the sense that the thesis focus on basolateral-related cellular events in the distal nephron and not apical-related effects in the proximal nephron as often done. Moreover, rather high doses of Cd^{2+} was used to achieve maximum response. Hence this study can be considered as a "functional study" trying to elucidate mechanisms behind the observed Cd^{2+}-evoked intracellular events, which was only possible using doses near or at the maximum response concentration, i.e. 1 mM Cd^{2+}. Nevertheless, along with the discussion of the above mentioned considerations, the following discussion will also deal with aspects concerning the physiological and pathophysiological relevance of the presented studies.

Human beings are continuously exposed to cadmium, primarily through inhalation and food intake (see chap. 3.2 and 3.3). Measurements between 1983-1987 demonstrated that the average weekly intakes of cadmium among the Danish population was about 140 µg, which corresponds to 30% of PTWI (the Danish EPA, publication No. 187, 1990). Due to variation in the population, the Danish EPA estimates that a small group of Danes have intakes of 50% of PTWI, which the Danish EPA consider to be unacceptably high. Thus, even though Denmark can be considered a "low-level" country due to the absence of important exposure sources of cadmium, e.g. mining, manufactory etc. still some citizens have high exposures not far from the PTWI. Probably, citizens near PTWI should be found among smokers as cigarettes significantly contributes to the overall cadmium intake. Lifelong ingestion and inhalation of cadmium give rice to concern because cadmium accumulates in the organs, especially the kidneys (see chap. 3.4). The kidney plays a very important role in the homoeostasis of electrolytes and water balance and as such clinical symptoms are often related to disturbances of the homoeostatic function of the kidney, e.g. chronic exposures of cadmium among workers leads to proteinuria, hypercalciuria, phosphaturia and recurrent kidney stone formation (see chap. 3.5). Overall, examination of cadmium-related effects are of main interest because of the constant exposure of human beings that in some parts of the world is expected to be near or above the PTWI (see table 3.2), and the fact that the clinical symptoms are more or less known, but the underlying mechanisms are largely unknown. Hence, mechanistic studies of cadmium-induced nephrotoxicity are therefore clearly necessary.

Renal toxicity following prolonged exposure to cadmium is characterized primarily by proteinuria and other disturbances of solute transport that reflect diminished proximal tubule function (Friedman, 1994). In proximal tubule the low molecular weight, Cd-MT, is readily filtered through the glomeruli and taken up by tubular reabsorption whereupon cadmium enters the lysosomes of the tubular cells. Like other proteins, Cd-MT is degraded in the lysosomes and free Cd^{2+} is released to react with sensitive sites in the cell (Nordberg, 1992). Thus, when it comes to cadmium-induced damage in the proximal tubule, the knowledge is present but the intracellular mechanisms needs still to be explored. Contrary to this, the focus on cadmium-induced damage of the distal segment is almost lacking. However, hormonal and pharmacologically regulated transport of solutes (exclusively for Ca^{2+}) and water takes place almost entirely in distal and connecting tubules (see chap. 3.8), which makes the cadmium-distal-interactions even more interesting to explore. Accordingly, studies indicate that cadmium may act as an distal nephron toxicant, e.g.; 1) in immortalized distal convoluted tubule cells cadmium is taken up (Friedman, 1994), 2) Kidney cell lines of proximal (LLC-PK_1) and distal (MDCK) tubular origins exposed to cadmium have also demonstrated that not only the proximal cell line but also, however to a lesser extend, the distal cell line accumulated cadmium (Zhang, 1995), 3) Immunohistochemical

localization of cadmium-induced metallothionein in rat kidney revealed intense staining in the distal tubule that was often more intense than in the proximal tubule (Tohyama, 1988; Zhang, 1995) and 4) Indirect evidence suggests that cadmium may be taken up by distal tubules as *in vivo* studies of cadmium-administered rats demonstrated increased excretion of urinary kallikrein, which is predominantly originates from the distal tubules(Girolami, 1989). Consequently, the small attention this topic has received in general and the important role the distal segment plays in hormonal water and electrolyte regulation, warrant a research on the distal effects of cadmium exposure.

The A6 cell line was used in all studies because of its obvious advantages (see chap. 3.9): 1) A6 cells exhibit morphological and functional properties of the mammalian distal epithelium, 2) A6 cells display active and electrogenic Na^+ and Cl^- ion transport and are sensitive to a variety of hormones, e.g. PTH, aldosterone and antidiuretic hormone, 3) A6 cells are grown at room temperature and 4) A6 cells form a polarised, highly differentiated epithelium with a large transepithelial resistance, R_{te} (> 1000 $\Omega \cdot cm^2$). In contrary to this, all cell lines representing the proximal tubule, e.g. LLC-PK_1, have low R_{te}. Because of high R_{te}, A6 cells are excellent for investigation of ion transport because high R_{te} indicates that the paracellular route is negligible allowing only transepithelial transport to occur. Furthermore, R_{te} serves as a sensitive marker for determination of cell integrity since low levels of R_{te} suggest that tight junctions are leaky or that the cell membranes are being destroyed. Therefore, this renal cell line provides an excellent model for distal tubular cells in the kidney, useful in studies attempting to characterize mechanisms of transepithelial ion transport and hormone action.

It is commonly believed that Cd-MT complex does not react with the basolateral membrane, whereas cadmium bound to e.g. cysteine or mercaptoethanol are responsible for the transfer of cadmium from peritubular blood to renal epithelia by interaction with anionic cadmium-binding sites on the cell membrane possessing much higher affinity for cadmium than does plasma albumin (Foulkes, 1990). Cadmium interactions with the basolateral membrane (see chap. 3.4) is interesting as the basolateral membrane posseses important potential targets for the maintenance of electrolyte and water balance, such as channels and receptors, by which cadmium due to its large affinity for ligands having -SH residues and nucleophilic sites (Jacobsen, 1980) might interact with. Moreover, the blood level of cadmium is homogenous and therefore one must expect that the "load" of cadmium in the distal tubule equals the exposure in the proximal tubule. Consequently, it was decided to focus on characterizing the mechanisms behind basolateral Cd^{2+} exposure only.

The findings suggest that the basolateral membrane is far more sensitive to Cd^{2+} exposure than the apical membrane since basolateral Cd^{2+} caused I_{sc} to increase in a transient and prompt manner that was not observed when applied to the apical side. Moreover, $\Delta I_{sc(Cd)}$ was dose-dependent with a maximal stimulation concentration at 1 mM. The side-specific effect is consistent with cell integrity studies, where basolateral Cd^{2+} exposure lowered R_{te} at much lower doses than observed when Cd^{2+} was applied to the apical surface. Similar results were observed in other epithelial cell lines such as Caco-2 (Rossi, 1996) and LLC-PK_1 (Bruggerman, 1992), but with other endpoints than R_{te}. The heterogenous effects on basolateral and apical I_{sc} and R_{te} suggest different mechanisms by which Cd^{2+} may disturb ion transport capacity and cause cytotoxic effects in A6 cells.

One of the major goals of the present thesis was to identify the cellular mechanisms behind the distinct $\Delta I_{sc(Cd)}$. The observed positive I_{sc}-deflection upon Cd^{2+} treatment of A6 cells is caused by either Na^+ reabsorption or Cl^- secretion. The ionic nature behind $\Delta I_{sc(Cd)}$ was examined using amiloride, a Na^+ channel inhibitor. Preexposure to amiloride demonstrated that $\Delta I_{sc(Cd)}$ was

undiminished showing that Na^+ transport was not involved in $\Delta I_{sc(Cd)}$. Thus, in order to determine if the Cd^{2+}-mediated positive I_{sc}-deflection was due to Cl^- secretion, Cl^- depletion and various Cl^- channel inhibitors were taken into use. Cl^- depletion and practical all the used inhibitors reduced $\Delta I_{sc(Cd)}$ compared with control level, which indirectly proves that Cl^- transport is involved in $\Delta I_{sc(Cd)}$. The two fenemates, FFA and NFA both significantly reduced $\Delta I_{sc(Cd)}$ with FFA being the most potent inhibitor of all tested inhibitors. Direct measurement of Cl^- transport was performed using the Cl^--sensitive fluorescent probe, SPQ to extend and confirm the obtained I_{sc}-results. Work under Cl^--free conditions was necessary to obtain maximal driving force for Cl^- as also proposed by (Scott *et al.*, 1995). One reasonable explanation for the lack of responsiveness during normal physiological conditions, i.e. in the presence of NRS, is the transient nature of Cd^{2+}-activated Cl^- transport by which only small amounts of Cl^- leave the cells, probably far below the detection level with SPQ.

In the present studies Cd^{2+} evoked an increase in Cl^--secretion measured as $\Delta F/F_0([\Delta Cl^-]_{Cd})$, which significantly exceeded the basal Cl^--secretion. Moreover, $\Delta F/F_0$ rapidly reached a plateau level suggesting that the kinetic is fast consistent with the kinetics in I_{sc}-experiments. However, under similar conditions, i.e. in the presence of Cl-free Ringer, no Cd^{2+}-evoked I_{sc}-transient was observed. The most plausible explanation for the conflicting results is that the cells were bathed in Cl^--free solution for more than 25 minutes before measuring $\Delta I_{sc(Cd)}$. In contrast, determination of $[\Delta Cl^-]_{Cd}$ took place within minutes after starting the Cl^--free protocol. Therefore, the intracellular Cl^- content resembles to some extend the physiological level. Preexposure with either FFA or NFA totally blocked the Cd^{2+}-induced Cl^--secretion without affecting the level of maximal fluorescence (figure 5.5). This shows that plenty of Cl^- ions were trapped inside the cells and that Cd^{2+} could not activate Cl^--exit due to the blockage of the apical Cl^--channels by the fenemates. Thus, the I_{sc}- and SPQ-results strongly indicate that Cd^{2+}-stimulated active ion transport indeed involves transepithelial Cl^-secretion. Only few papers have dealt with the effects of Cd^{2+} exposure on Cl^- transporting epithelia cells and to my knowledge no one has tried to measure Cd^{2+}-evoked Cl^--transport with fluorescence techniques. However, Cd^{2+} has been shown to evoke Cl^--secretion in shark rectal gland epithelia via cAMP-dependent mechanisms (Forrest *et al.*, 1997) and in rat colon epithelia via prostaglandines (Böhme *et al.*, 1992).

Among secretory chloride channels two main groups have been described, namely Ca^{2+}- and cAMP-regulated channels (Cliff & Frizzell, 1990; Greger, 1996; Guggino, 1994; Simmons, 1993). Apparently, two types (3-pS and 8-pS) of apical chloride channels controlled by Ca^{2+} and/or cAMP contribute to the transcellular chloride transport pathway in A6 cells (Marunaka, 1990; Marunaka, 1993; Shintani & Marunaka, 1996; Zeiske *et al.*, 1998). Since FFA and NFA, both known as inhibitors of Ca^{2+}-activated Cl^- channels (White, 1990), were the most potent inhibitors of $\Delta I_{sc(Cd)}$ and Ca^{2+}-induced activation of chloride secretion usually results from activation of apical Cl^- channels (Niisato & Marunaka, 1997), the involvement of intracellular Ca^{2+} in $\Delta I_{sc(Cd)}$ was investigated.

Preliminary I_{sc}-studies revealed that intracellular Ca^{2+} might be an important second messenger in $\Delta I_{sc(Cd)}$ as calcium depletion significantly reduced $\Delta I_{sc(Cd)}$ compared with control. Ca^{2+} mobilization evoked by TG and A23187 almost cancelled $\Delta I_{sc(Cd)}$. Furthermore, Cd^{2+} and TG could neutralize each other since neither Cd^{2+} nor TG could stimulate I_{sc} further when preexposed to the counterpart. Similar responses were obtained in SPQ-loaded cells as TG and Cd^{2+} also could neutralise the response of the counterparts. Thus, indirect evidence suggests that Ca^{2+}-mobilization is involved in $\Delta I_{sc(Cd)}$ why direct measurements of intracellular Ca^{2+} using fura-2 was implemented to further characterize Cd^{2+}-mediated intracellular events.

Measuring effects of Cd^{2+} and other divalent ions on intracellular Ca^{2+} homoeostasis using fura-2 can be hampered by the fact that Cd^{2+} also binds to the probe and mimic the effects of Ca^{2+}-binding to the probe (Hinkle, 1992). However, this requires that cadmium enters the cell in its free form. Therefore, the cell suspensions were pre-loaded with the membrane permeable heavy metal chelator TPEN. A pilot study showed that TPEN is actually able to chelate Cd^{2+} when the membranes are made permeable to Cd^{2+}. Moreover, addition of EGTA demonstrated that fura-2 was not present in the extracellular phase. Otherwise EGTA would, under those conditions, cause fluorescence to decrease immediately. This is expected as the cell suspensions were pre-loaded with probenecide, known as an inhibitor of the organic-anion transporter responsible for dye extrusion (Di Virgilio *et al.*, 1989; Di Virgilio *et al*, 1990; McDonough & Button, 1989). In fact, another pilot study using the fluorescent probe APTRA-BTC/AM has shown that probenecide in a dose-depended way abolished the dye extrusion why similar effect on fura-2 extrusion is to be expected. Accordingly, the leak rate of the fura-2 was estimated to be considerably lower than previously reported in A6 cells (Brochiero & Ehrenfeld, 1997) indicating that probenecid actually reduces the leakage rate.

Interestingly, using APTRA-BTC/AM, which is a specific Cd^{2+} (and Zn^{2+}) probe, to detect Cd^{2+}, offered no evidence for intracellular Cd^{2+} (figure 5.15). This suggests that perhaps Cd^{2+} does not pass the cell membranes in A6 cells within the time of measurements. In fact, pilot isotope studies support this idea as there was no significant difference in accumulation of Cd^{2+} in the cell supernatant, whereas the accumulation was significantly higher in the pellet after 60 minutes of exposure. Thus, the cell membranes of A6 cells might act as a barrier for Cd^{2+} intrusion ensuring, in combination with TPEN pre-loading, that Cd^{2+} does not interact with the fura-2-Ca^{2+}-complex. Evidence for that is strong as outlined in the discussion of manuscript VII, e.g. 1) Cd^{2+} evoked an immediate transient increase in fluorescence that is not to be expected if Cd^{2+} binds to the probe since the fluorescence would remain at high level as observed in ionomycin treated cells, 2) Addition of the heavy chelator, TPEN, showed no effect on $[Ca^{2+}]_{Cd}$ as expected if Cd^{2+} were bound to the probe, 3) Dose-response experiments revealed effects only above 10 μM. If an intracellular Cd^{2+}-fura-2-complex was present maximum intensity was obtained at much lower concentrations (500 nM Cd^{2+} gave maximum binding of fura-Na in pilot experiments), 4) Preexposure with the non-autofluorescence agents neomycin, TMB-8 and TG abolished the Cd^{2+}-evoked fluorescence intensity (figure 5.9), which would not occur if Cd^{2+} binds to the probe, 5) Depleting the cells for Ca^{2+} using TG reduced $[Ca^{2+}]_{Cd}$ significantly, 6) The observed Cd^{2+}-evoked Ca^{2+}-transients measured with fura-2 resemble Cd^{2+}-evoked Ca^{2+}-transients measured with $^{45}Ca^{2+}$ (Smith, 1989). In the light of this, it can be concluded that the observed effects on fluorescence in fura-2-loaded cells caused by extracellular Cd^{2+} are actually due to Ca^{2+}-mobilization and not the binding of Cd^{2+} to the probe.

It was found that Cd^{2+} evoked a Ca^{2+} transient in a hormone-like fashion, which has also been observed in human fibroblasts (Smith, 1989) and E367 neuroblastoma cells (Benters, 1997). Since no sustained elevation of the resting $Ca^{2+}{}_i$ was observed the possibility that Cd^{2+} simply interferes with the control of Ca^{2+} fluxes from outside the cells can be excluded. Furthermore, the very fast response (15 ± 1 sec) argues against physico-chemical interaction of Cd^{2+} with intracellular enzymes, e.g. PLC or Ca^{2+}-ATPases because such effects would require penetration of Cd^{2+} through the plasma membrane, which is slow. Moreover, inhibition of Ca^{2+} extruding systems often results in a sustained elevation of $Ca^{2+}{}_i$, which is not consistent with the transient nature observed in our studies. Measurements of the Na^+-K^+-ATPase activity using the nystatin technique supports this as Cd^{2+} did not inhibits the Na^+-K^+-ATPase activity in A6 cells, which is

indirectly responsible for Ca^{2+}-extrusion via the Na^{+}-Ca^{+}-exchanger (Friedman, 1998; White *et al.*, 1996).

To define the origin of the Ca^{2+}-release caused by Cd^{2+}, TG (and TMB-8) was applied to the cell suspensions. Consequently,$[\Delta Ca^{2+}]_{Cd}$ was almost annulled in cells pretreated with both TG and TMB-8 (VII). The $Ca^{2+}{}_{i}$-level was sustained when A6-cells were exposed to TG and subsequent addition of Cd^{2+} showed significant lower $Ca^{2+}{}_{i}$ than what was observed in control cells indicating that intracellular pools are the main source of $[Ca^{2+}]_{Cd}$. Subsequent addition of TG to Cd^{2+}-pretreated cells proved no significant difference in TG-amplitude compared with TG-control level suggesting that Cd^{2+}, probably due to the fast and transient nature of $[Ca^{2+}]_{Cd}$ does not empty the IP_3-sensitive $Ca^{2+}{}_{i}$ stores. Interestingly, the kinetic and dose-response characteristics of $[Ca^{2+}]_{Cd}$ correspond with those previously observed under similar conditions in I_{sc}-experiments (see figure 5.9 and inserted figure). Accordingly, the same kinetics and dose-response between I_{sc}-experiments and fura-2-experiments strongly suggest that Cd^{2+}-evoked Cl^{-}-secretion and $Ca^{2+}{}_{i}$-mobilization are closely connected. However, the fact that TG is unable to provoke further increases in I_{sc} in Cd^{2+}-treated A6 cells, but able to increase $Ca^{2+}{}_{i}$ further following Cd^{2+} treatment suggests that Cd^{2+}-mediated Cl^{-}-channels responsible for Cl^{-}-secretion become desensitized. Overall, it can be concluded that $[Ca^{2+}]_{Cd}$ originated from intracellular stores.

Transient Ca^{2+} responses are often caused by hormone stimulation, which involves binding of the agonist to its plasma membrane receptor, activation of the G-protein coupled PLC, resulting in generation of IP_3 and diacylglycerol (for reviews see Berridge, 1997; Clapham, 1995; Iino, 1999). Thus, to investigate if $[Ca^{2+}]_{Cd}$ involves hormonal signalling, experiments with the two PLC-inhibitors U73122 and neomycin were performed. I_{sc}-experiments revealed that U73122 could cancel $\Delta I_{sc(Cd)}$ whereas neomycin could only cancel $\Delta I_{sc(Cd)}$ at lower doses of Cd^{2+}. Contrary to the I_{sc}-experiments, U73122 could only abolish $[\Delta Ca^{2+}]_{Cd}$ at 100 μM Cd^{2+} whereas at 400 μM Cd^{2+} the cancellation, though significant, was partial (VII). This paradox is difficult to explain, but it may be due to different experimental setups as I_{sc}-experiments were measured on confluent cells and the fura-2-experiments were measured on cell suspensions. To address this topic further studies are necessary. Nevertheless, at 100 μM Cd^{2+} the fura-data are in accordance with the I_{sc}-experiment, which supports that Cd^{2+}-transients are a result of receptor-interactions that relies on PLC-activation. Besides being used as PLC-inhibitor, neomycin is also a well-known CaR-agonist (Hammerland *et al.*, 1999; Spurney *et al.*, 1999; Ye *et al.*, 1996). However, the fact that neomycin only inhibits $\Delta I_{sc(Cd)}$ at lower doses suggests that neomycin may function as a CaR-modulator rather than a PLC-inhibitor in A6 cells. This is in accordance with the idea that Cd^{2+} at a high dose probably displaces neomycin from the CaR as would be postulated if Cd^{2+} too functions as a CaR-agonist in A6-cells. In addition, the fact that Cd^{2+} selectively causes I_{sc} to increase at the basolateral surface suggests that the mechanism for triggering $\Delta I_{sc(Cd)}$ and $[\Delta Ca^{2+}]_{Cd}$ is due to extracellular events. Otherwise membrane penetration of Cd^{2+}, e.g. by diffusion, would cause similar responses at both cell surfaces. Therefore, if Cd^{2+} serves as an agonist of CaR, the receptor would necessarily have to be located at the basolateral surface. In fact, in the distal segment of rat kidney cells CaR was exclusively located at the basolateral surface (Riccardi *et al.*, 1998).

The CaR is unique in the sense that the physiological ligand is an inorganic ion, rather than an organic molecule. Activation of the receptor by increased levels of extracellular Ca^{2+} results in the breakdown of phosphoinositide 4,5-diphosphate by PLC and the formation of IP_3 and diacylglycerol. The resultant increase in levels of IP_3 mobilizes intracellular Ca^{2+} from the endoplasmic reticulum (ER). CaR presumably recognizes other divalent cations than Ca^{2+} and even polycations such as neomycin as mentioned (Brown, 1991) above. Previously studies have shown that Cd^{2+} and other divalent metals mobilized cell Ca^{2+} in human skin (Smith, 1989), in

E367 neuroblastoma cells (Benters, 1997) and bovine chromaffin cells (Yamagami *et al.*, 1998) via an increased generation of IP_3. Furthermore, the divalent metals appeared to trigger Ca^{2+}-mobilization via a reversible interaction with an external site on the cell surface, which the authors referred to as a "Cd^{2+}-receptor". Thus, PLC-inhibitor experiments point in the direction that PLC plays an important role for triggering $\Delta I_{sc(Cd)}$ and $[\Delta Ca^{2+}]_{Cd}$. Thus, the possible involvement of CaR was examined by measuring its second messenger, IP_3, directly. When A6 cell suspensions were exposed for 60 sec with 400 μM Cd^{2+} the concentration of intracellular IP_3 underwent a 1.45-fold increase proportional to the resting level, which is very similar to ratios reported in the studies listed above. In addition, preexposure to the U73122 completely abolished IP_3-generation stimulated by Cd^{2+} suggesting that U73122 likely inhibits PLC. Therefore, it seems very likely that Cd^{2+} causes Ca^{2+}-transients via the IP_3 signalling pathways. Taken together, direct measurements of IP_3 -generation and the Cd^{2+}-TG-interactions described above, suggest that $\Delta I_{sc(Cd)}$ and $[\Delta Ca^{2+}]_{Cd}$ involves IP_3-generation. This might go through the activation of CaR as it is likely that CaR is present in the basolateral membrane of A6 cells since the natural agonist, Ca^{2+}, also stimulated IP_3-generation, which significantly exceeded the control level.

Several studies have demonstrated that metals with similar chemical characteristics as Cd^{2+} are protective against biochemical and toxic effects of Cd^{2+} in a competitive manner (Benters, 1997; Blazka & Shaikh, 1992; Endo, 1996; Smith, 1994; Tang *et al.*, 1998). Both Zn^{2+} and Ni^{2+} induced Cl^--secretion with Zn^{2+} being most potent. Preexposure to Zn^{2+} or Ni^{2+} prevented $[\Delta Cl^-]_{Cd}$, which was comparable with the inhibiting actions of the fenemates. This observation demonstrates that Ni^{2+} and Zn^{2+} abolish $[\Delta Cl^-]_{Cd}$ completely probably due to similar mechanisms in A6 cells. Since Cd^{2+}-induced Cl^- secretion and Ca^{2+} mobilization probably are closely connected, the relationship between Zn^{2+}/Ni^{2+} and Ca^{2+}-mobilizations was examined. Both metals induced Ca^{2+}-mobilization in a Cd^{2+}-like fashion, i.e. they too displayed transient characteristics with very fast kinetics that resembled those obtained in I_{sc}-experiments. In fact, both metals were more potent inducers of $Ca^{2+}{}_i$ displaying significant higher peak levels than Cd^{2+}. In contrast, only Cd^{2+} induced an increase in $Ca^{2+}{}_i$ in E367 neuroblastoma cells whereas Zn^{2+} caused no change in $Ca^{2+}{}_i$ (Benters, 1997). Pretreatment with either Zn^{2+} or Ni^{2+} prevented $[\Delta Ca^{2+}]_{Cd}$ normally observed with Zn^{2+} being the most potent cancelling metal. These data confirm and extend the previous findings in the sense that the similar metals Cd^{2+}, Zn^{2+} and Ni^{2+} shares similar mechanisms regarding the ability to evoke Ca^{2+} transients and resulting Cl^--secretion in A6 cells. Could this also be due to the activation of the CaR as observed for Cd^{2+}? In human skin fibroblasts (Smith, 1989), bovine chromaffin cells (Yamagami *et al.*, 1998) and HEK 293-cells (Spurney *et al.*, 1999) divalent metals, other than Cd^{2+}, displayed Ca^{2+} mobilizing abilities that depended on IP_3-generation. Accordingly, Zn^{2+} and Ni^{2+}at 400 μM, like Cd^{2+}, could induce IP_3-generation significantly above control level and in accordance with their ability to induce $Ca^{2+}{}_i$-transients. Thus, it is likely that Zn^{2+} and Ni^{2+} share common mechanisms with Cd^{2+}, as the effects on I_{sc}, $Ca^{2+}{}_i$ and IP_3-generation were very similar, and as Zn^{2+} and Ni^{2+} could completely abolish Cd^{2+}-mediated effects. In fact, Zn^{2+} and Ni^{2+} have previously been proposed as CaR-agonists (Dwyer *et al.*, 1991; Shankar, Huang, Adebanjo, Simon, Alam, Moonga, Pazianas, Scott, & Zaidi, 1995), which therefore can account for the observed effects in A6 cells. Moreover, Mn^{2+} was used as a fura-2-quencher, however, when applied at high doses (10 mM) $Ca^{2+}{}_i$-peaks like those observed for the heavy metals were observed. Hence, the CaR potentially present in A6 cells presumably recognizes other cations than Ca^{2+}, and is apparently activated by a broad range of divalent metals including Ni^{2+}, leading to hormone-like Ca^{2+}-transients. Results presented in manuscript VIII indicate that Ni^{2+} probably is a "cleaner" agonist than Cd^{2+} as side-effects such

as capacitative calcium/cadmium entry (stimulation of Ca^{2+} channels when emptying intracellular Ca^{2+} stores) is not observed when Ni^{2+} is applied to A6 cells.

Activation of the CaR leads to a variety of biological activities caused by the subsequent activation of PKC and increased Ca^{2+}_i. However, one consequence of CaR-activation is inactivation of cAMP-dependent responses. Therefore, a physiological response upon CaR-activation is reduced water reabsorption due to reduction in cAMP levels, which serves as a second messenger for the antidiuretic hormone (see chap. 3.6). Thus, if Cd^{2+} serves as a CaR agonist one would expect Cd^{2+}, besides the effects described above on Ca^{2+}_i and IP_3-generation, to diminish the AVT-response. In fact, Cd^{2+} inhibited the AVT-induced increase in I_{sc}, which could not be caused by inhibition of the Na^+-K^+-ATPase as Cd^{2+} did not inhibit the transporter. Furthermore, the results showed that PDE-activity was unaffected, whereas cAMP production was reduced due to inhibition of AC-activity, which is a typical response upon CaR-activation.

Overall, from a physiological and pathophysiological point of view basolateral exposure of cadmium at the distal nephron is of interest due to: 1) equal proximal/distal "load" of cadmium as mentioned earlier. 2) The present results show that cadmium causes side-specific effects both in I_{sc}- and cytotoxic experiments, which are far more pronounced when cadmium is administered to the basolateral surface (Faurskov & Bjerregaard, 1997). 3) Traditionally, the proximal tubule is regarded as the main site of cadmium-mediated nephrotoxicity. Effects at this site are probably quantitatively most important. However, the distal nephron and the collecting duct are the main sites for hormonal regulation of ions (exclusively for Ca^{2+}-transport) and water transport. 4) One can argue that the doses used are unphysiologically high as $H_{0.5}$ was approximately 400 μM. Dose-response experiments have, however, revealed responses at doses as low as 1 μM Cd^{2+}, and that cadmium at 1 μM also could inhibit AVT-stimulated I_{sc} (Bjerregaard & Faurskov, 1997). Reported cadmium-blood levels for exposed workers lie generally between 5 and 50 μg/l (corresponding to 44 and 444 nM Cd^{2+}), but after extremely high exposures, blood levels as high as 300 μg/l (2.7 μM) were reported (see chap. 3.3). In blood, cadmium is bound to metallothionein and small ligands such as cysteine, glutathione, mercaptoethanol or albumin (Foulkes, 1990). A potential cellular target for cadmium could be the CaR since it contains highly conserved extracellular cysteine residues, which is believed to be involved in selective binding of divalent cations (Ray *et al.*, 1999; Ward *et al.*, 1998). Thus, the effects of cadmium are a results of the balance between affinities of cadmium bound to blood and membrane ligands. Accordingly, Cd^{2+} induced Ca^{2+}_i-transients in μM-range, which is far below the physiological range of the CaR-agonist, Ca^{2+}_o which works in mM-range indicating that Cd^{2+}-affinity towards the CaR is very high.

Hence, effects were observed under acute conditions that are not far from physiological blood concentrations of cadmium. The major effect of cadmium might, however, be when the distal part is exposed chronically and by that disturbing the Ca-homeostasis, hormonal regulation of water and electrolytes. This could lead to calcuria, osteoporosis and in severe cases to kidney-stone formation, which are well-known diseases accompanied chronic environmental exposure of cadmium (Järup *et al.*, 1998; Savolainen, 1995; Staessen *et al.*, 1991) and observed in patients suffering from an inherited human disorder of Ca^{2+} homoeostasis caused by CaR-overactivity (Brown, 1999; Pollak *et al.*, 1994).

7. CONCLUSION

Convincingly, the model for CaR-activation proposed by Hebert & Brown (Hebert & Brown, 1995) (figure 3.3) fits almost entirely with the results obtained in this thesis, which support the hypothesis that the CaR recognizes Cd^{2+}, and probably also Zn^{2+} and Ni^{2+}, as agonists leading to biological activities in A6 cells summarized below (see also figure 7.1).

The results indicate that an extracellular cation-sensing receptors may be present in the basolateral membrane of A6 cells, which is activated by extracellular Cd^{2+}. In previous reports, this receptor has been referred to as a "Cd^{2+}-receptor". It is, however, possible that the newly discovered calcium sensing receptor, CaR, is responsible for the observed effects, which is supported by the fact that CaR recognizes many other cations than Ca^{2+}, e.g. Mg^{2+}, Gd^{3+} (for reviews see (Chattopadhyay *et al.*, 1998; Hebert & Brown, 1995). Also, neomycin, which is often regarded as a CaR-agonist, extensively affected both $\Delta I_{sc(Cd)}$ and $[\Delta Ca^{2+}]Cd$. Additionally, the mechanism by which Cd^{2+} affects the Ca^{2+} homoeostasis is hormone-like due to the prompt and transient nature of $[\Delta Ca^{2+}]_{Cd}$ and not caused by inhibition of Ca^{2+}-ATPases, which would elicit a sustained Ca^{2+}-level. Furthermore, the I_{sc}-results suggest a polarized localization of the possible CaR, because Cd^{2+}-evoked I_{sc}-transient was observed only when Cd^{2+} was added to the basolateral surface of A6-cells. Moreover, an early event upon activation of CaR is the generation of IP_3 via PLC. All the tested cations provoked IP_3-generation that exceeded the control level. The PLC inhibitor, U73122, altered $[\Delta Ca^{2+}]_{Cd}$ and was able completely to cancel the Cd^{2+}-mediated IP_3-generation. Additional experiments with TG support the idea that Cd^{2+} (and Zn^{2+} and Ni^{2+}) provokes Ca^{2+} transients via IP_3-generation originating from ER, because TG-pretreatment significantly lowered Cd^{2+}-induced Ca^{2+}-mobilization. TMB-8 exhibited an even more pronounced cancelling effect on Cd^{2+}-evoked Ca^{2+}-transients, however, due to nonspecific effects, the origin of the TMB-8-related effects is difficult to pinpoint (VII). Finally, pretreatment with Zn^{2+} and Ni^{2+} completely abolished $[\Delta Ca^{2+}]_{Cd}$ suggesting that they too probably rely on the same mechanisms as Cd^{2+} in A6 cells.

Thus, it can be concluded that the obtained results confirm our previous observations that Cd^{2+} and possible also Zn^{2+} and Ni^{2+} mobilize intracellular Ca^{2+}, probably through the activation of an external receptor, which most likely is the CaR, leading to PLC-mediated IP_3-generation that stimulates TG-sensitive ER to release Ca^{2+} from its stores. Interestingly, the kinetics and dose-response characteristics of $[\Delta Ca^{2+}]_{Cd}$ correspond with those previously observed under similar conditions in I_{sc}-experiments. Moreover, these I_{sc}-experiments showed that the Cd^{2+}-transient consisted of Cl^--secretion entirely. Accordingly, the same kinetics and dose-response between I_{sc}-experiments and fura-2-experiments strongly suggest that Cd^{2+}-evoked Cl^--secretion and $Ca^{2+}{}_i$-mobilization are closely connected. However, the fact that TG is unable to provoke further increases in I_{sc} in A6 cells during Cd^{2+} exposure, but able to increase $Ca^{2+}{}_i$ further after pretreatment with Cd^{2+} suggests that Cd^{2+}-mediated Cl^--channels responsible for Cl^--secretion become desensitized. The transient increase of $Ca^{2+}{}_i$ is therefore likely to activate Ca^{2+}-sensitive Cl^--channels in the apical membrane of A6 cells leading to transcellular Cl^--secretion. Similar results have been obtained in RaKCaR cRNA-injected *Xenopus* oocytes, which responded to extracellular Ca^{2+}, Mg^{2+}, Gd^{3+} and neomycin with a characteristic activation of IP_3-dependent, intracellular Ca^{2+}-induced Cl^--secretion (Riccardi, 1995). Furthermore, extracellular cadmium and calcium both interferes with the hormonal regulation of electrolytes in the distal nephron since it has been shown that $Ca^{2+}{}_o$ decrease ADH-induced chloride transport by inhibiting cAMP pathway in rat kidney (De Jesus Ferreira & Bailly, 1998) in same way that Cd^{2+} did in A6 cells (Bjerregaard & Faurskov, 1997).

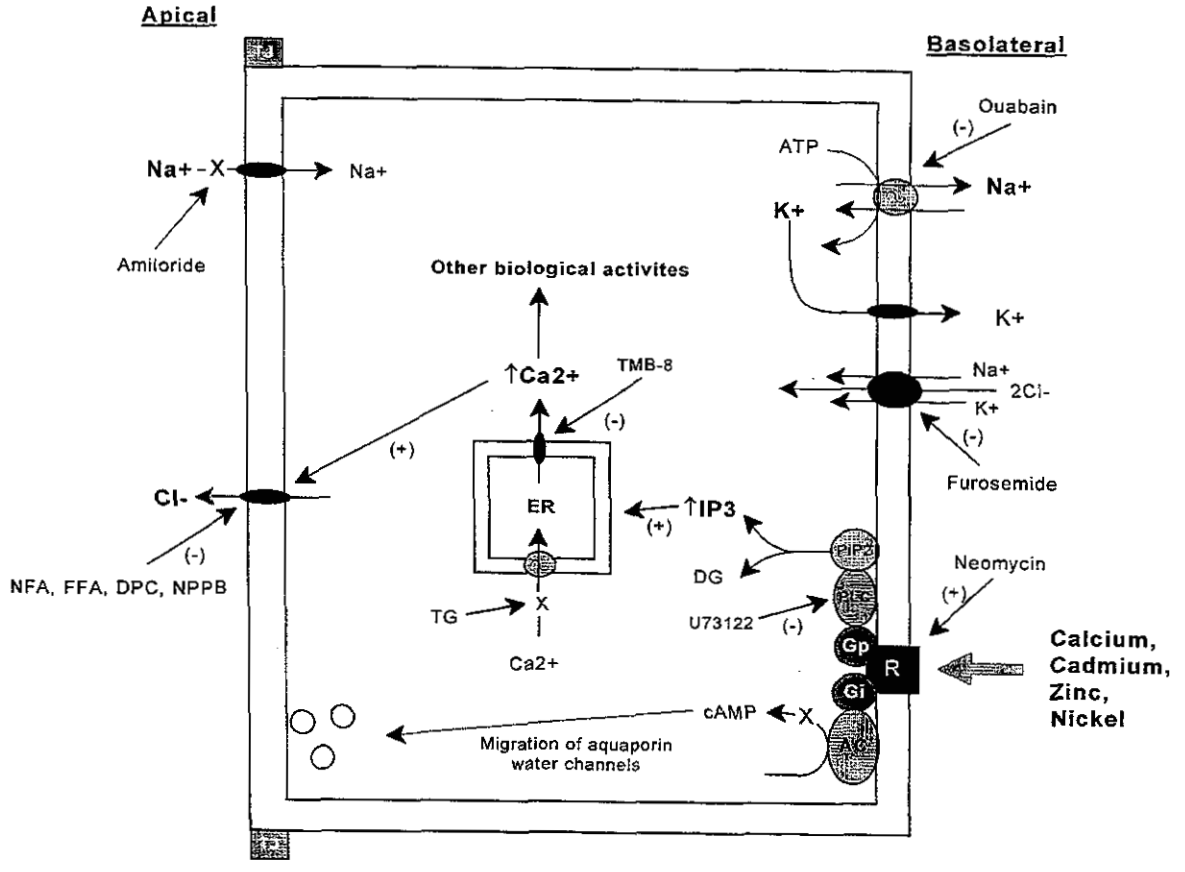

Figure 7.1. A model illustrating the manner in which cadmium, zinc and nickel act as extracellular messengers for the calcium-sensitive receptor (CaR). Activation of the CaR, by binding to negatively charged regions, activates phospholipase C (PLC) leading to increased levels of intracellular diacylglycerol (DG) and inositol 1,4,5-triphosphate (IP_3), and concomitant release of Ca^{2+} from internal stores. Activation of the CaR also reduces cAMP-levels by inhibition of adenylate cyclase (AC)-activity. The Cd^{2+}-induced changes in the activities of second messenger systems alter the biological activities of the cell, e.g. activation of apical Cl^- channels leading to transmembrane Cl^- secretion, reduced AVT-response leading to diminished water and electrolyte uptake. Long-term effect could be destabilisation of tight-junctions leading to reduced R_{te}, disturbances of water and electrolyte balance (especially Ca^{2+} in the distal nephron) and eventually cell death through induction of apoptosis. (-) and (+) indicate inhibitory or stimulative action of the particular test agent.

In figure 7.1, proposed mechanisms behind Cd^{2+}-mediated effects in A6 cells are summarized. In summary, the results indicate that an extracellular cation-sensing receptor may be present in the basolateral membrane of A6 cells, which is activated by extracellular Cd^{2+} and possible also Zn^{2+} and Ni^{2+}. Activation of the CaR leads to increased formation of IP_3 and subsequently release of Ca^{2+} from ER. Moreover, CaR-activation suppress cAMP pathway, which reduces the overall ADH-response. $\Delta[Ca^{2+}]_{Cd}$ then activates Ca^{2+}-sensitive Cl^--channels in the apical membrane of A6 cells leading to transcellular Cl^--secretion. Long-term effects caused by excessive Cd^{2+} concentrations leads to destabilisation of tight junctions and by that lowering R_{te} as observed in IC_{50}-measurements. Later, Cd^{2+}-mediated Ca^{2+}-disturbances may lead to cell death by induction

of apoptosis, as Ca^{2+}_i plays an important role in the transduction of apoptogenic signals (see section 3.6). However, the importance of cadmium-mediated disturbances of distal nephron functions at subtoxic doses may be underestimated because of overwhelming proximal tubule damage and that disturbances of calcium homoeostasis and water/electrolyte balance in the distal tubule cause nonspecific symptoms, the origin of which is difficult to decide. Overall, it is suggested that distal tubule nephrotoxicity may be a part of overall renal cadmium toxicity leading to clinical symptoms related to disturbances of calcium homoeostasis in the distal nephron.

8. PERSPECTIVES

It is suggested that cadmium (and zinc and nickel) acts as a CaR-agonists in A6-cells leading to intracellular Ca^{2+}mobilization and subsequently activation of apical chloride channels and AVT-response. However, this hypothesis calls for supplementing studies as proposed below;

1. In the present study inorganic cadmium was used, however, using inorganic cadmium does not reflect the *in vivo* conditions as cadmium has high affinity towards proteins such as MT, albumin, sulfhydryl groups etc. and therefore mainly exists as stabile ligand-cadmium complexes in blood. The optimal experimental *in vitro* condition would be to perform the experiments in the presence of serum or albumin and/or the use of Cd-MT. However, like in most other *in vitro* studies, experiments were performed under serum-free conditions to avoid the presence of unknown substances that could lead to incontrollable conditions and subsequently misinterpretations of obtained results. Nevertheless, supplementary *in vitro* experiments using serum, albumin or Cd-MT are necessary to perform in future.

2. This study has focussed on short-term effects, but exploring long-term effects would perhaps tell more about cadmium as a distal nephron toxicant as damage to this nephron segment can be difficult to detect in short-term. Moreover, long-term effects should be supplemented with *in vivo* studies, e.g. determination of urinary Ca^{2+} and kallikrein excretion, to explore the physiological relevance of cadmium as a distal nephron toxicant.

3. The studies indicate that Cd^{2+} hardly transverse the membrane of A6 cells - at least within 60 minutes of exposure. However, direct evidence for cadmium transport could be elucidated using the Cd^{2+}-specific probe, BTC-5N, which is more sensitive and selective to Cd^{2+} than the used APTRA-BTC/AM. This would also bring in a more direct evidence of no Cd^{2+}-fura-2-interaction that presently is based upon indirect evidence although it seems massive.

4. The results imply that the CaR is present in the basolateral membranes of A6 cells, however, direct evidence is necessary to be certain. This could for instance be accomplished by using the PCR-technique. Moreover, CaR-transfection of *Xenopus laevis* eggs could lead to functional studies of the substrate specificity of the CaR derived from A6 cells and actually prove if Cd^{2+} activated the CaR.

5. The blocker experiments in SPQ-studies, using FFA and NFA, ought to be supplemented using blockers, which do not affect $\Delta I_{sc(Cd)}$, e.g. DIDS, to ensure that the observed blocking effects are specific.

6. The specificity of the PLC-inhibitor, U73122, compared to its inactive counterpart, U73343, should have been rigorously tested. However, all the performed experiments suggest that U73122 indeed inhibits PLC.

7. The studies also show that there might be a connection between Cd^{2+}-mediated lowering of R_{te} and increased levels of $Ca^{2+}{}_i$. However, this subject needs to be elucidated further. Also, whether long-term exposure of Cd^{2+} causes destruction of tight-junctions and/or apoptosis that both are mediated in part by $Ca^{2+}{}_i$-changes. Long-term measurements of Cd^{2+}-evoked Ca^{2+} increases using fura-2 could answer some of these questions.

9. REFERENCES

Abdel-Mageed, A.B. & Oehme, F.W. (1990). A review of the biochemical roles, toxicity and interactions of zinc, copper and iron: I. Zinc. *Vet Hum Toxicol*, **32**, 34-39.

Ala-Opas M (1995). Concentrations of Cadmium and Lead in Renal Cell Cancer. *J.Trace Elements Med.Biol.*, 176-180.

Alessio, L., Apostoli, P., Duca, P.G., & Braga, M. (1992). Definition of reference values for Cd-B and Cd-U: methodological aspects and preliminary results. In G.F. Nordberg, R.F.M. Herber, & L. Alessio (Eds.), *Cadmium in the Human Environment: Toxicity and Carcinogenicity* (pp. 93-99). Lyon: International Agency for Research on Cancer.

Alison, M. (1995). Apoptosis: Regulation and relevance to toxicology. *Hum.Exp.Toxicol.*, **14**, 234-247.

Amlal, H., Legoff, C., Vernimmen, C, Paillard, M., and Bichara, M. Na^+-K^+-(NH_4^+)-$2Cl^-$ cotransport in medullary thickascending limb: control by PKA, PKC and 20-HETE. Amer J Physiol Cell Physiol 40, C455-C463. 1996.

Andersen, O. Factors affecting the intestinal uptake of cadmium from the diet. Nordberg, GF., Herber, RFM., and Alessio, L. 118, 173-187. 1992. United Kingdom, International Agency for Research on Cancer. Cadmium in the environment: Toxicity and Carcinogenicity.

Aylett BJ (1979). The chemistry and bioinorganic chemistry of cadmium. In BJ. Aylett (Ed.), *The Chemistry, Biochemistry and Biology of Cadmium* (pp. 1-43).

Baum, M.A. & Harris, H.W. (1998). Recent insights into the coordinate regulation of body water and divalent mineral ion metabolism. *American Journal Of The Medical Sciences*, **316**, 321-328.

Benters, J. (1997). Study of the interactions of cadmium and zinc ions with cellular calcium homoeostasis using ^{19}F-NMR spectroscopy. *Biochem.J.*, **322**, 793-799.

Bernard, A., Buchet, J.P., Cardenas, A., & Lauwerys, R. (1992). Cadmium and Health: the Belgian experience. In G.F. Nordberg, R.F.M. Herber, & L. Alessio (Eds.), *Cadmium in the Human Environment: Toxicity and Carcinogenicity* (pp. 15-33). Lyon: International Agency for Research on Cancer.

Berridge, M. J. Elementary and global aspects of calcium signalling - Annual Review Pr ize Lecture. J.Physiol London. 499(2), 291-306. 1997.

Beyersmann, D and Hectenberg, S. Cadmium, Gene Regulation, and Cellular Signalling in Mammalian. Toxicol Appl Pharmacol 144, 247-261. 1997.

Bindels, R. (1988). Stimulation of sodium transport by aldosterone and arginine vasotocin in A6 cells. *Biochem.Biophys.Acta*, **972**, 320-330.

Bindels, RJM. Calcium handling by the mammalian kidney. J.Exp.Biol. 184, 89-104. 1993.

Biwersi, J., Tulk, B., and Verkman, A. S. Long-Wavelength Chloride-Sensitive Fluorescent Indicators. Anal.Biochem. 219, 139-143. 1994.

Biwersi, J., Farah, N., Wang, Y. X., Ketcham, R., and Verkman, A. S. Synthesis of cell-impermeable Cl-sensitive fluorescent indicators with improved sensitivity and optical properties. Amer J Physiol Cell Physiol 262(31), C243-C250. 1992.

Bjerregaard, H. F. and Faurskov, B. Cadmium-induced inhibition of ADH-stimulated ion transport in cultured kidney-derived epithelial cells (A6). ATLA 25(3), 271-277. 1997.

Bjerregaard HF (1995). Side-specific Toxic effects on the Membranes of Cultered Renal Epithelial Cells (A6). *ATLA*, **23**, 485-490.

Bjerregaard HF (1992). Effect of aldosterone on ADH-induced stimulation of active Na^+ transport in A6 epithelia. *Renal Physiological and Biochemistry*, **15**, 190

BlazerYost, B. L. and Helman, S. I. The amiloride-sensitive epithelial Na+ channel: Binding sites and chan nel densities. Amer.J.Physiol Cell Physiol 41(3), C761-C769. 1997.

Blazka, M. (1991). Differences in cadmium and mercury uptakes by hepatocytes: role of calcium channels. *Toxicol.Appl.Pharmacol.*, **110**, 355-363.

Blazka, M. & Shaikh, Z. (1992). Cadmium and Mercury Accumulation in Rat Hepatocytes: Interactions with Other Metal Ions. *Toxicology and Applied Pharmacology*, **113**, 118-125.

Bofetta, P. (1992). Methodological aspects of the epidemiological association between cadmium and cancer in humans. In G.F. Nordberg, R.F.M. Herber, & L. Alessio (Eds.), *Cadmium in the Human Environment* (pp. 425-434). Lyon: International Agency for Research on Cancer.

Böhme, M., Diener, M., & Rummel, W. (1992). Chloride secretion Induced by Mercury and Cadmium: Action sites and mechanism. *Toxicology and Applied Pharmacology*, **114**, 295-301.

Bradford, M. (1976). A rapid and Sensitive Method for the Quantitation of Microgram Quantities of Protein Utilizing the Principle of Protein-Dye Binding. *Anal.Biochem.*, **72**, 248-254.

Brochiero, E and Ehrenfeld, J. Characterisation of Ca^{2+} Membrane Permeability of Renal A6 Cells upon Different Osmotic Conditions. Kidney Blood Press Res 20, 381-390. 1997.

Brown, A. J., Dusso, A., and Slatopolsky, E. Invited review: Vitamin D. Amer J Physiol Renal Physiol 277(46), F157-F175. 1999.

Brown, E.M. (1991). Extracellular Ca^{2+} sensing, regulation of parathyroid cell function, and role of Ca^{2+} and other ions as extracellular (first) messengers. *Physiol.Rev.*, **71**, 371-411.

Brown, E., Gamba, G., & Riccardi, D. (1993). Cloning and characterization of an extracellular Ca^{2+}-sensing receptor from bovine parathyroid. *Nature*, **366**, 575-580.

Brown, E.M., Pollak, M., & Hebert, S.C. (1998). The extracellular calcium-sensing receptor: Its Role in Health and Disease. *Annu.Rev.Med.*, **49**, 15-29.

Brown, E.M. (1999). Physiology and pathophysiology of the extracellular calcium-sensing receptor. *Am J Med*, **106**, 238-253.

Bruggerman, IM. (1990). Transport and toxicity of $CdCl_2$ in LLC-PK_1 cells. *Toxicology Letters*, **53**, 167-168.
Carafoli, E and Stauffer, T. Calcium pump of the plasma membrane. J.Biol.Chem. 267, 2115-2118. 1992.

Bruggerman, IM. (1992). Effect of glutathione and cysteine on apical and basolateral uptake and toxicity of $CdCl_2$ in kidney cells (LLC-PK_1). *Toxic.in Vitro*, **6**, 195-200.

Cabantchik, Z. & Greger, R. (1992). Chemical probes for anion transporters of mammalian cell membranes. *Amer.J.Physiol.Cell Physiol.*, **262**, C803-C827

Cereijido, M., Valdés, J., Shoshani, L., and Contreras, R. G. Role of tight junctions in establishing and maintaining cell polarity. Annu Rev Physiol 60, 161-177. 1998.

Chalfant ML (1993). Distinct regulation of Na^+ reabsorption and Cl^- secretion by arginine vasopressin in the amphibian cell line A6. *Amer.J.Physiol.*, **264**, C1480-C1488

Champe, C.P. & Harvey, R.A. (1987). Nutrition. In D. Barnes (Ed.), *Lippincott's Illustrated Reviews: Biochemistry* (pp. 296-309). Philadelphia: J. B. Lippincott Company.

Chattopadhyay, N., Vassilev, P. M., and Brown, E. M. Calcium-Sensing Receptor: Roles in and beyond Systemic Calcium Homeostasis. Biol.Chem. 378, 759-768. 1997.

Chattopadhyay, N., Yamaguchi, T., & Brown, E.M. (1998). Ca2+ receptor from brain to gut: Common stimulus, diverse actions. *Trends In Endocrinology And Metabolism*, **9**, 354-359.

Clapham, D. E. Calcium Signalling. Cell 80, 259-268. 1995.

Cliff, W. & Frizzell, R. (1990). Separate Cl^- conductances activated by cAMP and Ca^{2+} in Cl^- secreting epithelial cells. *Proc.Natl.Acad.Sic.USA*, **87**, 4956-4960.

Costanzo, L.S. & Windhager, E.E. (1992). Renal regulation of calcium balance. In D.W. Seldin & G. Giebisch (Eds.), *The Kidney* (pp. 2375-2394). New York: Raven Press.

De Jesus Ferreira, M. C. and Bailly, C. Extracellular Ca^{2+} decreases chloride reabsorption in rat CTAL by inhibiting cAMP pathway. Amer J Physiol Renal Physiol 275(44), F198-F203. 1998.

De Luca, F. & Baron, J. (1998). Molecular biology and clinical importance of the Ca(2+)-sensing receptor. *Curr Opin Pediatr*, **10**, 435-440.

Di Stefano, A., Wittner, M, Schlatter, E, Lang, H. J, Englert, H., and Greger, R. Diphenylamine-2-carboxylate, a blocker of the Cl^- conductive pathway in Cl^--transporting epithelia. Pfluegers Arch. 405(Suppl. 1), S95-S100. 1985.

Di Virgilio, F., Steinberg, T.H., & Silverstein, S.C. (1990). Inhibition of Fura-2 sequestration and secretion with organic anion transport blockers. *Cell Calcium*, **11**, 57-62.

Di Virgilio, F., Fasolato, C., & Steinberg, T.H. (1988). Inhibitors of membrane transport system for organic anions block fura-2 excretion from PC12 and N2A cells. *Biochem J*, **256**, 959-963.

Di Virgilio, F., Steinberg, T.H., & Silverstein, S.C. (1989). Organic-anion transport inhibitors to facilitate measurement of cytosolic free Ca2+ with fura-2. *Methods Cell Biol*, **31**, 453-462.

Doucet, A. & Katz, A.I. (1982). High-affinity Ca-Mg-ATPase along the rabbit nephron. *Am J Physiol*, **242**, 346-352.

Draper, M.P., Martell, R.L., & Levy, S.B. (1997). Active efflux of the free acid form of the fluorescent dye 2',7'-bis(2-carboxyethyl)-5(6)-carboxyflyuorescein in multidrug-resistance-protein-overexpressing murine and human leukemia cells. *Eur.J.Biochem.*, **243**, 219-224.

Dwyer, S. D., Zhuang, Y., and Smith, JB. Calcium Mobilization by Cadmium or Decreasing Extracellular Na+ or pH in Coronary Endothelial Cells. Experimental Cell Research 192, 22-31. 1991.

Endo, T. (1996). Effects of Zinc and Copper on Uptake of Cadmium by LLC-PK_1 Cells. *Biol.Pharm.Bull.*, **19**, 944-948.

Endo, T., Kimura, O., & Sakata, M. (1999). Further analysis of cadmium uptake from apical membrane of LLC-PK1 cells via inorganic anion exchanger. *Pharmacol Toxicol*, **84**, 187-192.

Erkilic, A. B., Isbir, M., Ozdem, S., and Ogutman, C. The influence of blood pressure on intracellular Ca2+ content in erythrocytes: Effects of cadmium chloride and nifedipine. Clin.Exp.Hypertension 18(1), 77-86. 1996.

Essodaïgui, M., Broxterman, H.J., & Garnier-Suillerot, A. (1998). Kinetic Analysis of Calcein and Calcein - Acetoxymethylester Efflux Mediated by the Multidrug Resistance Protein and P-Glycoprotein. *Biochemistry*, **37**, 2243-2250.

Faurskov, B. & Bjerregaard HF (1997). Effect of cadmium on active ion transport and cytotoxicity in cultured renal epithelia cells (A6). *Toxicology in Vitro*, **11**, 717-722.

Forrest, J., Stephen, G.A., Stephen, J.W., Ratner, M.A., Forrest, J.K., & Kelley, G.G. (1997). Cadmium Disrupts the Signal Transduction Pathway of Both Inhibitory and Stimulatory Receptors Regulating Chloride Secretion in the Shark Rectal Gland. *The Journal of Experimental Biology*, **279**, 530-536.

Foulkes, EC. & Blanck, S. (1990). Acute Cadmium Uptake by Rabbit Kidneys: Mechanism and Effects. *Toxicology and Applied Pharmacology*, **102**, 464-473.

Foulkes, E.C. (1990). Transport of heavy metals by the kidney. *Toxicol Lett*, **53**, 29-31.

Foulkes, EC. (1988). On the mechanism of transfer of heavy metals across cell membranes. *Toxicology*, **52**, 263-272.

Friberg L (1986). Cadmium. In Friberg L, Nordberg GF, & Vouk VB (Eds.), *Handbook on the Toxicology of Metals* (pp. 130-184). Amsterdam-NY-Oxford: Elsevier.

Friedman, P.A. (1988). Renal calcium transport: Sites and insights. *News Physiol.Sci.*, **3**, 17-21.

Friedman, P. & Gesek, F.A. (1993). Calcium transport in renal epithelial cells. *Amer.J.Physiol.Renal Fl.Elect.*, **264**, F181-F198.

Friedman, P. (1994). Cadmium Uptake by Kidney Distal Convuluted Tubule Cells. *Toxicology and Applied Pharmacology*, **128**, 257-263.

Friedman, P. A. Codependence of renal calcium and sodium transport. Annu Rev Physiol 60, 179-197. 1998.

Gachot, B. & Poujeol, P. (1992). Effects of cadmium and copper on zinc transport kinetics by isolated renal proximal cells. *Biol.Tr.Elem.Res.*, **35**, 93-103.

Galal-Gorchev, H. (1993). Dietary intake, levels in food and estimated intake of lead, cadmium, and mercury. *Food Addit Contam*, **10**, 115-128.

Garty, H. (1988). Physiological Reviews: Characteristics and Regulatory Mechanisms of the Amiloride-Blockable Na^+ Channel. *The American Physiological Society*, **68**, 309-373.

Geisler, A., Klysner, R., Thams, P, and Christensen, S. A simple and inexpensive protein binding assay for cyclic AMP in biological materials. Acta pharmacol.et toxicol. 40, 356-368. 1977.

Girolami, JP. (1989). Renal kallikrein excretion as a distal nephrotoxicity marker during cadmium exposure in rats. *Toxicology*, **55**, 117-129.

Gollapudi, S., Kim, C.H., Tran, B.-N., Sangha, S., & Gupta, S. (1997). Probenecid reverses multidrug resistance in multidrug resistance-associated protein-overexpressing HL60/AR and H69/AR cells but not in P-glycoprotein-overexpressing HL60/Tax and P388/ADR cells. *Cancer Chemother Pharmacol*, **40**, 150-158.

Goyer, R. A. Mechanisms of lead and cadmium nephrotoxicity. Toxicology Letters 46, 153-162. 1989.

Goyer, R. A., Miller, C. R., Zhu, S. Y., and Victery, W. Non-metallothionein-bound cadmium in the pathogenesis of cadmium nephrotoxicity in the rat. Toxicol Appl Pharmacol 101, 232-244. 1989.

Goyer, R.A., Epstein, S., Bhattacharyya, M., Korach, K.S., & Pounds, J. (1994). Environmental risk factors for osteoporosis. *Environ Health Perspect*, **102**, 390-394.

Goyer, R. A. Toxic and essential metal interactions. Annu.Rev.Nutr. 17, 37-50. 1997.

Greger, R. The membrane transporters regulating epithelial NaCl secretion. Pflugers Arch.Eur.J.Physiol. 432(4), 579-588. 1996.

Grynkiewicz, G., Poenie, P., & Tsien, R. (1985). A new Generation of Ca^{2+} Indicators with Greatly Improved Fluorescence Properties. *J Biol Chem*, **260**, 3440-3450.

Guggino, WB. (1994). *Chloride Channels*. San Diego: Academic Press, Inc.

Hammerland, L.G., Krapcho, K.J., Garrett, J.E., Alasti, N., Hung, B.C., Simin, R.T., Levinthal, C., Nemeth, E.F., & Fuller, F.H. (1999). Domains determining ligand specificity for Ca2+ receptors. *Mol Pharmacol*, **55**, 642-648.

Hansen, J.C. (1989). Cadmium exposure in Denmark. *Dan Med Bull*, **36**, 499-502.

Hartwig, A. (1994). Role of DNA repair inhibition in lead and cadmium induced genotoxicity: a review. *Environ.Health Perspect.*, **102**, 45-50.

Hays, R. M. Cellular and molecular events in the action of antidiuretic hormone. Kidney Int. 49(6), 1700-1705. 1996.

Hebert, S. C. and Andreoli, T. E. Control of NaCl transport in the thick ascending limb. Am.J.Physiol. 246, F745-F756. 1984.

Hebert, S. C. and Brown, EM. The extracellular calcium receptor. Curr.Opin.Cell Biol. 7, 484-492. 1995.

Hebert, S. (1996). Extracellular calcium-sensing receptor: Implications for calcium and magnesium handling in the kidney. *Kidney International*, **50**, 2129-2139.

Hebert, S.C. & Brown, E.M. (1996). The scent of an ion: calcium-sensing and its roles in health and disease. *Current Opinion in Nephrology & Hypertension*, **5**, 45-53.

Hebert, S.C., Brown, E., & Harris, W. (1997). Role of the Ca^{2+}-sensing receptor in divalent mineral ion homeostasis. *The Journal of Experimental Biology*, **200**, 295-302.

Hechtenberg, S., Schafer, T., Benters, J., and Beyersmann, D. Effects of cadmium on cellular calcium and proto-oncogene expression. Ann.Clin.Lab.Sci. 26(6), 512-521. 1996.

Heinrich, U. (1992). Pulmonary carcinogenicity of cadmium by inhalation in animals. In G.F. Nordberg, R.F.M. Herber, & L. Alessio (Eds.), *Cadmium in the Human Environment: Toxicity and carcinogenicity* (pp. 405-413). Lyon: International Agency for Research on Cancer.

Helman SI (1994). A6 epithelia: Aldosterone and corticosterone increase apical membrane Na channel density and not open probability. *The FASEB Journal*, **8**, A294(Abstract)

Helman SI (1995). Vesicle Trafficking and Aldosterone-Stimulated Na^+ Transport in A6 Epithelia. *The Journal of General Physiology*, **106**, 42a-43a.(Abstract)

Herber, R.F.M. (1994). Cadmium. In H.G. Seiler, A. Sigel, & H. Sigel (Eds.), *Handbook on Metals in Clinical and Analytical Chemistry* (pp. 283-297). New York: Marcel Dekker.

Hildebrandt, J.P., Plant, T.D., & Meves, H. (1997). The effects of bradykinin on K^+ in NG108-15 cells treated with U73122, a phospholipase C inhibitor, or neomycin. *Br.J.Pharmacol.*, **120**, 841-850.

Hinkle, P. (1992). Measurement of Intracellular Cadmium with Flourescent Dyes. *J.Biol.Chem.*, **267**, 25553

Iino, M. (1999). Dynamic regulation of intracellular calcium signals through calcium release channels. *Mol Cell Biochem*, **190**, 185-190.

Ikeda, M. (1992). Biological monitoring of the general population for cadmium. In G.F. Nordberg, R.F.M. Herber, & L. Alessio (Eds.), *Cadmium in the Human Environment: Toxicity and Carcinogenicity* (pp. 65-72). Lyon: International Agency for Research on Cancer.

Jackson, T. Structure and function og G protein coupled receptors. Pharmacol Ther 50, 425-442. 1991.

Jacobsen, K. (1980). The interaction of cadmium and certain other metal ions with proteins and nucleic acids. *Toxicology*, **16**, 1-37.

Järup, L., Alfvén, T., Persson, B., Toss, G., & Elinder, C.G. (1998). Cadmium may be a risk factor for osteoporosis. *Occup Environ Med*, **55**, 435-439.

Johnson DR (1980). On the Proposed Role of Metallothionein in the Transport of Cadmium. *Environ.Res.*, **21**, 360-365.

Jones, S.W. (1998). Overview of voltage-dependent calcium channels. *Journal Of Bioenergetics And Biomembranes* , **30**, 299-312.

Jovov, B. (1994). Role of intracellular Ca^{2+} in modulation of tight junction resistance in A6 cells. *Renal Fluid Electrolyte Physiol.*, **35**, F775-F784

Kao, J. (1994). Practical Aspects of Measuring [Ca^{2+}] with Fluorescent Indicators. In Anonymous*Methods in Cell Biology* (pp. 155-181). Academic press.

Kazantzis, G., Blanks, R.G., & Sullivan, K.R. (1992). Is cadmium a human carcinogen? *IARC Sci Publ*, 435-446.

Kemendy, A. E., Kleym, , T. R., and Eaton, D. C. Aldosterone alters the open probability of amiloride-blockable sodium channelsin A6 epithelia. Amer J Physiol Cell Physiol 263, C825-C837. 1992.

Kimura, O., Endo, T., and Sakata, M. Comparison of cadmium uptakes from apical and basolateral membranes of LLC-PK1 cells. Toxicol.Appl.Pharmacol. 137(2), 301-306. 1996.

King, L. M., Anderson, M. B., Sikka, S. C., and George, W. J. Murine strain differences and the effects of zinc on cadmium concentra tions in tissues after acute cadmium exposure. Arch Toxicol 72(10), 650-655. 1998.

Kiss, T. & Osipenko, O.N. (1994). Toxic effects of heavy metals on ionic channels. *Pharmacol.Rev.*, **46**, 245-267.

Kjellström, T. (1985). L. Friberg, C.G. Elinder, T. Kjellström, & G.F. Nordberg (Eds.), *Cadmium and Health. A toxicological and Epidermiological Apparaisal* Florida: CRC Press, Boca Raton.

Kjellström, T. (1992). Mechanism and epidemiology of bone effects of cadmium. In G.F. Nordberg, R.F.M. Herber, & L. Alessio (Eds.), *Cadmium in the Human Environment: Toxicity and Carcinogenicity* (pp. 301-310). Lyon: Internation Agency for Research on Cancer.

Klaassen, C. D., Liu, J., and Choudhuri, S. Metallothionein: An intracellular protein to protect against cadmium toxicity. Ann.Rev.Pharmacol. 39, 267-294. 1999.

Koudrine, A. V. Trace elements and apoptosis - Review. J Trace Elem Med Biol 12(2), 65-76. 1998.

Kroemer, G. (1995). The biochemistry of programmed cell death. *FASEB J.*, **9**, 1277-1287.

Lang, M. A., Muller, J., Preston, A. S, and Handler, J. S. Complete response to vasopressin requires epithelial organization in A6 cell in culture. Amer J Physiol Cell Physiol 250, C138-C145. 1986.

Lansman, J. (1986). Blockade of current through single calcium channels by Cd^{2+}, Mg^{2+} and Ca^{2+}. Voltage and concentration dependence of calcium entry into the pore. *J.Gen.Physiol.* , **88**, 321-347.

Long, G. J. Cadmium perturbs calcium homeostasis in rat osteosarcoma (ROS 17/2.8) cells; A possible role for protein kinase C. Toxicol.Lett. 91(2), 91-97. 1997.

Marples, D., Frøkiaer, J., and Nielsen, S. Long-term regulation of aquaporins in the kidney. Amer J Physiol Renal Physiol 276(45), F331-F339. 1999.

Marunaka Y (1990). Chloride channels in the apical membrane of a distal A6 cell lines. *Amer.J.Physiol.Cell Physiol.*, **258**, C352-C368

Marunaka (1993). Modification of Ca^{2+}-Activated Cl^- Channel by Vasopressin and Cholera Toxin. *Jpn.J.Physiol.*, **43**, 553-560.

Marunaka, Y. (1997). Hormonal and osmotic regulation of NaCl transport in renal distal nephron epithelium. *Jpn J Physiol*, **47**, 499-511.

Matsuoka M (1995). Cadmium-induced expression of immediate early genes in LLC-PK_1 cells. *Kidney International*, **48**, 383-389.

Maximilien, R., Poncy, J.L., Monchaux, G., rin, M., & sse, R. (1992). Validity and limitations of animal experiments in assessing lung carcinogenicity of cadmium. In G.F. Nordberg, R.F.M. Herber, & L. Alessio (Eds.), *Cadmium in the Human Environment: Toxicity and carcinogenicity* (pp. 415-424). Lyon: International Agency for Research on Cancer.

McDonough, P. M. and Button, D. C. (1989). Measurement of cytoplasmic calcium concentration in cell suspensions: correction for extracellular Fura-2 through use of Mn2+ and probenecid. *Cell Calcium* 10 (3):171-180.

Mishima, A., Yamamoto, C., Fujiwara, Y., and Kaji, T. Tolerance to cadmium cytotoxicity is induced by zinc through non-metal lothionein mechanisms as well as metallothionein induction in cultured cells. Toxicology 118(2-3), 85-92. 1997.

Mitsui, M., Abe, A., Tajimi, M., & Karaki, H. (1993). Leakage of the fluorescent Ca2+ indicator fura-2 in smooth muscle. *Jpn J Pharmacol*, **61**, 165-170.

Moreira, J.C. (1996). Threats by heavy metals: human and environmental contamination in Brazil. *Sci Total Environ*, **188 Suppl 1**, S61-S71

Nakahari, T. & Marunaka, Y. (1994). Whole cell conductance regulated by cytosolic [Cl-] and ADH-activated Cl-channels in a distal nephron cell line (A6). *Jpn J Physiol*, **44 Suppl 2**, S295-S300

Newberne, P.M. (1988). Naturally occuring food-borne toxicants. In M.E. Shills & V.R. Young (Eds.), *Modern Nutrition in Health and Disease* (pp. 685-697). Philidelphia: Lea & Febiger.

Niisato, N. & Marunaka, Y. (1997). Regulation of Cl^- transport by IBMX in renal A6 epithelium. *Pflügers Arch-Eur.J.Physiol*, **434**, 227-233.

Nordberg, GF., Kjellström, T., & Nordberg, M. (1985). Kinetics and Metabolism. In L. Friberg, T. Kjellström, CF. Elinder, & GF. Nordberg (Eds.), *Cadmium and Health. A Toxicological and Epidemiological Appraisal* (pp. 103-178). Boca Raton, Florida: CRC Press.

Nordberg, M. cadmium, metallothionein and renal tubular toxicity. Nordberg, GF., Herber, RFM., and Alessio, L. 118, 293-297. 1992. United Kingdom, International Agency for Research on Cancer. Cadmium in the environment: Toxicity and Carcinogenicity.

Nordberg, G.F. (1992). Application of the "critical effect" and "critical concentration" concept to human risk assessment for cadmium. In G.F. Nordberg, R.F.M. Herber, & L. Alessio (Eds.), *Cadmium in the Human Environment: Toxicity and Carcinogenicity* (pp. 3-14). Lyon: Internatiolnal Agency for Research on Cancer.

Nordberg, M. cadmium, metallothionein and renal tubular toxicity. Nordberg, GF., Herber, RFM., and Alessio, L. 118, 293-297. 1992. United Kingdom, International Agency for Research on Cancer. Cadmium in the environment: Toxicity and Carcinogenicity.

Paccolat, M. P., Geering, K., Gaeggler, H. P, and Rossier, B. C. Aldosterone regulation of Na^+ transport and Na^+-K^+-ATPase in A6 cells: role of growth conditions. Amer J Physiol Cell Physiol 252, C468-C476. 1987.

Paulsen, I. T. and Saier, M. H. A novel family of ubiquitous heavy metal ion transport proteins. The Journal of Membrane Biology 156(2), 99-103. 1997.

Perkins, FM. (1981). Transport properties of toad kidney epithelia in culture. *Amer.J.Physiol.*, **41**, C154-C159

Pigman, E. A., Blanchard, J. and Laird, H. E.(1997). A study of cadmium transport pathways using the Caco-2 cell model. *Toxicol. Appl. Pharmacol.* **142** (2):243-247.

Pilas, B. & Durack, G. (1997). A Flow Cytometric Method for Measurement of Intracellular Chloride Concentration in Lymphocytes Using the Halide-Specific Probe 6-methoxy-N-(3-sulfopropyl) quinolinium (SPQ). *Cytometry*, **28**, 316-322.

Pollak, M., Brown, E. M., Chou, Y. W., Hebert, S. C. Steinmann (1993). Mutations in the human Ca2+-sensing receptor gene cause familial hypocalciuric hypercalcemia and neonatal severe hyperparathyrodism. *Cell* 75:1297-1303.

Pollak, M., Brown, E. M., Estep, H., McLaine, P., Kifor, O., and Park, J. Autosomal dominant hypocalcemia caused by Ca2+-sensing gene mutation. Nat.Genet. 8, 303-307. 1994.

Prozialeck, WC. (1991). Cadmium (Cd^{2+}) disrupts intercellular junctions and actin filaments in LLC-PK_1 cells. *Toxicology and Applied Pharmacology*, **107**, 81-97.

Prozialeck, WC. (1993). Surface binding and uptake of cadmium (Cd^{2+}) by LLC-PK_1 cells on permeable membrane supports. *Archives of Toxicology*, **67**, 113-119.

Quamme, G. (1992). Free cadmium activity in renal epithelial cells is anhanced by Mg^{2+}depletion. *Kidney International*, **41**, 1237-1244.

Rafferty, KA. (1969). Mass culture of amphibian cells; methods and observations concerning stability of cell type. In M. Mizell (Ed.), *Biology of Amphibian Tumors* (pp. 52-81). New York: Springer Verlag.

Ramachandran, C. and Brunette, G. The renal Na^+/Ca^{2+} exchange system is located exclusively in the distal tubule. Biochem J 257, 259-264. 1989.

Ray, K., Hauschild, B. C., Steinbach, P. J., Goldsmith, P. K., Hauache, O., and Spiegel, A. M. Identification of the Cysteine residues in the Amino-terminal Extracellular Domain of the Human Ca2+ Receptor Critical for Dimerization. The Journal of Biological Chemistry 274(39), 27642-27650. 1999.

Reed, P.W. & Lardy, H.A. (1972). A23187: A divalent cation ionophore. *J Membrane Biol*, **247**, 6970-6977.(Abstract)

Rehn, M., Weber, W.-M., & Clauss, W. (1996). The use of kidney epithelial cell cultures (A6) in the study of Na^+ transport regulation. *Zoology*, **99**, 221-226.

Riccardi, D. (1995). Clonning and functional expression of a rat kidney extracellular calcium/polyvalent cation-sensing receptor. *Proc.Natl.Acad.Sci.USA*, **92**, 131-135.

Riccardi, D., Hall, A.E., Chattopadhyay, N., Xu, J.Z., Brown, E.M., & Hebert, S.C. (1998). Localization of the extracellular Ca^{2+}/polyvalent cation-sensing protein in rat kidney. *Amer J Physiol Renal Physiol*, **274**, F611-F622

Richardson, A and Taylor, CW. Effects of Ca^{2+} Chelators on Purified Inositol 1,4,5-Triphosphate ($InsP_3$) Recptors and $InsP_3$-stimulated Ca^{2+} Mobilization. The Journal of Biological Chemistry 268(16), 11528-11533. 1993.

Rodriguez-Commes, J. (1995). Parathyroid Hormone Stimulates Electrogenic Sodium Transport in A6 cells. *Biochem.Biophys.Res.Commun.*, **213**, 688-698.

Rossi, A. (1991). Modifications of Cell Signaling in the Cytotoxicity of Metals. *Pharmacology & Toxicology*, **68**, 424-429.
Rossi, A. (1996). Heavy Metal Toxicity Following Apical and Basolateral Exposure in the Human Intestinal Cell Line Caco-2. *Toxicology in Vitro*, **10**, 27-36.

Rossman, T.G., Roy, N.K., & Lin, W. (1992). Is cadmium genotoxic? In G.F. Nordberg, R.F.M. Herber, & L. Alessio (Eds.), *Cadmium in the Human Environment: Toxicity and Carcinogenicity* (pp. 367-375). Lyon: International Agency for Research on Cancer.

Salomonsson, M. & Arendshorst, W.J. (1999). Calcium recruitment in renal vasculature: NE effects on blood flow and cytosolic calcium concentration. *Am J Physiol*, **276**, F700-F710

Sariban-Sohraby, S. (1983). Apical sodium uptake in toad kidney epithelial cell line A6. *Amer.J.Physiol.*, **245**, C167-C171

Savolainen, H. (1995). Cadmium-associated renal disease. *Ren Fail*, **17**, 483-487.

Schoenmakers, T.J., Klaren, P.H., Flik, G., Lock, R.A., Pang, P.K., & Bonga, S.E. (1992). Actions of cadmium on basolateral plasma membrane proteins involved in calcium uptake by fish intestine. *J Membr Biol*, **127**, 161-172.

Scott, R.H., Sutton, K.G., Griffin, A., Stapleton, S.R., & Currie, K.P. (1995). Aspects of calcium-activated chloride currents: a neuronal perspective. *Pharmacol Ther*, **66**, 535-565.

Scott, R.H., & Zaidi, M. (1995). Effect of membrane potential on surface Ca2+ receptor activation in rat osteoclasts. *J Cell Physiol*, **162**, 1-8.

Seldin, D.W. (1999). Renal handling of calcium. *Nephron*, **81 Suppl 1**, 2-7.

Shaikh, Z. (1995). Metal transport in cells: cadmium uptake by rat hepatocytes and renal corcitical epithelial cells. *Environ.Health Perspect.*, **103**, 73-75.

Shankar, V.S., Huang, C.L., Adebanjo, O., Simon, B., Alam, A.S., Moonga, B.S., Pazianas, M.,

Sherlock JC (1986). Cadmium in foods and the diet. *Experimentia*, **40**, 152-156.

Shintani, Y. and Marunaka, Y. Regulation of chloride channel trafficking by cyclic AMP via protein kinase A-independent pathway in A6 renal epithelial cells. Biochem.Biophys.Res.Commun. 223(2), 234-239. 1996.

Simmons, NL. (1993). Renal epithelial Cl^- secretion. *Experimental Physiology*, **78**, 117-137.

Sipma, H., Van der Zee, L., Den Hertog, A., & Nelemans, A. (1996). Neomycin inhibits histamine and thapsigargin mediated Ca2+ entry in DDT1 MF-2 cells independent of phospolipase C activation. *Eur.J.Pharmacol.*, **305**, 207-212.

Smith, J. (1989). Cadmium evokes inositol polyphosphate formation and calcium mobilization. *J.Biol.Chem.*, **264**, 7115-7118.

Smith, J. (1994). Transmembrane signals and protooncogene induction evoked by carcinogenic metals and prevented by zinc. *Environ.Health Perspect.*, **102**, 181-189.

Snitsarev, VA, McNulty, TJ, and Taylor, C. Endogenous Heavy Metal Ions Perturb Fura-2 Measurements of Basal and Hormone-Evoked Ca^{2+} Signals. Biophys J 71, 1048-1056. 1996.

Solomons, N.W. (1988). zinc and copper. In M.E. Shills & V.R. Young (Eds.), *Modern Nutrition in Health and Disease* (pp. 238-262). Philadelphia: Lea & Febiger.

Spurney, R.F., Pi, M., Flannery, P., & Quarles, L.D. (1999). Aluminum is a weak agonist for the calcium-sensing receptor. *Kidney Int*, **55**, 1750-1758.

Staessen, J., Bernard, A., Buchet, J.P., Claeys, F., Dekempeneer, L., Ducoffre, G., Fagard, R., Lauwerys, R., Lijnen, P., Roels, H., Rondia, D., Sartor, F., Thijs, L., & Amery, A. (1992). Effects of cadmium exposure on the cardiovascular system and on calcium metabolism: results of a cross-sectional population study. In G.F. Nordberg, R.F.M. Herber, & L. Alessio (Eds.), *Cadmium in the Human Environment: Toxicity and Carcinogenicity* (pp. 263-269). Lyon: International Agency for Research on Cancer.

Staessen, J., Amery, A., Bernard, A., Bruaux, P., Buchet, J.P., Claeys, F., De Plaen, P., Ducoffre, G., Fagard, R., & Lauwerys, R.R. (1991). Effects of exposure to cadmium on calcium metabolism: a population study. *Br J Ind Med*, **48**, 710-714.

Tang, W., Sadovic, S., and Shaikh, Z. A. Nephrotoxicity of Cadmium-Metallothionein: Protection by Zinc and Role of Glutathione. Toxicol.Appl.Pharmacol. 151, 276-282. 1998.

Taylor, A. & Palmer, L. (1982). Hormonal Regulation of Sodium Chloride and Water Transport in Epithelia. In RF. Goldberger & K. Yamamoto (Eds.), *Biological Regulation and Development* (pp. 253-298). Plenum Publishing Corporation.

Templeton, DM. (1990). Cadmium uptake by cells of renal origin. *J.Biol.Chem.*, **21**, 21764-21770.

Thastrup O (1989). Thapsigargin, a novel molecular probe for studying intracellular calcium release and storage. *Agents and Actions*, **27**, 17-23.

Thornton, I. (1992). Sources and pathways of cadmium in the environment. In G.F. Nordberg, R.F.M. Herber, & L. Alessio (Eds.), *Cadmium in the Human Environment: Toxicity and Carcinogenicity* (pp. 149-162). Lyon: Internatial Agency for Research on Cancer.

Tohyama, C. (1988). Immunohistochemical localization of metallothionein in the liver and kidney of cadmium- or zinc-treated rats. *Acta Histochemica et Cytochemica*, **21**, 91-102.

Tsuchiya, K. (1992). Health effects of cadmium with special reference to studies in Japan. *IARC Sci Publ*, 35-49.

Ussing HH (1953). Active Transport of Sodium as the Source of Electric Current in the Short-Circuited Isolated Frog Skin. *Acta Physiologica Scandinavica*, 110-127.

Verbost, P. (1987). Nanomolar concentrations of Cd^{2+} inhibit Ca^{2+} transport system in plasma membranes and intracellular Ca^{2+} stores in intestinal epithelium. *Biochem.Biophys.Acta*, **902**, 247-252.

Verkman, A. (1990). Development and biological applications of chloride-sensitive fluorescent indicators. *Amer.J.Physiol.Cell Physiol.*, **259**, C375-C388

Verrey, F. (1993). Polarized Membrane Movements in A6 Kidney Cells Are Regulated by Aldosterone and Vasopressin/Vasotocin. *J.Membrane.Biol.*, **133**, 213-226.

Verrey, F. (1994). Antidiuretic Hormone Action in A6 Cells: Effcet on Apical Cl and Na Conductances and Synergism with Aldosterone for NaCl Reabsorption. *J.Membrane.Biol.*, **138**, 65-76.

Verrey, F. Transciptional control of sodium transport in tight epithelia by adrenal steroids. J Membrane Biol 144, 93-110. 1995.

Vio, C. P. and Figueroa, C. P. Subecellular localization of renal kallikrein by ultra-structural immunocytochemistry. Kidney Int. 28, 36. 1985.

Wangemann, P., Wittner, M., Di Stefano, A., Englert, H., Lang, H.J., Schlatter, E., & Greger, R. (1986). Cl^--channel blockers in the thick ascending limb of the loop og Henle. Structure activity relationship. *Pfluegers Arch.*, **407**, S128-S141

Ward, D.T., Brown, E.M., & Harris, H.W. (1998). Disulfide bonds in the extracellular calcium-polyvalent cation-sensing receptor correlate with dimer formation and its response to divalent cations in vitro. *J Biol Chem*, **273**, 14476-14483.

White, M. M. (1990) . Niflumic and Flufenamic Acids are Potent Reversible Blockers of Ca^{2+}-Activated Cl^- Channels in *Xenopus* Oocytes. *Molecular Pharmacology* **37**:720-724.

White MM (1990). Niflumic and Flufenamic Acids are Potent Reversible Blockers of Ca^{2+}-Activated Cl^- Channels in *Xenopus* Oocytes. *Molecular Pharmacology*, **37**, 720-724.

White, K. E., Gesek, F. A., and Friedman, P. A. Structural and functional analysis of Na+/Ca2+ exchange in distal conv oluted tubule cells. Amer.J.Physiol.Renal Fl.Elect. 40(3), F560-F570. 1996.

Wills, N. K. Antibiotics as tools for studying the elctrochemical properties in tight epithelia. Fed.Proc. 40, 2202-2205. 1981.

World Health Organization (1980). Recommended Health-based Limits in Occupational Exposure to Heavy Metals. *WHO Technical Report Series*, **647**, 21-22.

World Health Organization (1992). G.F. Nordberg, R.F.M. Herber, & L. Alessio (Eds.), *Cadmium in the Human Environment: Toxicity and Carcinogenicity (WHO)* Lyon: International Agency for Research on Cancer.

Yamagami, K., Nishimura, S., and Sorimachi, M. Cd2+ and Co2+ at micromolar concentrations mobilize intracellular Ca2+ via the generation of inositol 1,4,5-triphosphate in bovine chromaffin cell s. Brain Res 798(1-2), 316-319. 1998.

Ye, C., Rogers, K., Bai, M., Quinn, S.J., Brown, E.M., & Vassilev, P.M. (1996). Agonists of the Ca(2+)-sensing receptor (CaR) activate nonselective cation channels in HEK293 cells stably transfected with the human CaR. *Biochem Biophys Res Commun*, **226**, 572-579.

Zeiske, W., Atia, F., & Van Driessche, W. (1998). Apical Cl- channels in A6 cells. *J Membr Biol*, **166**, 169-178.

Zhang, B. Difference in Cadmium Cytotoxicity in two Kidney Cell Lines ($LLC-PK_1$ and MDCK) with Special Reference to Metallothionein). Toxic.in Vitro 9(5), 765-772. 1995.

APPENDIXES

ARTICLE/MANUSCRIPT I

Pergamon

Toxicology in Vitro 11 (1997) 717–722

Toxicology in Vitro

Effect of Cadmium on Active Ion Transport and Cytotoxicity in Cultured Renal Epithelial Cells (A6)

B. FAURSKOV* and H. F. BJERREGAARD

Department of Life Sciences and Chemistry, Roskilde University, PO Box 260, 4000 Roskilde, Denmark

Abstract—A cultured epithelial cell line from toad kidney (A6) was used to study the mechanism by which cadmium (Cd) affects transepithelial resistance (TER) and active transepithelial ion transport measured as short-circuit current (SCC) *in vitro*. The influence of Cd on cell integrity was investigated by measuring time-dependent TER under controlled conditions and the half-maximal inhibition concentration (IC_{50}) 24 hr after exposure to 1 mM $CdCl_2$. The data suggest that Cd deterioration of cell integrity is stronger when applied to the apical relative to the basolateral solution (IC_{50} = 173.9 and 147.8 μM, respectively). Also, the data demonstrate that addition of Cd to the basolateral solution results in a prompt and transient stimulation of the active ion transport from 2.6 ± 0.4 to 8.7 ± 1.1 $\mu A/cm^2$. Use of the sodium channel blocker amiloride indicate that Na transport is not involved in Cd-stimulated SCC. Substitution of Cl with SO_4^{2-} in the basolateral solution and use of the Cl channel inhibitors, diphenylamine-2-carboxylase (DPC) and niflumic acid indicate strongly that Cd increases Cl secretion in A6 epithelium. Thapsigargin (TG), an intracellular Ca-ATPase blocker, inhibits Cd-stimulated active ion transport indicating that Ca-activated Cl channels are probably involved. Therefore, we suggest that Cd by interaction with the basolateral membrane, become internalized and increase Ca intracellularly. In a dose- and time-dependent way an increase in Ca activates specific Cl channels leading to an increased SCC. Thereafter, the increase in Ca leads to disruption of tight junctions thereby decreasing TER. This may lead to deterioration of cell integrity and perhaps even cell death.

Abbreviations: DPC = diphenylamine-2-carboxylase; Fur = furosemide; IC_{50} = half maximal inhibition concentration; SCC = short-circuit current; TER = transepithelial resistance; TG = thapsigargin.

Keywords: cadmium; active sodium-chloride transport; transepithelial resistance; renal epithelial cells (A6); cell integrity; *in vitro* toxicity.

ARTICLE/MANUSCRIPT II

Cadmium-induced Inhibition of ADH-stimulated Ion Transport in Cultured Kidney-derived Epithelial Cells (A6)

Henning F. Bjerregaard and Brian Faurskov

Department of Life Sciences and Chemistry, Roskilde University, P.O. Box 260, 4000 Roskilde, Denmark

Summary — An epithelial cell line (A6) derived from the distal tubule of toad kidney, was used to study the effect of cadmium (Cd^{2+}) on the increase in active ion transport induced by anti-diuretic hormone (ADH). Addition of Cd^{2+} (1mM) to the basolateral solution of A6 epithelia generated an immediate and transient increase in active ion transport, measured as short circuit current (SCC). This increase was not affected by prior addition of ADH. However, there was a distinct inhibition of ADH-induced stimulation of SCC in epithelia pre-treated with Cd^{2+}. Since cAMP serves as an intracellular messenger for ADH by increasing the ion permeability of the apical membrane in A6 epithelial cells, the effects of Cd^{2+} on enzymes involved in cAMP metabolism were measured. The results showed that Cd^{2+} markedly inhibits cAMP production by inhibiting adenylate cyclase (which had been stimulated with forskolin, magnesium or a non-hydrolysed GTP-analog), indicating that Cd^{2+} inhibits the catalytic subunit of adenylate cyclase. Furthermore, degradation of cAMP by phosphodiesterase was not stimulated by Cd^{2+}, also suggesting that the mechanism by which Cd^{2+} inhibits the ADH-induced ion transport could be through inhibition of adenylate cyclase. Taken together, these results indicate that, in addition to the well-known toxic effect on the proximal tubule, Cd^{2+} could also have an effect on the distal part of the kidney, where the important hormonal regulation of salt and water homeostasis takes place.

Key words: cadmium, active ion transport, ADH, adenylate cyclase, phosphodiesterase, distal renal epithelial cell culture (A6).

ARTICLE/MANUSCRIPT III

PERGAMON

Toxicology in Vitro 13 (1999) 611–617

www.elsevier.com/locate/toxinvit

Effect of Cisplatin on Transepithelial Resistance and Ion Transport in the A6 Renal Epithelial Cell Line

B. FAURSKOV* and H. F. BJERREGAARD

Department of Life Sciences and Chemistry, Roskilde University, Universitetsvej 1, 4000 Roskilde, Denmark

Abstract—Cisplatin is a platinum-containing antitumour agent, the usefulness of which is limited by nephrotoxicity. In the present study, we examined the effects of cisplatin on the established renal epithelial A6 cell line, which forms a polarized monolayer *in vitro* with active transmembrane ion transport. The effect of cisplatin (0–800 μM) on transepithelial ion transport and transepithelial resistance (TER) was monitored by the short-circuit current (SSC) technique. Cell integrity was determined by monitoring TER at increasing concentration of cisplatin during 24 hours. The half-maximal inhibition concentration was 49 and 540 μM when applied to either the basolateral or apical surface, respectively. This suggests that cisplatin-mediated deterioration of cell integrity is far more pronounced when cisplatin is applied basolaterally than apically. Continuous measurements of TER demonstrated a dose- and time-dependent decline in TER/TER_0 (TER at time zero). In addition, cisplatin from the basolateral side had no prompt effect on transepithelial ion transport. Instead a slow, but dose-dependent decline which at the highest concentration resembled the decline observed when ouabain was added. Inhibition of Na-K-ATPase by cisplatin was examined by the use of nystatin, a membrane permeabilizer, and data suggest that cisplatin at 800 μM inhibits Na-K-ATPase by about 50% after 60 minutes of exposure. Morphological examinations of subcultured cisplatin treated cells indicate that cell death is probably due to apoptosis rather than necrosis.

Keywords: cisplatin; short-circuit current; transepithelial resistance; renal epithelial cells (A6); nystatin; Na-K-ATPase.

Abbreviations: AVT = arginine vasotocin; DMEM = Dulbecco's modified Eagle's medium; SSC = short-circuit current; TER = transepithelial resistance.

ARTICLE/MANUSCRIPT IV

Toxicology and Applied Pharmacology **163**, 267–278 (2000)
doi:10.1006/taap.1999.8852, available online at http://www.idealibrary.com on IDEAL®

Chloride Secretion in Kidney Distal Epithelial Cells (A6) Evoked by Cadmium

B. Faurskov*,[1] and H. F. Bjerregaard†

*Grenaa Central Hospital, Sygehusuej 6, 8500 Grenaa, Denmark; and †Department of Life Sciences and Chemistry, Roskilde University, P.O. Box 260, DK-4000 Roskilde, Denmark

Received September 16, 1999; accepted November 9, 1999

Chloride Secretion in Kidney Distal Epithelial Cells (A6) Evoked by Cadmium. Faurskov, B., and Bjerregaard, H. F. (2000). *Toxicol. Appl. Pharmacol.* 163, 267–278.

The effect of Cd^{2+} on chloride secretion was examined in A6 renal epithelia cells by chloride-sensitive fluorescence (SPQ probe) and by the short-circuit-current (I_{sc}) technique. Depleting the cells of Cl^- suggests that the Cd^{2+}-activated I_{sc} ($\Delta I_{sc(Cd)}$) is dependent on the presence of Cl^- ions. Among the Cl^--channel inhibitors the fenemates, flufenamic acid (FFA) and niflumic acid (NFA), and 5-nitro-2-(3-phenylpropylamino)-benzoate (NPPB) significantly lowered $\Delta I_{sc(Cd)}$ compared with control level. In SPQ-loaded A6 cells, Cd^{2+} evoked an increase in Cl^- secretion ($[\Delta Cl^-]_{Cd}$), which significantly exceeded the basal Cl^- transport and was blockable by FFA and NFA. The closely related metals, Zn^{2+} or Ni^{2+}, were also able to activate Cl^- secretion. Preexposure of Zn^{2+} or Ni^{2+} completely prevented $[\Delta Cl^-]_{Cd}$, suggesting that Zn^{2+} and Ni^{2+} probably use similar mechanisms. Like Cd^{2+}, thapsigargin (TG), an inhibitor of intracellular Ca^{2+}-ATPase and the Ca^{2+}-ionophore A23187, induced an increase in I_{sc}. Moreover, TG and Cd^{2+} were able to neutralize the responses of the counterparts as also observed in I_{sc} measurements, which indicates that Cd^{2+} activates Cl^- secretion in a Ca^{2+}-dependent manner. Hence, this study supports the idea that basolateral Cd^{2+} (possibly also Zn^{2+} and Ni^{2+}), probably through a Ca^{2+}-sensing receptor, causes calcium mobilization that activates apical fenemate-sensitive chloride channels leading to chloride secretion in A6 cells.

Key Words: cadmium; calcium; chloride-channel blockers; chloride secretion; fluorescence; heavy metals; renal epithelial cells (A6); short-circuit-current; 6-methoxy-*N*-(sulfopropyl)quinolinium (SPQ).

ARTICLE/MANUSCRIPT V

Cadmium mobilizes intracellular calcium in a hormone-like manner in renal distal epithelial A6 cells

B. Faurskov* & H. F. Bjerregaard‡

*Corresponding author: Grenaa Central Hospital, Klinisk Biokemisk Område, Sygehusvej 6, 8500 Grenaa, Denmark. Phone: +45 89585871, Fax: +45 89585677.E-mail: bf@get2net.dk

‡Department of Life Sciences and Chemistry, Roskilde University, PO Box 260, 4000 Roskilde, Denmark

Running headline: Cd^{2+}-evoked Ca^{2+}-mobilization in A6 cells

Number of figures: 10

Number of tables: 1

ABSTRACT
The effect of Cd^{2+} on intracellular Ca^{2+} homoeostasis was examined in renal epithelial A6 cells loaded with fura-2. Cd^{2+} produced a large transient hormone-like spike in cytosolic Ca^{2+} in a dose-dependent manner. Recently, a calcium-sensing receptor (CaR) has been identified in the kidney that may transduce the biological effects of Cd^{2+}. Activation of the receptor by increased levels of extracellular Ca^{2+} results in the breakdown of phosphoinositide 4,5-diphosphate by phospholipase C (PLC) and the formation of 1,4,5-inositol-triphosphate (IP_3) and diacylglycerol. The resultant increase of the IP_3-levels mobilizes intracellular Ca^{2+} from endoplasmic reticulum (ER). CaR presumably recognizes other cations than Ca^{2+}, e.g. Mg^{2+} and Gd^{3+}, and even polycations such as neomycin. The PLC-inhibitor U73122 and the CaR-agonist, neomycin, both affected Cd^{2+}-evoked increase in intracellular Ca^{2+} ($[\Delta Ca^{2+}]_{Cd}$) suggesting the involvement of CaR in Cd^{2+}-mediated cell signalling. Further, thapsigargin, an inhibitor of intracellular Ca^{2+}-ATPases that deplete intracellular Ca^{2+}-stores, significantly reduced $[\Delta Ca^{2+}]_{Cd}$. Extending these observations, IP_3-binding studies showed that the concentration of intracellular IP_3 underwent a 1.45-fold increase proportional to the resting level when exposed to Cd^{2+}. Finally, we found that the Cd^{2+}-related heavy metals, Zn^{2+} and Ni^{2+}, were even more potent inducers of Ca^{2+}-mobilization than Cd^{2+}. Zn^{2+} was also able to significantly increase the IP_3-generation above control level. Moreover, both Zn^{2+} and Ni^{2+} completely abolished the transient increase in $Ca^{2+}{}_i$ evoked by Cd^{2+}. It can be concluded that Cd^{2+}, and possibly Zn^{2+} and Ni^{2+}, may act as a CaR-agonist leading to IP_3-mediated release of Ca^{2+} from intracellular stores.

Keywords: heavy metals, calcium-sensitive receptor, fura-2, fluorescence, short-circuit-current.

Introduction

The kidney is believed to be the most critical organ for cadmium toxicity. Often mechanisms and effects of inorganic cadmium (Cd^{2+}) is focussed on epithelial cells originating from the renal proximal tubule since this nephron segment reabsorbs the bulk of ultrafiltered Cd^{2+} (for reviews see 26, 33). However, evidence for distal tubule toxicity suggests that cadmium may also act at this nephron site (27).

To elucidate the effect of Cadmium on epithelial cells from the distal part of the kidney we used A6 cells. A6 cells, originating from *Xenopus laevis* (African clawed toad) was used since this cell model exhibits morphological and functional properties of the mammalian distal epithelium (47). A6 cells respond to various hormones and intracellular second messengers and exhibit Na^+ and Cl^--transport similar to what is observed *in vivo* (47, 48, 54, 67). In previous studies we found that Cd^{2+} administered to the basolateral surface of renal epithelia A6 cells, induced a prompt and transient increase in short-circuit-current ($\Delta I_{sc(Cd)}$), which was independent of Na^+ transport (23), but exclusively involved Cl^--secretion (25). Moreover, Ca^{2+}-mobilization was apparently crucial for these events.

Cellular calcium homoeostasis and calcium-mediated functions are being increasingly recognized as sensitive and critical targets for the action of toxic metals such as Cd^{2+} (3, 52, 58, 65). Cd^{2+} and other toxic metals are known to bind to and interact with receptor proteins on the cell surface, with ion channels proteins, or with intracellular proteins controlling Ca^{2+} homoeostasis. The listed studies above have shown that Cd^{2+} provokes an immediate production of IP_3 supporting that Cd^{2+} may interfere with receptors responsible for IP_3-dependent Ca^{2+}-signalling.

Recent studies have provided evidence that Ca^{2+} besides serving as an intracellular second messenger also serves a hormone-like role as an extracellular "first-messenger". Evidence for that came about with the cloning of an extracellular Ca^{2+}-sensing receptor (CaR) from bovine parathyroid gland (13). This receptor plays a central role in the homoeostatic system responsible for maintenance of constant blood Ca^{2+}-levels. When subjected to increased levels of extracellular Ca^{2+} ($Ca^{2+}{}_o$), cells expressing CaR respond with activation of PLC leading to accumulation of IP_3 and consequent release of Ca^{2+} from intracellular stores (for reviews see 14, 15, 31). Moreover, the kidney, like the parathyroid, is able to respond directly to alterations in extracellular Ca^{2+} with the resultant modulation of mineral ion transport, i.e. elevations of $Ca^{2+}{}_o$ activate the CaR in the thick ascending limb (TAL)/distal segment

and lead to reduced reabsorption of Ca^{2+} (and Mg^{2+}) and hence increased Ca^{2+}/Mg^{2+} excretion in the urine. (see refs. 1, 16, 32). Also, it is likely that CaR is expressed in many different nephron segments and that the polarity varies with cell type along the nephron, e.g. CaR is exclusively expressed at the basolateral surface of distal tubule cells (16, 50).

It is also possible that CaR recognizes other agonists than Ca^{2+}_o, e.g. CaR is activated by extracellular Mg^{2+}, Gd^{3+}, organic polycations as neomycin (12, 46). Even Cd^{2+} has been recognized as a possible CaR-agonist due to the stimulation of IP_3-generation (21, 57). Therefore, in order to confirm and extend our previous observations we decided to examine whether Cd^{2+} evokes Ca^{2+}-mobilization in A6 cells by extending the previous obtained I_{sc}-experiments with additional experiments and by direct measurements of intracellular Ca^{2+} using the fluorescent probe, fura-2. Also, the involvement of IP_3 was examined by using IP_3-binding studies.

MATERIALS & METHODS

Cell culture

A6 cells, a line derived from the distal tubule of *Xenopus laevis* kidney, were purchased from the American Type Culture Collection (Rockville, MD, USA), at serial passage 67. All experiments were conducted with cells at passage 80-113 grown at 26°C in a humidified atmosphere of 5% CO_2 in air. The cells were cultured as previously described (23). When cells were confluent and exhibited dome formation (5-10 days), they were subcultured by incubation in 2 ml Ca^{2+}-Mg^{2+}-free amphibian salt solution with 0.25% (w/v) trypsin containing 110 mM NaCl, 2.5 mM $NaHCO_3$, 3 mM KCl, 1 mM KH_2PO_4, 1 mM EGTA and 5 mM glucose (pH 7.6). Upon detachment from the culture flask (3-5 minutes), the subculture medium was removed. Five to ten minutes later, the effect of trypsin was neutralized by adding 5 ml culture medium. The cells were resuspended and used for experiments. In electrochemical experiments, the cells were seeded onto membrane inserts in snap wells (Transwell, 0.45 μm poresize, Costar) at a seeding density of about $5 \cdot 10^5$ cells/well (1 cm^2). The cells were supplemented with growth medium for 7-8 days to obtain confluent monolayers. The ion transport capacities were improved by preincubation of the epithelia with 1 μM aldosterone 24 hours before performing the experiments (7). In fluorescent experiments, cell suspension at a density of about $5 \cdot 10^5$ cells/cuvette (500 μl) was used.

Electrophysiological measurements

To study active transepithelial ion transport, monolayers of cells were mounted in a modified Ussing chamber bathed from both sides in aerated Ringer solutions as described below and kept at room temperature. Each half-chamber housed a potential-sensing KCl-electrode (agar bridge saturated with KCl) and an Ag-AgCl current passing electrode. All electrodes were connected to a multichannel Voltage/Current Clamp amplifier (WPI EVC-4000) enabling one to measure the potential difference and short-circuit-current (I_{sc}) across the monolayer. Conductance (G_{te}) was determined at 300-s intervals by passing a 10-mv pulse of 3 sec duration. The I_{sc} and G_{te} were continuously recorded on a strip-chart recorder. Cell integrity was assessed by monitoring the transepithelial resistance (R_{te}) giving that G_{te} equals $1/R_{te}$.

IP_3-binding

The A6 cells were subcultured as described above and $0.8 \cdot 10^6$ cells/300 μl were prepared in accordance with the guidelines given for the assay system (Kit: TRK 1000) purchased from Amersham (Life Science, UK). Shortly, 300 μl cell suspension were mixed with 0.2 volume ice-cold 20% perchloric acid, and incubated on ice for 20 minutes. A small amount was decanted for protein determination according to the Bradford method (10). The cell suspension was then centrifuged at 2000 g for 15 min. at 15°C whereupon the supernatant were decanted into plastic tubes and neutralized with ice-cold 10 M KOH to pH 7.5. Finally, the neutralized supernatant was diluted 4 × in millipore water

before running the assay. The principle behind the assay is that unlabelled IP_3 competes with a fixed amount of [^{3}H]-labelled IP_3 for a limited number of bovine adrenal IP_3 binding proteins. The bound IP_3 is then separated from the free IP_3 by centrifugation. The free IP_3 in the supernatant is discarded by simple decantation, leaving the bound fraction adhering to the tube. The amount of unlabelled IP_3 in the sample is calculated from a standard curve using the ^{3}H counts. Nonspecific binding measured in the presence of 1 nM IP_3 was typically 10% of the total count. Specific binding was typically 30 % of the total count. Moreover, the used concentration of $CdCl_2$ did not affect the binding capacity of the binding protein. The measurements were performed on a Wallack scintillation counter model 1409. Data were analysed by computer assisted curve-fitting to a logistic equation, which together with the protein content allowed calculation of the specific IP_3-content as pmol IP_3/mg protein. Pilot experiments indicated that the IP_3-content of control cells did not change significantly during a typical time course of experiment, i.e. 60 sec of exposure.

Ca^{2+}_i measurements

All experiments were performed with isolated A6 cells after 4-8 days of growth. To monitor intracellular calcium concentrations, the fluorescent probe Fura-2/AM (Molecular Probes, Leiden, NL) was used. In order to increase uptake of the dye was mixed 1:1 with pluronic acid, a mild nonionic surfactant (Molecular Probes, Leiden, NL) prior to the loading of cells. Isolated cells suspended in DMEM were loaded with 500 μM Fura-2/AM on a rocking device at room temperature for 30 minutes while covered in aluminium foil. Ten minutes before the end of loading, 50 μM TPEN (tetrakis-(2-pyridylmethyl)-ethylenediamine) and probenecid were added to the cell suspension. TPEN is a membrane permeant chelator with extremely high affinity for heavy metals (35, 51) and 5 mM probenecid is capable of inhibiting the organic anion-transporter responsible for the efflux of the dye (19, 20, 43, 44). TPEN treatment did not affect the basal Fura-2 -fluorescence but reversed the 50 μM Cd^{2+}-induced fura-2 fluorescence increase. Since we had a high signal/background ratio, we concluded that the loading procedure was acceptable. Furthermore, we assume that the use of DMEM during loading and the short time of loading help prevent cell damage (11). After the loading, a small volume of isolated cells (about $5 \cdot 10^5$ cells per experimental datum) was washed and resuspended three times (two minutes at 180 g) in normal Ringer solution (NRS) under gentle stirring in a plastic tube. Ca^{2+}-free experiments were performed by replacing NRS with Ca^{2+}-free Ringer solution during the last washing of the cells. All experiments were carried out in a quartz cuvette with a total sample volume of 500 μl containing 5 mM probenecid. Preliminary studies revealed that probenecid at the concentration used did not damage the cells during the time course of the experiments. Also, probenecid did not influence the basal level of Ca^{2+}_i. Fluorescence was measured on a Perkin Elmer Luminescence spectrophotometer, model LS50B. The excitation wavelength was set to alternate between 340 and 380 nm (10 nm slit width) and the emission wavelength was monitored at 540 nm (10 nm slit width). The fluorescence intensity ratio (I_{340}/I_{380}) was measured every 20 ms and plotted graphically using the FLDM-software connected to the Luminescence spectrometer. Routinely, a calibration program was done on the same cell batch (8 samples in total) as the one used during experiments to determine the limiting values of the ratio I_{340}/I_{380} when the probe is in its Ca^{2+}-saturated form (R_{max}) and in its Ca^{2+}-free form (R_{min}) by adding the detergent triton X-100 and excess of EGTA (50 mM) to the cell suspension, respectively. The calcium concentration used to obtain R_{max} was 1 mM. Autofluorescence of the chemicals used and cells not loaded with fura-2 was also measured and subtracted from all test values.

A small fura-2 leak occurred through the cell membranes into the extracellular space in presence of 100 mM Mn^{2+}, which quenches fura-2 fluorescence. The leak was estimated to be 0.63 ± 0.05 % per min. (n = 3). In addition, the last wash was examined for Fura-2-content by adding 1 mM Cd^{2+} and comparing the deflection with the one obtained when 1 mM Cd^{2+} was added to Fura-Na dissolved in Ca^{2+}-free NRS. We found that Cd^{2+} caused a deflection of 2.8 % of what was observed when Cd^{2+} was added to Fura-Na solution indicating that only a very small part of Fura-2 was present in the extracellular space when the experiments began. As the majority of our experiments showed effects that was greater

than 100%, the small leak of fura-2 could not explain the changes in the fluorescent Ca^{2+}_i signal. Furthermore, the extend of fura-2 compartmentalization was estimated by adding the membrane permeabilizer, digitonin (50 μM) and next triton X-100 (1 % v/v), which permeabilize and release dye from subcellular organelles. The fraction of total intracellular dye that was compartmentalized was calculated according to Kao (1994) and was 8.5 ± 0.6 % (n = 4).

Statistics and calculations

We have previously shown that basolateral addition of 1 mM $CdCl_2$ to A6 epithelia did not change R_{te} markedly in the first 40 minutes (23). Therefore, to assure that cell integrity during I_{sc}-experiments was not influenced by Cd^{2+}, all experiments were terminated within 40 minutes after addition of Cd^{2+}. The increase in I_{sc} (ΔI_{sc}) was calculated as the difference in I_{sc} before addition of the agent and the steady or maximal I_{sc}-level reached after addition of the agent. At least one monolayer from the same platting served as control for the other monolayers. Fluorescence results will often be presented as the difference in I_{340}/I_{380}-ratio before and after addition of an agent and are expressed as relative fluorescence ΔF_{agent}. To calculate the intracellular Ca^{2+} concentration, Grynkiewicz' equation was used, with a K_d-value of 224 nM as reported by Grynkiewicz *et al.* (1985).

$$[Ca^{2+}]_i = K_d \cdot \left(\frac{R - R_{min}}{R_{max} - R}\right) \cdot \left(\frac{s_{f2}}{s_{b2}}\right)$$

The factor s_{f2}/s_{b2} represents the ratio of the measured fluorescence intensity when all dye is Ca^{2+} free and the intensity measured when all the dye is saturated with Ca^{2+}, both measurements taken at 380 nm.

Results are expressed as means ± SEM and were analysed statistically using one-way ANOVA multiple comparisons of mean values between groups. If ANOVA detected differences between groups analysed, the data were tested by F-test to evaluate for differences in variance and then further by using two-tailed Student t-test. P-values of less than 5% were considered significant.

Chemicals & Solutions

The solutions used both in electrochemical and fluorescence experiments had the following compositions: Normal Ringer solution, NRS (in mM): Na^+, 115; K^+, 2.5; Cl^-, 117; Ca^{2+} 1; CO_3^{2-}, 2.5. Ca^{2+}-free Ringer (in mM): Na^+, 115; K^+, 2.5; Cl^-, 115; CO_3^{2-}, 2.5; EGTA, 0.1. The pH was in all cases 7.4. A final concentration of 5 mM glucose was used during all experiments.

Metals, thapsigargin, neomycin, triton X-100, U73122 and 3, 4, 5, -trimethoxybenzoic acid-8-(diethylamino)octyl ester (TMB-8) were purchased either from Sigma, USA or from Aldrich, Germany. Fura-2/AM, digitonin, BAPTA/AM and TPEN were purchased from Molecular Probes (Leiden, NL). If the chemicals were dissolved in dimethylsulphoxide (DMSO) a final maximum concentration of 1% (v/v) of the solvent was allowed. In control epithelia, DMSO at 1% (v/v) had no effect on baseline I_{sc} or fluorescence intensity. All drugs were of the highest purity available.

RESULTS

Apical versus basolateral effects of Cd^{2+} on I_{sc}

Addition of Cd^{2+} to the basolateral surface of A6-monolayers caused a dose-dependent increase of I_{sc} showing a prompt and transient nature with a half maximal stimulation concentration ($H_{0.5}$) of 385.9 ± 10.7 μM (n = 6, figure 1). The maximum stimulation concentration, 1 mM, caused I_{sc} to increase from 2.3 ± 0.3 to 10.6 ± 0.8 μA/cm² (n=25, p<0.001) within seconds after administration. The activation was sustained for less than five minutes before I_{sc} returned to basal level. Previously we showed that Na^+-transport was not involved in the observed Cd^{2+}-mediated activation of I_{sc} (23). To examine whether the observed Cd^{2+}-induced I_{sc} ($\Delta I_{sc(Cd)}$) was a side-specific effect or a general effect due to the movement of

Cd^{2+} across the cell membranes, 1 mM Cd^{2+} was applied to both surfaces of A6 cell monolayers in order to achieve maximal response. As demonstrated in figure 1, when 1 mM Cd^{2+} was added to the basolateral side the response differed completely from that observed when Cd^{2+} was applied to the apical side, as basolateral Cd^{2+} exposure caused a $\Delta I_{sc(Cd)}$ of 8.3 ± 0.6 (n = 25) and apical exposure a $\Delta I_{sc(Cd)}$ of -1.5 ± 0.1 (n = 3). This suggests that the action of Cd^{2+} is side-specific, justifying further examination of both apical and basolateral Cd^{2+}-exposure. However, because of the prompt and transient nature of $\Delta I_{sc(Cd)}$ during basolateral treatment, further studies focussed on basolateral Cd^{2+}-treatment only.

Indirect evidence suggests that Ca^{2+}-mobilization is involved in $\Delta I_{sc(Cd)}$ (23) why direct measurements of intracellular Ca^{2+} using fura-2 were implemented. To examine how Cd^{2+} may cause Ca^{2+}-mobilization, the possible role of CaR activation was studied by use of known inhibitors and stimulators of its action.

Actions of PLC-inhibitors on Cd^{2+}-stimulated I_{sc}

The involvement of PLC-dependent activation of Cd^{2+}-stimulated I_{sc} was examined using U73122, a membrane permeable aminosteroid that blocks the phosphatidylinositol-specific PLC (34). As shown in figure 2, preexposure of confluent A6 cell monolayers to 10 μM U73122 at the basolateral side resulted in almost total cancellation of $\Delta I_{sc(Cd)}$ at both 100 μM Cd^{2+} and 1 mM Cd^{2+} as $\Delta I_{sc(Cd)}$ was diminished to 17.4 ± 9.0 % and 9.3 ± 3.5 % of control level, respectively (n = 4 and $p < 0.01$ in both cases). Further experiments were carried out with neomycin, an aminoglycoside antibiotic that has often been used as an inhibitor of PLC-mediated signalling processes (6, 34, 56). Pretreatment with 500 μM neomycin completely abolished $\Delta I_{sc(Cd)}$ at 100 μM of Cd^{2+}-exposure as $\Delta I_{sc(Cd)}$ was diminished to 6.3 ± 4.1 % (n = 3, $p < 0.01$). However, at 1000 μM Cd^{2+} neomycin had no significant effect on $\Delta I_{sc(Cd)}$ compared with cells not pretreated with neomycin (figure 2) suggesting that neomycin is not as potent or specific a PLC-inhibitor as U73122. Subsequent permeabilization of the apical membrane with 300 U/ml nystatin, resulted in a prompt increase of I_{sc} showing that Cd^{2+} did not inhibits the basolateral Na-K-ATPase activity prior to treatment with nystatin as has been shown in another study (41).

$[Ca^{2+}]_i$-mobilization caused by external Cd^{2+}

The test concentration of Cd^{2+} was set at $H_{0.5}$-level, i.e. 400 μM in the subsequent experiments. The basal concentration of free calcium ions in the cytoplasm ($[Ca^{2+}]_i$) of isolated, fura-2-loaded A6 cells were 111 ± 7 nM determined in 73 experiments. $[Ca^{2+}]_i$ rose steeply to peak-values of 579 ± 61 nM (n = 23) within 15 ± 1 seconds when stimulated with 400 μM Cd^{2+}, and declined afterwards to control level or slightly above control level within 3 minutes (figure 3). When the fluorescence intensity at peak height was compared with the basal level, Cd^{2+} displayed a peak/basal-ratio of 6.1 ± 0.6 (n = 23). Consistent with the previously obtained I_{sc}-results, dose-response studies showed that below 10 μM Cd^{2+} fura-2 loaded A6-cells responded marginally whereas above this threshold the response was dose-dependent (figure 3, inserted).

Studies of the effects of Cd^{2+} on intracellular Ca^{2+} homoeostasis using fura-2 is hampered by the fact that divalent metal ions like Cd^{2+} also binds to the probe and cause fluorescence often more intense than that of the Ca^{2+} complex (35). However, this requires that cadmium enters the cells in its free form. As described in methods the cells were incubated with the heavy metal chelator, TPEN, before carrying out the experiments to prevent interactions with Ca^{2+}-fura-complex. To examine whether Cd^{2+} entered the cells and were processed by TPEN, pilot experiments under Ca^{2+}-free conditions were performed. A6 cells were bathed in Ca^{2+}-free Ringer and after 10 minutes 400 μM Cd^{2+} was added to the cell suspension preexposed with 0.8 μM thapsigargin (TG), a potent inhibitor of ATPases in ER (37, 63), or to TG-untreated cells. As demonstrated in figure 4, TG significantly reduced the Cd^{2+}-induced increase of fluorescence from 1.1 ± 0.2 (n = 4, $p < 0.01$) in TG-untreated cells to 0.4 ± 0.1 (n = 7) in TG-pretreated cells. Thus, the obtained results suggest that the observed Cd^{2+}-evoked fluorescence transients depend on Ca^{2+} mobilization.

Actions of PLC-inhibitors on Cd^{2+}-induced Ca^{2+}-mobilization

Using U73122 and neomycin in Ca^{2+}-measurements demonstrated that 10 μM U73122 partially suppressed $[\Delta Ca^{2+}]_{Cd}$ at 400 μM and totally at 100 μM. (figure 5A & table 1). Thus, pretreatment with U73122 and subsequent addition of 100 μM Cd^{2+} prevented the increase in $[Ca^{2+}]_i$ that occurred in the absence of U73122 as $[Ca^{2+}]_i$ was 69 ± 16 nM (n = 3, $p < 0.05$) compared with 503 ± 106 nM (n = 4) in control cells. Neomycin was an even more potent inhibitor of Cd^{2+}-mediated $Ca^{2+}{}_i$-increase ($[\Delta Ca^{2+}]_{Cd}$) than U73122 as 250 μM neomycin almost cancelled the control response at 400 μM Cd^{2+} (figure 5B and table 1). Hence, $[\Delta Ca^{2+}]_{Cd}$ dropped from 579 ± 61 nM (n = 23) in control cells to 50 ± 13 nM (n = 5) in neomycin preexposed cells ($p < 0.001$) corresponding to peak/basal-ratios of 6.1 ± 0.6 and 0.4 ± 0.1, respectively. These data indicate that $[\Delta Ca^{2+}]_{Cd}$ is dependent upon PLC-sensitive pools with neomycin being the most potent inhibitor of $[\Delta Ca^{2+}]_{Cd}$ at the given concentrations used.

Origin of the Cd^{2+}-induced Ca^{2+} increase

To investigate the origin of the Cd^{2+}-induced transient increase in $Ca^{2+}{}_i$, TG and TMB-8, a benzoic acid derivative reported to abolish the Ca^{2+}-mobilization from IP_3-sensitive stores in rat kidney (53), were used. As illustrated in figure 6 and 7 the two agents displayed different effects on $Ca^{2+}{}_i$. TG (0.8 μM) induced an increase in $Ca^{2+}{}_i$ which remained at a plateau level of 337 ± 59 nM (n = 8). TMB-8 (100 μM) induced a fast and transient $Ca^{2+}{}_i$ increase with a peak level of 1269 ± 233 nM (n = 6) corresponding to a peak/basal-ratio of 14.9 ± 3.7 (table 1) before returning to values similar to those measured before TMB-8 addition. Pretreatment with TMB-8 or TG almost abolished $[\Delta Ca^{2+}]_{Cd}$ as the peak/basal-ratio in both cases was 0.4 ± 0.1 (n = 7 for TMB-8 and n = 4 for TG) compared with a control level of 6.1 ± 0.6 (n = 23, table 1). Preexposure with Cd^{2+} and subsequent addition of TG or TMB-8 increased $[\Delta Ca^{2+}]_{Cd}$ to 383 ± 67 nM or to 1084 ± 252 nM (n = 7 in both cases), respectively, which was insignificantly different from their respective control levels mentioned above (figure 6 and 7 and table 1). This demonstrates that the intracellular pools are the main source of $[\Delta Ca^{2+}]_{Cd}$. Moreover, Cd^{2+} pre-exposure did not completely empty the pools as the subsequent addition of TG or TMB-8 showed responses that resembled the corresponding control responses.

Interactions between Cd^{2+} and related metals

Unpublished data indicates that Zn^{2+} and Ni^{2+} probably share similar effects with Cd^{2+} regarding their ability to induce Cl^--secretion in A6-cells, which is why the effect of these cations on $[\Delta Ca^{2+}]_{Cd}$ was examined. As shown in figure 8, both metals induced Ca^{2+}-mobilization in a Cd^{2+}-like fashion, i.e. they too displayed transient characteristics with a very fast kinetic. In fact, both metals (400 μM) were more potent inducers than Cd^{2+}; peak-levels for Zn^{2+} and Ni^{2+} were 1116 ± 210 nM (n = 7) within 14 ± 1 seconds and 868 ± 119 nM (n = 5) within 16 ± 2 seconds, respectively (table 1). This corresponds to peak/basal-ratios of 14.0 ± 2.7 and 11.0 ± 1.8, respectively and was about twofold higher than the corresponding Cd^{2+}-level of 6.1 ± 0.6 (n = 23). Pretreatment with either Zn^{2+} or Ni^{2+} prevented the Cd^{2+}-inducible Ca^{2+}-increase normally observed with Zn^{2+} being the most potent cancelling metal. Hence, Zn^{2+} and Ni^{2+} reduced the peak/basal-ratio of Cd^{2+} to 0.3 ± 0.1 and 0.8 ± 0.1 (n = 4 in both cases), respectively. These data confirm and extend the previous findings in the sense that the similar metals Cd^{2+}, Zn^{2+} and Ni^{2+} evoke Ca^{2+} transients and Cl^--secretion in A6 cells by similar mechanisms. Finally, we determined if Cd^{2+} triggers the mobilization of Ca^{2+} via the IP_3-signalling pathway as expected if intracellular stores are involved.

IP_3 accumulation in cation activated cells

Resting IP_3-levels, measured with the receptor binding assay, were 272.2 ± 51.7 pmol · mg protein in A6 cell suspension (n = 30) which is about a factor 20 higher than observed in neuroblastoma × glioma

cells (34) and a factor 4 higher than observed in E367 neuroblastoma cells (3). As shown in figure 9, exposure to 400 μM Cd^{2+} showed a time dependency as the IP_3-concentration rose to 257.3 ± 114.2 (n = 3), 399.6 ± 132.3 (n = 14) and 668.2 ± 156.6 pmol/mg protein (n = 18, $p < 0.05$ compared with resting level) in cells exposed for 15, 30 and 60 sec, respectively. The exposure time was set at 60 sec in the subsequent experiments to obtain a high IP_3-response.

Both Cd^{2+} and Zn^{2+} were able to increase the IP_3-content significantly above control level (figure 10). Hence, activation of the cells for 60 sec with 400 μM Cd^{2+} and Zn^{2+} increased the IP_3-content significantly to 668.2 ± 156.6 (n = 18, $p < 0.02$) and 957.6 ± 229.0 (n = 8, $p < 0.01$) in comparison with resting levels as mentioned above.

Preincubation of cells with the PLC-inhibitor U73122 (5 μM) for 2 min completely suppressed Cd^{2+}-induced IP_3-generation (figure10, inserted). Thus, the Cd^{2+}/control-ratio of IP_3-accumulation increased to 2.2 ± 0.5 (n = 4) whereas U73122 pretreated cells demonstrated a Cd^{2+}/control-ratio of 0.2 ± 0.2 (n = 3). This suggests that U73122 function as an effective inhibitor of PLC since the IP_3-level was not different from the resting level. Moreover, these data show that U73122 is a potent inhibitor of Cd^{2+}-inducible IP_3-generation.

DISCUSSION

When A6 cells are treated with Cd^{2+} a persistent, prompt and transient increase in I_{sc} is observed only when administered to the basolateral surface. Previously we have shown that the transient increase was independent on Na^+-transport (23) and entirely relied on Cl- transport (25). Furthermore, the studies suggested the involvement of Ca^{2+}-mobilization as Ca^{2+}-depletion and pretreatment with TG almost cancelled $\Delta I_{sc(Cd)}$. In regard to this, we were encouraged to perform additional Ca^{2+}-experiments.

Cadmium and fura-2

Cd^{2+} exhibits high affinity towards fura-2 blunting the measurements of intracellular Ca^{2+} and subsequent interpretation of the obtained results. In the following a number of arguments will be listed, which demonstrate that intracellular Ca^{2+} is in fact being measured and not the binding of Cd^{2+} to the probe: 1) Cd^{2+} evoked an immediate transient increase in fluorescence that is not to be expected if Cd^{2+} binds to the probe since the fluorescence would remain at high level as observed when Cd^{2+} was added to Fura-Na (data not presented). 2) Addition of the Cd^{2+}-chelator TPEN showed no effect on $[\Delta Ca^{2+}]_{Cd}$ as expected if Cd^{2+} were bound to the probe. Furthermore, figure 4 also demonstrates that fura-2 was not present in the extracellular phase. Otherwise EGTA would cause the fluorescence to drop immediately due to the presence of Cd^{2+}. This is expected as the cell suspensions were pre-loaded with probenecid (see methods). Accordingly, the leak rate of the fura-2 was estimated to be considerably lower than previously reported in A6 cells (11) indicating that probenecid actually reduces the leakage rate. Finally, using BAPTA/AM, a membrane permeable Ca^{2+} chelator proved that Cd^{2+}-induced increase in fluorescence only involves Ca^{2+} as BAPTA/AM caused fluorescence to dropped to basal level. 3) Dose-response experiments revealed marked effects only above 10 μM. If an intracellular Cd^{2+}-fura-2-complex was present maximum intensity was obtained at much lower concentrations (500 nM Cd^{2+} gave maximum binding of fura-Na in pilot experiments). 4) Preexposure with the non-autofluorescence $Ca^{2+}{}_i$-modulating agents neomycin, TMB-8 and TG abolished $[Ca^{2+}]_{Cd}$, which would not occur if Cd^{2+} binds to the probe. 5) Depleting the cells for Ca^{2+} using TG reduced $[Ca^{2+}]_{Cd}$ significantly. In the light of this, it can be concluded that the observed effects on fluorescence in fura-2-loaded cells caused by extracellular Cd^{2+} are actually due to Ca^{2+}-mobilization and not the binding of Cd^{2+} to the probe.

Involvement of $Ca^{2+}{}_i$ in Cd^{2+}-induced transients

In subsequent fura-2 experiments, we decided to use Cd^{2+} at a concentration that corresponds to the $H_{0.5}$-level determined in I_{sc}-experiments, i.e. 400 μM. We found that Cd^{2+} evoked a Ca^{2+} transient in a hormone-like fashion, which has also been observed in human fibroblasts (57) and E367 neuroblastoma

cells (3). To emphasize the importance of Ca^{2+}-mobilization during Cd^{2+}-evoked transients, experiments were performed under Ca^{2+}-free conditions. Hence, the typical transient peak as seen under physiological conditions was totally absent in cells pretreated with TG. Moreover, $[\Delta Ca^{2+}]_{Cd}$ was about 64 % lower in TG-pretreated cells than in control cells. Since total depletion of internal Ca^{2+} stores is very difficult to achieve and as reported by Brochiero & Ehrenfeld (1997) even cell treatment with Ca^{2+}-free medium for 10 minutes did not deplete the internal stores in A6 cells, total Ca^{2+}-depletion was not expected. Moreover, Cd^{2+} may under those non-physiological conditions, i.e. very low or free Ca^{2+} intracellular environment, enter the cells through Ca^{2+} channelsas emptying of intracellular Ca^{2+} stores stimulate entry of extracellular Ca^{2+} (capacitative calcium entry) (37, 61). In spite of that, the results strongly suggest that Ca^{2+}-mobilization is crucial for the generation of a transient peak evoked by Cd^{2+}.

Since no sustained elevation of the resting $Ca^{2+}{}_i$ was observed the possibility that Cd^{2+} simple interferes with the control of Ca^{2+} fluxes from outside the cells can be excluded. Furthermore, the very fast response (15 ± 1 sec) argues against physico-chemical interaction of Cd^{2+} with intracellular enzymes, e.g. PLC or Ca^{2+}-ATPases because such effects would require penetration of Cd^{2+} through the plasma membrane, which is slow. Moreover, inhibition of Ca^{2+} extruding systems often results in a sustained elevation of $Ca^{2+}{}_i$, which is not consistent with the transient nature observed in our studies. Measurements of the Na^+-K^+-ATPase activity using the nystatin technique (24) supports this as Cd^{2+} did not inhibits the Na^+-K^+-ATPase activity in A6 cells (data not presented), which is indirectly responsible for Ca^{2+}-extrusion via the Na^+-Ca^+-exchanger (28; 64).

Origin of $[Ca^{2+}]_{Cd}$

To define the origin of the Ca^{2+} release caused by Cd^{2+}, TG and TMB-8 were applied to the cell suspensions. We found that $[\Delta Ca^{2+}]_{Cd}$ was completely annulled in cells pretreated with TMB-8. In addition, TMB-8 induced a prompt and transient increase in $Ca^{2+}{}_i$ that exceeded the levels observed for Cd^{2+}. This is unlikely to be an artifact because TMB-8 did not interfere with fura-2 fluorescence. Moreover, similar findings have been observed in fura-2-loaded MDCK-cells using various TMB-8 derivates (38). As pointed out in other studies, TMB-8 is not a specific blocker of Ca^{2+} store release, e.g. TMB-8 has been reported to act as an a muscarinic (42) and nicotinic acetylcholine (2) receptor antagonist. Accordingly, it is likely that TMB-8 demonstrates mixed actions on the Ca^{2+}-dependent signalling system since mutual cancellation of the Cd^{2+}- and TMB-8-evoked Ca^{2+}-mobilizations did not occur. In contrast, the $Ca^{2+}{}_i$-level was sustained when A6-cells were exposed to TG and subsequent addition of Cd^{2+} showed significant lower $Ca^{2+}{}_i$ than what was observed in control cells indicating that intracellular pools are the main source of $[\Delta Ca^{2+}]_{Cd}$. Subsequent addition of TG to Cd^{2+}-pretreated cells proved no significant difference in TG-amplitude compared with TG-control level suggesting that Cd^{2+}, probably due to the fast and transient nature of $[Ca^{2+}]_{Cd}$, does not empty TG-sensitive stores. Furthermore, under the present experimental conditions we can rule out the possibility that Cd^{2+} inhibits the TG-sensitive Ca^{2+}-ATPases as has been observed for the ER-derived hepatic microsomal Ca^{2+}-ATPase (68) because Cd^{2+} pretreatment did not prevent TG to induce a sustained $Ca^{2+}{}_i$ increase (inhibiting effect on Ca^{2+}-ATPases evoked by Cd^{2+} is reviewed by Beyersmann & Hectenberg, 1997). Nevertheless, we cannot rule out that Cd^{2+} is able to inhibit TG-sensitive ATPase under different experimental conditions since the cells were pre-loaded with TPEN allowing no intracellular Cd^{2+} to occur in its active ionic form.

PLC-inhibitor studies

Transient Ca^{2+} responses are often caused by hormone stimulation, which involves binding of the agonist to its plasma membrane receptor, activation of the G-protein coupled PLC, resulting in generation of IP_3 and diacylglycerol (for reviews see 4, 17, 36). Thus, to investigate if $[Ca^{2+}]_{Cd}$ involves hormonal signalling, experiments with the two PLC-inhibitors U73122 and neomycin were performed. I_{sc}-experiments revealed that U73122 cancelled $\Delta I_{sc(Cd)}$ whereas neomycin could only cancel $\Delta I_{sc(Cd)}$ at lower

doses of Cd^{2+}. Contrary to the I_{sc}-experiments, U73122 abolished $[\Delta Ca^{2+}]_{Cd}$ at 100 μM Cd^{2+} whereas at 400 μM Cd^{2+} the cancellation, though significant, was partial. This paradox is difficult to explain, but it may be due to different experimental setups as I_{sc}-experiments were measured on confluent cells and the fura-2-experiments were measured on cell suspensions. To address this topic further studies are necessary. Nevertheless, at 100 μM Cd^{2+} the fura-data are in accordance with the I_{sc}-experiment, which supports the notion that Cd^{2+}-transients are a result of receptor-interactions that relies on PLC-activation. Besides being used as PLC-inhibitor, neomycin is also a well-known CaR-agonist (30, 59, 66). The fact that neomycin only inhibits $\Delta I_{sc(Cd)}$ at lower doses suggests that neomycin may function as a CaR-modulator rather than a PLC-inhibitor in A6 cells. The different effects of neomycin and U73122 have also been observed in NG108-15 neuroblastoma×glioma cells where neomycin (3 mM), in contrast to U73122 (10 μM), failed to inhibit bradykinin-induced IP_3-generation (34). Similar results were obtained in MDCK-cells as bradykinin-evoked Ca^{2+}_i-transients were abolished by U73122 (5-10 μM) and only partially inhibited by neomycin (3 mM) (38). This supports that neomycin is not a selective PLC-inhibitor but rather exhibits different inhibiting characteristics depending on cell type. U73122 demonstrated noticeable effect on $\Delta I_{sc(Cd)}$ even at high doses and as in NG108-15 neuroblastoma×glioma cells, U73122 showed pronounced effect on the IP_3-generation as discussed below. Thus, assuming that neomycin acts as a CaR-modulator, subsequent addition of 400 μM Cd^{2+} to neomycin pre-treated cells failed to increase Ca^{2+}_i, which suggests that Cd^{2+} mimic or interfere with the mechanism(s) of neomycin.

Cd^{2+} might function as a CaR-agonist in A6 cells

The fact that Cd^{2+} selectively causes I_{sc} to increase at the basolateral surface suggests that the mechanism for triggering $\Delta I_{sc(Cd)}$ and $[\Delta Ca^{2+}]_{Cd}$ are due to extracellular events. Otherwise membrane penetration of Cd^{2+}, e.g. by diffusion, would cause similar responses at both cell surfaces. Therefore, if Cd^{2+} serves as an agonist of CaR, the receptor would necessarily have to be located at the basolateral surface. In fact, in the distal segment of rat kidney cells CaR was exclusively located at the basolateral surface (50). The CaR is unique in the sense that the physiological ligand is an inorganic ion, rather than an organic molecule. Activation of the receptor by increased levels of extracellular Ca^{2+} results in the breakdown of phosphoinositide 4,5-diphosphate by PLC and the formation of IP_3 and diacylglycerol. The resultant increase in levels of IP_3 mobilizes intracellular Ca^{2+} from ER. CaR presumably recognizes other divalent cations than Ca^{2+} and even polycations such as neomycin (12, 45). Previously studies have shown that Cd^{2+} and other divalent metals mobilized cell Ca^{2+} in human skin (57), in E367 neuroblastoma cells (3) and bovine chromaffin cells (65) via an increased generation of IP_3. Furthermore, the divalent metals appeared to trigger Ca^{2+}-mobilization via a reversible interaction with an external site on the cell surface, which the authors referred to as a "Cd^{2+}-receptor". Thus, PLC-inhibitor experiments point in the direction that PLC plays an important role for triggering $\Delta I_{sc(Cd)}$ and $[\Delta Ca^{2+}]_{Cd}$. Direct measurements of IP_3 demonstrated that the IP_3-generation underwent a 1.45-fold increase proportional to the resting level in A6 cell suspensions, which is very similar to ratios reported in the studies listed above. In addition, preexposure to U73122 completely abolished IP_3-generation stimulated by Cd^{2+} suggesting that U73122 likely inhibits PLC. Therefore, it seems likely that $[\Delta Ca^{2+}]_{Cd}$ involves PLC-mediated IP_3 signalling pathway. Furthermore, extracellular cadmium and calcium both interferes with the hormonal regulation of electrolytes in the distal nephron since it has been shown that Ca^{2+}_o decrease anti-diuretic hormone-induced chloride transport by inhibiting cAMP pathway in rat kidney (18) in same way that Cd^{2+} did in A6 cells (8).

Interaction studies

Several studies have demonstrated that metals with similar chemical characteristics as Cd^{2+} are protective against biochemical and toxic effects of Cd^{2+} in a competitive manner (3, 9, 22, 58, 62). The results obtained in fura-2-loaded cells resembled those observed in I_{sc}- and Cl^--transport experiments (25) since pre-treatment with Zn^{2+} or Ni^{2+} at 400 μM completely abolished $[\Delta Ca^{2+}]_{Cd}$. Furthermore, Zn^{2+}

and Ni^{2+} were even more potent inducers of Ca^{2+}-mobilization than Cd^{2+}. In contrast, only Cd^{2+} induced an increase in $Ca^{2+}{}_i$ in E367 neuroblastoma cells whereas Zn^{2+} caused no change in $Ca^{2+}{}_i$ (3). Nevertheless, in human skin fibroblasts (57), bovine chromaffin cells (65) and HEK 293-cells (59) divalent metals, other than Cd^{2+}, displayed Ca^{2+} mobilizing abilities which depended on IP_3-generation. Accordingly, Zn^{2+}, like Cd^{2+}, was able to induce IP_3-generation significantly above control level and in accordance with their ability to induce $Ca^{2+}{}_i$-transients Zn^{2+}, though non-significantly, was the most potent inducer of IP_3-generation. Hence, the results confirm and extend our previous findings in the sense that the similar metals Cd^{2+}, Zn^{2+} and Ni^{2+} share similar mechanisms regarding the ability to evoke Ca^{2+} transients and resulting Cl^--secretion in A6 cells.

Conclusion

The results indicate that an extracellular cation-sensing receptor may be present in the basolateral membrane of A6 cells, which is activated by extracellular Cd^{2+} and possible also Zn^{2+} and Ni^{2+}. In previous reports, this receptor has been referred to as a "Cd^{2+}-receptor". We believe, however, that the newly discovered calcium sensing receptor, CaR, is responsible for the observed effects, which is supported by the fact that CaR recognizes many other cations. Interestingly, the kinetic and dose-response characteristics of $[\Delta Ca^{2+}]_{Cd}$ correspond with those we have previously observed under similar conditions in I_{sc}-experiments (25) suggesting that Cd^{2+}-evoked Cl^--secretion and $Ca^{2+}{}_i$-mobilization are closely connected. We therefore suggest that $\Delta[Ca^{2+}]_{Cd}$ activates Ca^{2+}-sensitive Cl^--channels in the apical membrane of A6 cells leading to transcellular Cl^--secretion. Similar results have been obtained in RaKCaR cRNA-injected *Xenopus* oocytes which responded to extracellular Ca^{2+}, Mg^{2+}, Gd^{3+} and neomycin with a characteristic activation of IP_3-dependent, intracellular Ca^{2+}-induced Cl^--secretion (49). Overall, it is suggested that distal tubule nephrotoxicity may be a part of overall renal cadmium toxicity leading to clinical symptoms such as calcuria and in severe cases kidney-stone formation (39, 55, 60) related to disturbances of calcium homoeostasis in the distal nephron.

REFERENCES

1. Baum, M. A. & Harris, H. W. Recent insights into the coordinate regulation of body water and divalent mineral ion metabolism. *American Journal of the Medical Sciences*. 316: 321-328, 1998.

2. Bencherif, M., Eisenhour, C. M., Prince, R. J., Lippiello, P.M., & Lukas, R. J. The calcium antagonist TMB-8 [3,4,5-trimethoxybenzoic acid 8-(diethylamino)octyl ester] is a potent, non-competitive, functional antagonist at diverse nicotinic acetylcholine receptor subtypes. *J. Pharmacol. Exp. Ther.* 275: 1418-1426, 1995.

3. Benters, J. Study of the interactions of cadmium and zinc ions with cellular calcium homoeostasis using ^{19}F-NMR spectroscopy. *Biochem. J.* 322: 793-799, 1997.

4. Berridge, M. J. Elementary and global aspects of calcium signalling - Annual Review Prize Lecture. *J. Physiol London.* 499 (2): 291-306, 1997.

5. Beyersmann, D. and Hectenberg, S. Cadmium, Gene Regulation, and Cellular Signalling in Mammalian. *Toxicol. Appl. Pharmacol.* 144: 247-261, 1997.

6. Bian, J. S., Zhang, W. M., Xia, Q., & Wong, T.M.. Phospholipase C inhibitors attenuate arrhythmias induced by kappa-receptor stimulation in the isolated rat heart. *Journal of Molecular and Cellular Cardiology*, 30: 2103-2110, 1998.

7. Bjerregaard, H. F. Effect of aldosterone on ADH-induced stimulation of active Na^+ transport in A6 epithelia. *Renal Physiological and Biochemistry*. 15: 190, 1992.

8. Bjerregaard, H. F. and Faurskov, B. Cadmium-induced inhibition of ADH-stimulated ion transport in cultured kidney-derived epithelial cells (A6). *ATLA.* 25 (3): 271-277, 1997.

9. Blazka, M. & Shaikh, Z. Cadmium and Mercury Accumulation in Rat Hepatocytes: Interactions with Other Metal Ions. *Toxicology and Applied Pharmacology.* 113: 118-125, 1992.

10. Bradford, M. A rapid and Sensitive Method for the Quantitation of Microgram Quantities of Protein Utilizing the Principle of Protein-Dye Binding. *Anal. Biochem.* 72: 248-254, 1976.

11. Brochiero, E. and Ehrenfeld, J. Characterisation of Ca^{2+} Membrane Permeability of Renal A6 Cells upon Different Osmotic Conditions. *Kidney Blood Press. Res.* 20: 381-390, 1997.

12. Brown, E. M. Extracellular Ca^{2+} sensing, regulation of parathyroid cell function, and role of Ca^{2+} and other ions as extracellular (first) messengers. *Physiol. Rev.* 71: 371-411, 1991.

13. Brown, E. M., Gamba, G., & Riccardi, D. Cloning and characterization of an extracellular Ca^{2+}-sensing receptor from bovine parathyroid. *Nature.* 366: 575-580, 1993.

14. Brown, E. M., Pollak, M., & Hebert, S.C.. The extracellular calcium-sensing receptor: Its Role in Health and Disease. *Annu. Rev. Med.* 49: 15-29, 1998.

15. Brown, E. M. Physiology and pathophysiology of the extracellular calcium-sensing receptor. *Am. J. Med.* 106: 238-253, 1999.

16. Chattopadhyay, N., Yamaguchi, T., & Brown, E.M. Ca2+ receptor from brain to gut: Common stimulus, diverse actions. *Trends in Endocrinology and Metabolism.* 9: 354-359, 1998.

17. Clapham, D. E. Calcium Signalling. *Cell.* 80: 259-268, 1995.

18. De Jesus Ferreira, M. C. and Bailly, C. Extracellular Ca^{2+} decreases chloride reabsorption in rat CTAL by inhibiting cAMP pathway. *Amer. J. Physiol. Renal Physiol.* 275 (44): F198-F203, 1998.

19. Di Virgilio, F., Steinberg, T. H., & Silverstein, S. C. Organic-anion transport inhibitors to facilitate measurement of cytosolic free Ca2+ with fura-2. *Methods Cell Biol.* 31: 453-462, 1989.

20. Di Virgilio, F., Steinberg, T. H., & Silverstein, S. C. Inhibition of Fura-2 sequestration and secretion with organic anion transport blockers. *Cell Calcium.* 11: 57-62, 1990.

21. Dwyer, S. D., Zhuang, Y., and Smith, J. B. Calcium Mobilization by Cadmium or Decreasing Extracellular Na+ or pH in Coronary Endothelial Cells. *Experimental Cell Research.* 192: 22-31, 1991.

22. Endo, T. Effects of Zinc and Copper on Uptake of Cadmium by LLC-PK_1 Cells. *Biol. Pharm. Bull.* 19: 944-948, 1996.

23. Faurskov, B. & Bjerregaard, H. F. Effect of cadmium on active ion transport and cytotoxicity in cultured renal epithelia cells (A6). *Toxicology in Vitro.* 11: 717-722, 1997.

24. Faurskov, B and Bjerregaard, H. F. Effect of Cisplatin on Transepithelial Resistance and Ion Transport in the A6 Renal Epithelial Cell Line. *Toxic. in Vitro.* 13: 611-617, 1999.

25. Faurskov, B. and Bjerregaard, H. F. Chloride secretion in kidney distal epithelial cells (A6) evoked by cadmium. *Toxicol. Appl. Pharmacol.* 163: 267-278, 2000.

26. Friberg, L. Cadmium. In Friberg L, Nordberg GF, & Vouk VB (Eds.), *Handbook on the Toxicology of Metals.* pp. 130-184. Amsterdam-NY-Oxford: Elsevier, 1986.

27. Friedman, P. Cadmium Uptake by Kidney Distal Convoluted Tubule Cells. *Toxicology and Applied Pharmacology.* 128: 257-263, 1994

28. Friedman, P. A. Codependence of renal calcium and sodium transport. *Annu. Rev. Physiol.* **60**:179-197, 1998.

29. Grynkiewicz, G., Poenie, P., & Tsien, R. A new Generation of Ca^{2+} Indicators with Greatly Improved Fluorescence Properties. *J. Biol. Chem.* 260: 3440-3450, 1985.

30. Hammerland, L. G., Krapcho, K. J., Garrett, J. E., Alasti, N., Hung, B. C., Simin, R.T., Levinthal, C., Nemeth, E. F., & Fuller, F. H. Domains determining ligand specificity for Ca2+ receptors. *Mol. Pharmacol.* 55: 642-648, 1999.

31. Hebert, S. C. and Brown, E. M. The extracellular calcium receptor. *Curr. Opin. Cell Biol.* 7: 484-492, 1995.

32. Hebert, S. Extracellular calcium-sensing receptor: Implications for calcium and magnesium handling in the kidney. *Kidney International.* 50: 2129-2139, 1996.

33. Herber, R. F. M. Cadmium. In H. G. Seiler, A. Sigel, & H. Sigel (Eds.), *Handbook on Metals in Clinical and Analytical Chemistry.* pp. 283-297. New York: Marcel Dekker, 1994

34. Hildebrandt, J. P., Plant, T.D., & Meves, H. The effects of bradykinin on K^+ in NG108-15 cells treated with U73122, a phospholipase C inhibitor, or neomycin. *Br. J. Pharmacol.* 120: 841-850, 1997.

35. Hinkle, P. Measurement of Intracellular Cadmium with Flourescent Dyes. *J. Biol. Chem.* 267: 25553, 1992.

36. Iino, M. Dynamic regulation of intracellular calcium signals through calcium release channels. *Mol. Cell. Biochem.* 190: 185-190, 1999.

37. Inesi, G. Specific Inhibitors of Intracellular Ca2+ Transport ATPases. *The Journal of Membrane Biology.* 141: 1-6, 1994.

38. Jan, C. R., Ho, C. M., Wu, S. N., & Tseng, C. J. Bradykinin-evoked Ca2+ mobilization in Madin Darby canine kidney cells. *Eur. J. Pharmacol.* 355: 219-233, 1998.

39. Järup, L., Alfvén, T., Persson, B., Toss, G. and Elinder, C. G. Cadmium may be a risk factor for osteoporosis. *Occup. Environ. Med..* 55(7):435-439, 1998.

40. Kao, J. Practical Aspects of Measuring [Ca^{2+}] with Fluorescent Indicators. In *Methods in Cell Biology.* Academic press. pp. 155-181, 1994.

41. Kinne-Safran, E., Hulseweh, M., Pfaff, C. and Kinne, R. K. H. Inhibition of Na/K-ATPase by cadmium: different mechanisms in different species. *Toxicol. Appl. Pharmacol.* 121: 22-29, 1993.

42. Leipziger, J., Thomas, J., Rubini-Illes, P., Nitschke, R., & Greger, R. 8-(N,N-diethylamino)octyl 3,4,5-trimethoxybenzoate (TMB-8) acts as a muscarinic receptor antagonist in the epithelial cell line HT29. *Naunyn Schmiedebergs Arch. Pharmacol.* 353: 295-301, 1996.

43. McDonough, P. M. & Button, D. C. Measurement of cytoplasmic calcium concentration in cell suspensions: correction for extracellular Fura-2 through use of Mn2+ and probenecid. *Cell Calcium.* 10: 171-180, 1989

44. Mitsui, M., Abe, A., Tajimi, M., & Karaki, H. Leakage of the fluorescent Ca2+ indicator fura-2 in smooth muscle. *Jpn. J. Pharmacol.* 61: 165-170, 1993.

45. Nemeth, E. F. Ca^{2+} Receptor-Dependent Regulation of Cellular Functions. *Am. Physiol. Soc.* 10: 1-5, 1995.

46. Paulais, M., Baudouin-Legros, M., and Teulon, J. Functional evidence for a Ca^{2+}/polyvalent cation sensor in the mouse thick ascending limb. *Amer. J. Physiol. Renal Physiol.* 271 (40): F1052-F1060, 1996.

47. Perkins, F. M. Transport properties of toad kidney epithelia in culture. *Amer. J. Physiol.* 41: C154-C159, 1981.

48. Rehn, M., Weber, W.-M., & Clauss, W. The use of kidney epithelial cell cultures (A6) in the study of Na^+ transport regulation. *Zoology.* 99: 221-226, 1996.

49. Riccardi, D. Clonning and functional expression of a rat kidney extracellular calcium/polyvalent cation-sensing receptor. *Proc. Natl. Acad. Sci. USA.* 92: 131-135, 1995.

50. Riccardi, D., Hall, A. E., Chattopadhyay, N., Xu, J. Z., Brown, E. M., & Hebert, S. C. Localization of the extracellular Ca^{2+}/polyvalent cation-sensing protein in rat kidney. *Amer. J. Physiol. Renal Physiol.* 274: F611-F622, 1998.

51. Richardson, A. and Taylor, C. W. Effects of Ca^{2+} Chelators on Purified Inositol 1,4,5-Triphosphate ($InsP_3$) Receptors and $InsP_3$-stimulated Ca^{2+} Mobilization. *The Journal of Biological Chemistry.* 268 (16): 11528-11533, 1993.

52. Rossi, A. Modifications of Cell Signaling in the Cytotoxicity of Metals. *Pharmacology & Toxicology.* 68: 424-429, 1991.

53. Salomonsson, M. & Arendshorst, W. J. Calcium recruitment in renal vasculature: NE effects on blood flow and cytosolic calcium concentration. *Am. J. Physiol.* 276: F700-F710, 1999.

54. Sariban-Sohraby, S. Apical sodium uptake in toad kidney epithelial cell line A6. *Amer. J. Physiol.* 245: C167-C171, 1983.

55. Savolainen, H. Cadmium-associated renal disease. *Ren. Fail.* 17 (5): 483-487, 1995.

56. Sipma, H., Van der Zee, L., Den Hertog, A., & Nelemans, A. Neomycin inhibits histamine and thapsigargin mediated Ca2+ entry in DDT1 MF-2 cells independent of phospolipase C activation. *Eur. J. Pharmacol.* 305: 207-212, 1996.

57. Smith, J. Cadmium evokes inositol polyphosphate formation and calcium mobilization. *J. Biol. Chem.* 264: 7115-7118, 1989.

58. Smith, J. Transmembrane signals and protooncogene induction evoked by carcinogenic metals and prevented by zinc. *Environ. Health Perspect.* 102: 181-189, 1994.

59. Spurney, R. F., Pi, M., Flannery, P., & Quarles, L. D.. Aluminum is a weak agonist for the calcium-sensing receptor. *Kidney Int.* 55: 1750-1758, 1999.

60. Staessen, J., Amery, A., Bernard, A., Bruaux, P., Buchet, J. P., Claeys, F., De Plaen, P., Ducoffre, G., Fagard, R. and Lauwerys, R. R. Effects of exposure to cadmium on calcium metabolism: a population study. *Br. J. Ind. Med.* 48 (10):710-714, 1991.

61. Takemura, H. Activation of Calcium Entry by the Tumor Promotor Thapsigargin in Parotid Acinar cells. *The Journal of Biological Chemistry.* 264: 12266-12271, 1989.

62. Tang, W., Sadovic, S., and Shaikh, Z. A. Nephrotoxicity of Cadmium-Metallothionein: Protection by Zinc and Role of Glutathione. *Toxicol. Appl. Pharmacol.* 151: 276-282, 1998.

63. Thastrup, O. Thapsigargin, a novel molecular probe for studying intracellular calcium release and storage. *Agents and Actions.* 27: 17-23, 1989.

64. White, K. E., Gesek, F. A. and Friedman, P. A. Structural and functional analysis of Na+/Ca2+ exchange in distal convoluted tubule cells. *Amer.J.Physiol.Renal Fl.Elect.* 40 (3): F560-F570, 1996.

65. Yamagami, K., Nishimura, S., and Sorimachi, M. Cd2+ and Co2+ at micromolar concentrations mobilize intracellular Ca2+ via the generation of inositol 1,4,5-triphosphate in bovine chromaffin cells. *Brain Res.* 798 (1-2): 316-319, 1998.

66. Ye, C., Rogers, K., Bai, M., Quinn, S. J., Brown, E. M., & Vassilev, P. M. Agonists of the Ca(2+)-sensing receptor (CaR) activate nonselective cation channels in HEK293 cells stably transfected with the human CaR. *Biochem. Biophys. Res. Commun.*. 226: 572-579, 1996.

67. Zeiske, W., Atia, F., & Van Driessche, W. Apical Cl- channels in A6 cells. *J. Membr. Biol.* 166: 169-178, 1998.

68. Zhang, G. Effects of Heavy Metal on Rat Liver Microsomal Ca^{2+}-ATPase and Ca^{2+} Sequestering. *The Journal of Biological Chemistry.* 265: 2184-2189, 1990.

FIGURE LEGENDS

Figure 1. Time course of short-circuit-current (I_{sc}) experiment on confluent A6 cell monolayers. Cadmium (1 mM) exposure of the apical (dotted line) or basolateral (full line) side had completely different effects as 1 mM Cd^{2+} added to the basolateral side. Inserted figure shows dose-response relationoship between I_{sc}, expressed as % of control, and increasing concentrations of cadmium administered to the basolateral surface of A6 cells. The half maximal stimulation concentration ($H_{0.5}$) was calculated as the 50%-level of maximal Cd^{2+}-induced stimulation of I_{sc}. The monolayer was washed with normal Ringer solution between each addition of Cd^{2+}. Data are expressed as mean ± SE of six experiments.

Figure 2. (A). Typical time course showing the effects of the PLC-inhibitors, U73122 (full line) and neomycin (dotted line) on basolateral Cd^{2+}-induced I_{sc} ($I_{sc(Cd)}$). The control response at 100 μM Cd^{2+} is illustrated as the upper punctuated line. U73122 and neomycin were added to the basolateral side of the A6 cell monolayers at 10 μM and 500 μM, respectively. The apical membrane was permeabilized by nystatin (300 U/ml) to illustrate that the basolateral membrane transport still was intact. (B). Bar diagram displaying the effect of U73122 (10 μM) and neomycin (500 μM) on $\Delta I_{sc(Cd)}$ at concentrations of 100 μM and 1000 μM, respectively. n-values are as follows for control, neomycin and U73122 at 100 μM; 4, 3, 4 and at 1000 μM; 24, 4, 4.

Figure 3. $[Ca^{2+}]_i$ measurements in suspensions of fura-2 loaded A6 cells at rest and after application of 400 μM Cd^{2+}. Cd^{2+} evokes a fast and transient increase in $[Ca^{2+}]_i$, which within 3 minutes declines to or slightly above basal level. The transient increase is dose dependent as showed in the inserted figure and responds at concentrations of Cd^{2+} above 10 μM which is consistent with the I_{sc}-results, which is consistent with the I_{sc}-results. The cell suspension was preloaded with the Cd^{2+}-chelator, TPEN, 10 minutes before the start of experiment.

Figure 4. A typical time course of fluorescence ($R_{340/380}$) performed on fura-2 loaded A6 cells bathed in Ca^{2+}-free Ringer solution. Pretreatment with 0.8 μM thapsigargin causes the 400 μM Cd^{2+}-evoked increase in $R_{340/380}$ to drop significantly and alter the course to a non-transient nature. 5 mM EGTA has only a minor effect on $R_{340/380}$ implying that extracellular Cd^{2+} does not contribute to the fluorescence signal and that fura-2 is located in the intracellular environment. Addition of the heavy metal chelator TPEN (50 μM) does not lower $R_{340/380}$ whereas the intracellular Ca^{2+} chelator, BAPTA/AM (100 μM) demonstrates a steep drop in $R_{340/380}$.

Figure 5. Typical time course showing effect of PLC-inhibitors on Cd^{2+}-induced Ca^{2+}-mobilization in fura-2 loaded A6-cells (full line). (A) Control cells exposed to 100 μM Cd^{2+} (dotted line) and cells pretreated with 10 μM U73122. (B) Control cells exposed to 100 μM Cd^{2+} (dotted line) and cells pretreated with 250 μM neomycin (full line).

Figure 6. Time course showing $[Ca^{2+}]_i$ when cells are exposed to Cd^{2+} (400 μM) and subsequently to TMB-8 (100 μM, dotted line) or conversely (full line). Note that preexposure with TMB-8 almost cancel the Cd^{2+}-induced increase of $Ca^{2+}{}_i$ normally observed.

Figure 7. Time course showing $[Ca^{2+}]_i$ when cells are exposed to Cd^{2+} (400 μM) and subsequently to TG (0.8 μM, dotted line) or conversely (straight line). See legend belonging to figure 6 for additional informations. Inserted figure shows a typical time course of an I_{sc}-experiment when TG is added to Cd^{2+}-preexposed A6 cells (data obtained from Faurskov & Bjerregaard, 1997). Note that TG is unable to provoke further increase in I_{sc} but able to further increase $Ca^{2+}{}_i$ following Cd^{2+} treatment.

Figure 8. Interactions between Cd^{2+} and the two related metals, Zn^{2+} and Ni^{2+}. Both Zn^{2+} and Ni^{2+} (both 400 μM) displayed time-courses very alike those observed when A6 cells are exposed to 400 μM Cd^{2+}.

Pretreatment with either Zn^{2+} or Ni^{2+} prevented the Cd^{2+}-inducible Ca^{2+}-increase normally observed suggesting that both metals exhibit similar mechanisms regarding their ability to evoke Ca^{2+} transients in A6 cells.

Figure 9. IP_3-generation in A6 cells at rest (zero sec) and after application of 400 μM Cd^{2+} for 15, 30 and 60 seconds expressed as mean ● SE from 30, 3, 14 and 18 experiments, respectively. Only 60 seconds of exposure differed significantly ($p < 0.05$) from the controls. Thus, to obtain maximum IP_3-response the exposure time was set at 60 seconds in subsequent experiments.

Figure 10. IP_3-accumulation in A6 cells when exposed for 60 seconds to 400 μM $Cd^{2+}$and Zn^{2+}obtained from 18 and 8 experiments, respectively. Both cations increased the IP_3-content significantly compared with the non-treated control cells. Inserted: Cd^{2+}-induced IP_3-generation with and without U73122 treatment. Data are expressed as mean ± SE.

Table 1. Summary of results of fura-2 loaded A6-cells obtained from control experiments, interactions studies and TG-experiments. The data is expressed either as Ca^{2+}_i-concentration given in nM or as the peak to basal-ratio (in some cases as the maximum to basal-ratio). p-values are given at 5% significance level (further details are stated in the text). Data are compared with Cd^{2+}-values except for TG-interactions data which are compared with TG-control values. NS = non significant.

	Ca^{2+}_i-concentration		Peak/basal-ratio	
Control experiments (n)	Peak/maximum ($\Delta[Ca^{2+}]_i$ in nM)	p-value	Peak/maximum	p-value
Cd^{2+} (23)	579 ± 61		6.1 ± 0.6	
Zn^{2+} (7)	1116 ± 210	< 0.001	14.0 ± 2.7	< 0.001
Ni^{2+} (5)	868 ± 119	< 0.05	11.0 ± 1.8	< 0.01
TG (8)	337 ± 58	< 0.05	3.1 ± 0.5	< 0.02
TMB-8 (6)	1269 ± 233	< 0.001	14.9 ± 3.7	< 0.001
Interactions (n) (pretreatment)	Cd^{2+}-induced Ca^{2+}-increase ($\Delta[Ca^{2+}]_i$ in	p-value	Cd^{2+}-peak	p-value
400 μM control (23)	579 ± 61		6.1 ± 0.6	
100 μM control (4)	503 ± 106		4.5 ± 0.7	
Zn^{2+} (4)	50 ± 9	< 0.001	0.3 ± 0.1	< 0.01
Ni^{2+} (4)	42 ± 6	< 0.001	0.8 ± 0.1	< 0.01
TG (4)	262 ± 108	< 0.05	0.4 ± 0.1	< 0.01
TMB-8 (7)	55 ± 12	< 0.001	0.4 ± 0.1	< 0.001
U73122 (3) (Cd = 400 μM)	238 ± 40	NS	2.1 ± 0.9	< 0.05
U73122 (3) (Cd = 100 μM)	69 ± 16	< 0.05*	1.1 ± 0.5	< 0.02*
Neomycin (5)	50 ± 13	< 0.001	0.4 ± 0.1	< 0.001
TG-experiments (n) (pretreatment)	TG-maximum ($\Delta[Ca^{2+}]_i$ in nM)	p-value	TG-maximum	p-value
Control (8)	337 ± 58		3.1 ± 0.5	
Cd^{2+} (7)	383 ± 67	NS	2.3 ± 0.3	NS
Neomycin (5)	492 ± 84	NS	2.8 ± 0.6	NS
Zn^{2+} (5)	532 ± 74	NS	2.7 ± 0.4	NS
Ni^{2+} (4)	611 ± 161	NS	5.3 ± 0.8	NS
TMB-8 (5)	355 ± 94	NS	2.2 ± 0.6	NS
U73 → Cd^{2+} (6)	458 ± 117	NS	3.6 ± 0.7	NS

* compared with 100 μM Cd^{2+}-control.

FIG. 1

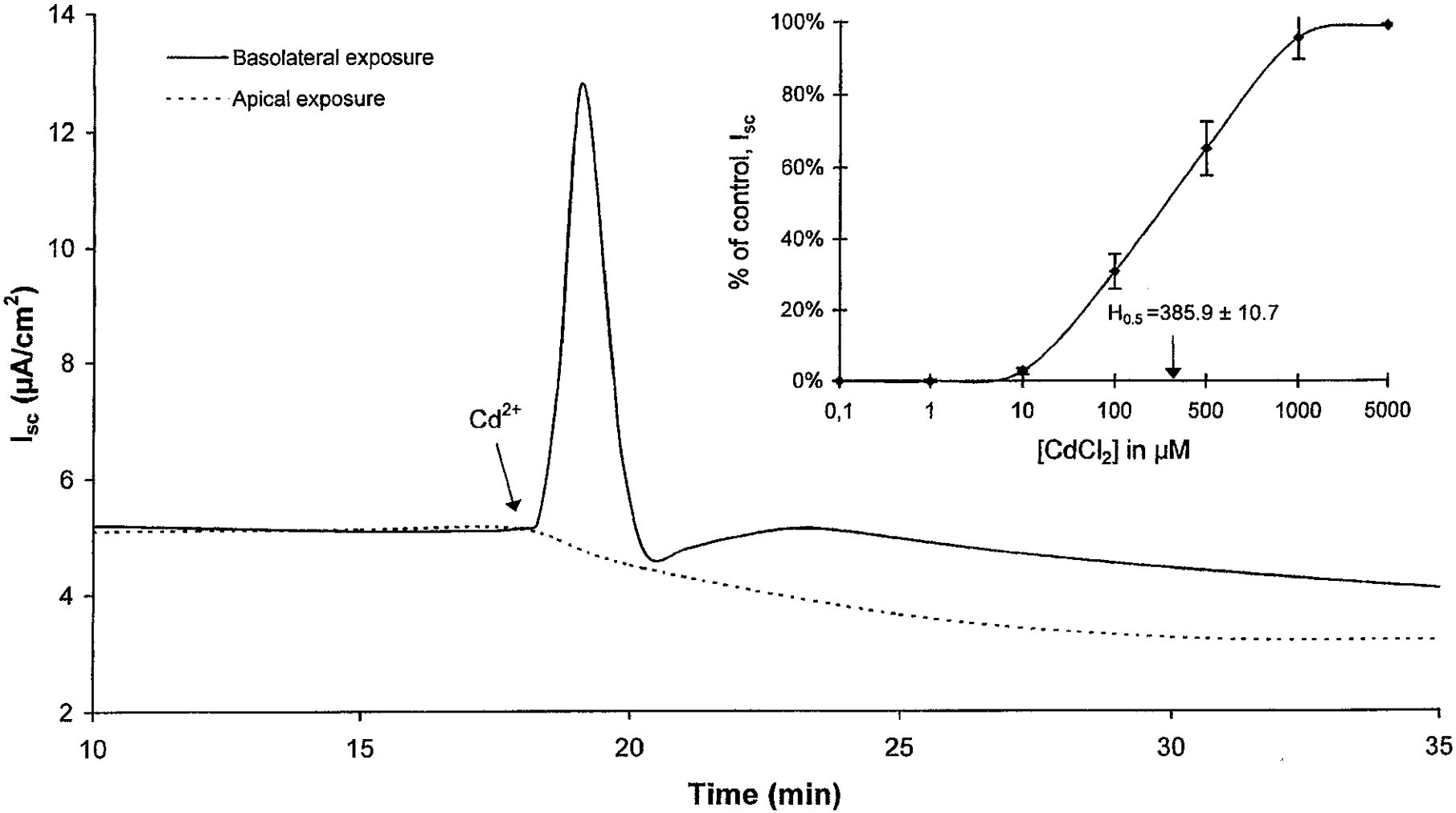
Basolateral exposure
Apical exposure
Cd^{2+}
I_{sc} (µA/cm²)
Time (min)
14
12
10
8
6
4
2
10
15
20
25
30
35
% of control, I_{sc}
100%
80%
60%
40%
20%
0%
$H_{0.5}$ =385.9 ± 10.7
0,1
1
10
100
500
1000
5000
[$CdCl_2$] in µM

FIG.2

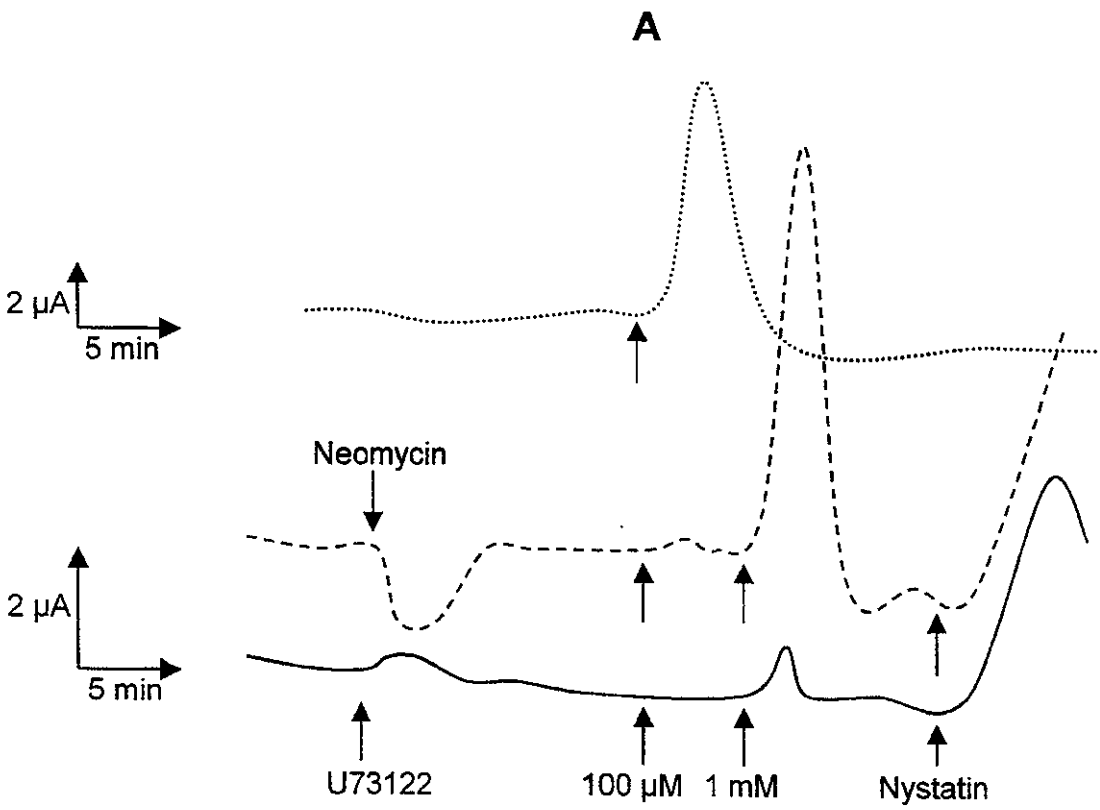
A
2 µA
5 min
Neomycin
2 µA
5 min
U73122
100 µM
1 mM
Nystatin

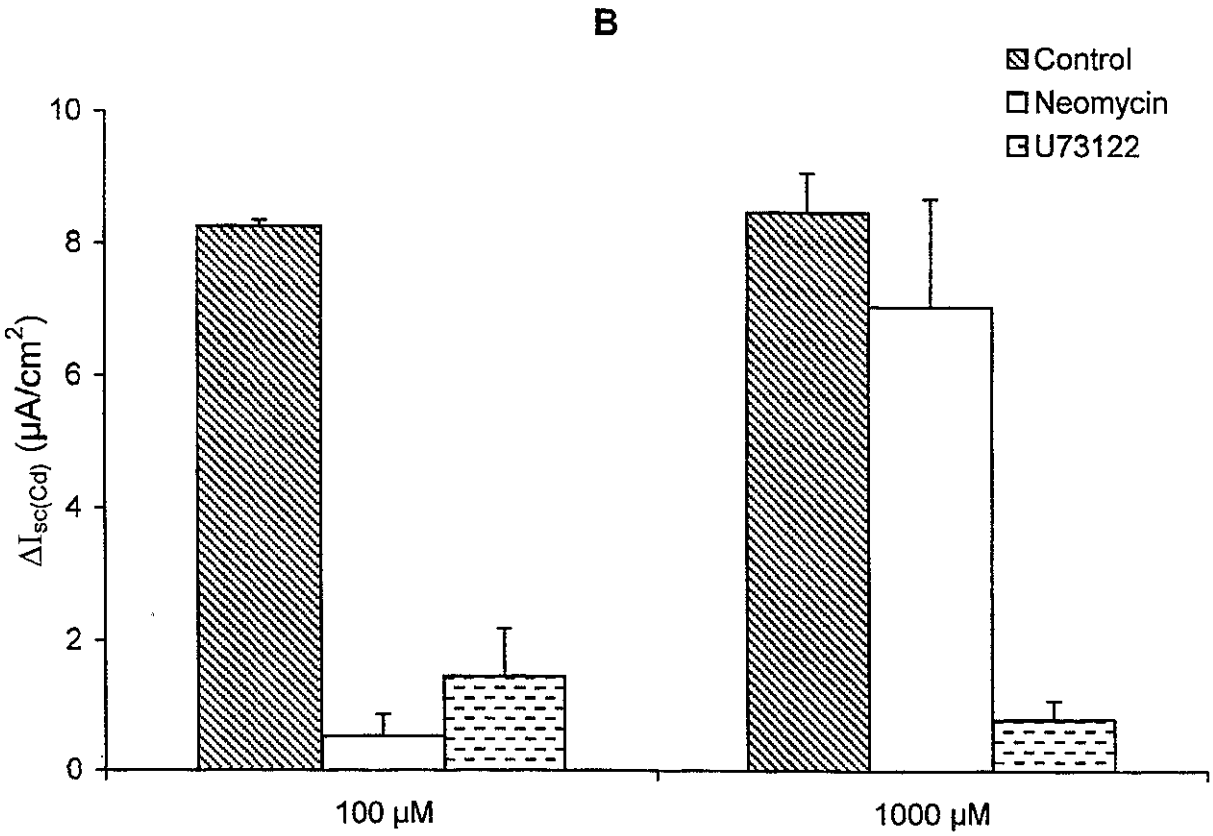
B
Control
Neomycin
U73122
10
8
6
4
2
0
$\Delta I_{sc(Cd)}$ (µA/cm^2)
100 µM
1000 µM

FIG.3

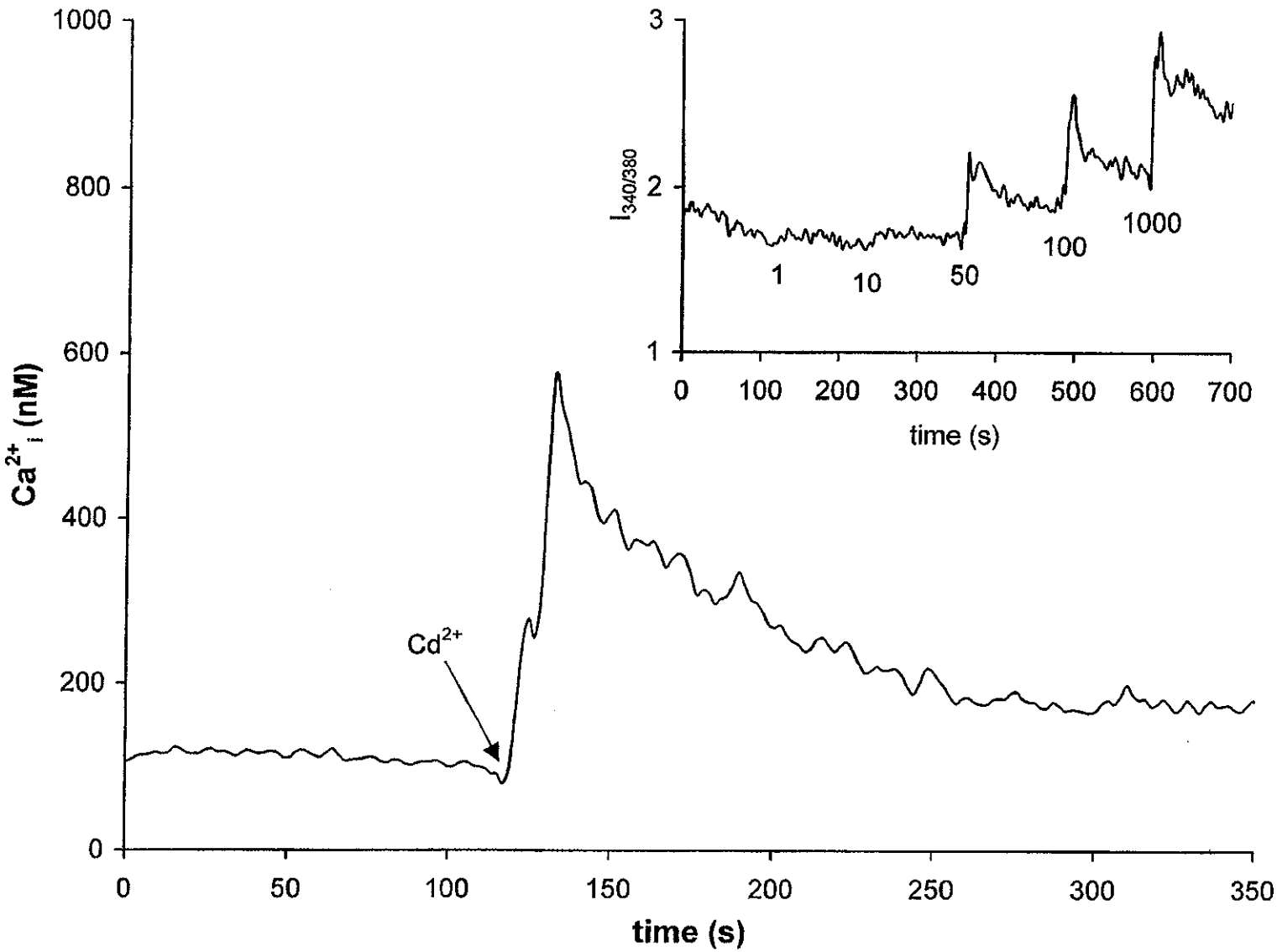
1000
800
600
400
200
0
Ca^{2+}_i (nM)
0
50
100
150
200
250
300
350
time (s)
Cd^{2+}
3
2
1
$I_{340/380}$
1
10
50
100
1000
0
100
200
300
400
500
600
700
time (s)

FIG. 4

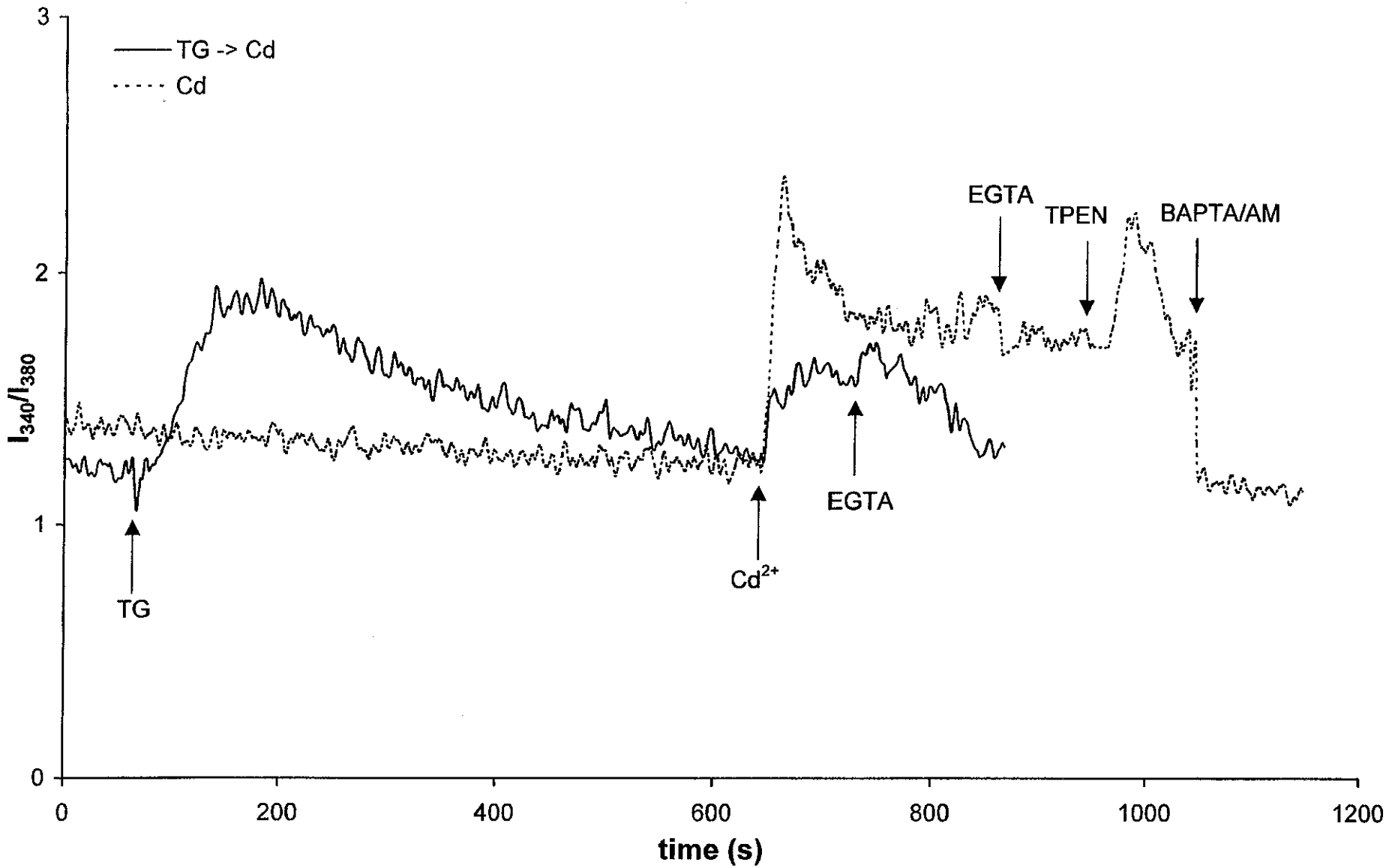
TG -> Cd
Cd
EGTA
TPEN
BAPTA/AM
EGTA
TG
Cd2+
I340/I380
time (s)
0
1
2
3
0
200
400
600
800
1000
1200

FIG. 5

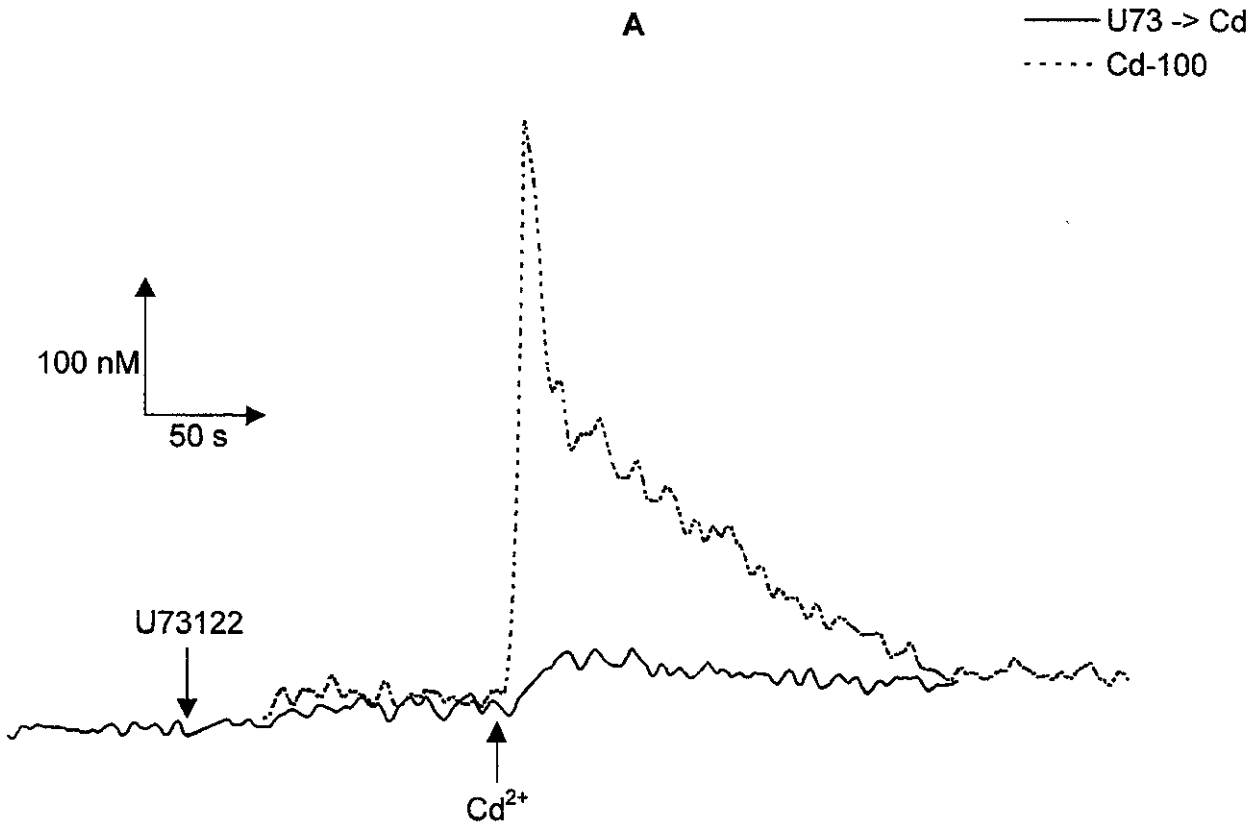
A
U73 -> Cd
Cd-100
100 nM
50 s
U73122
Cd2+

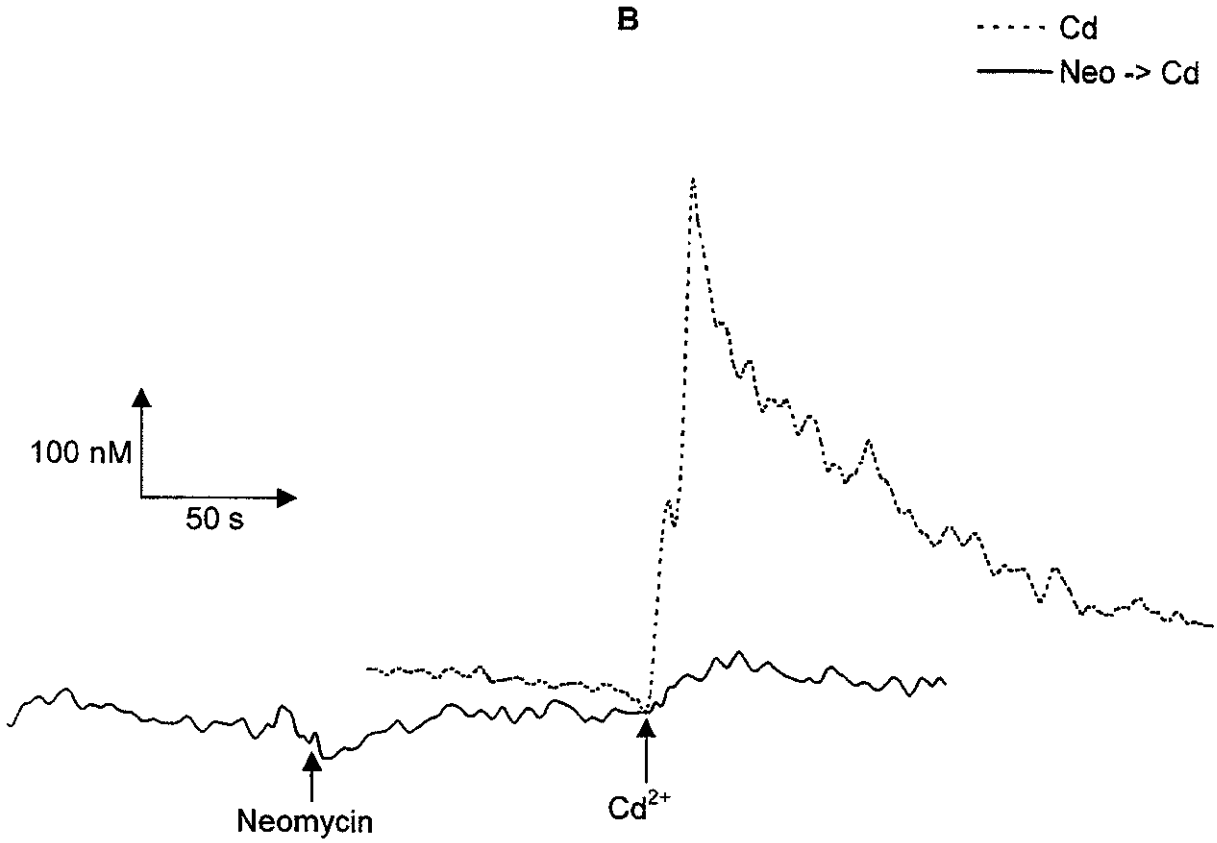
B
Cd
Neo -> Cd
100 nM
50 s
Neomycin
Cd2+

FIG.6

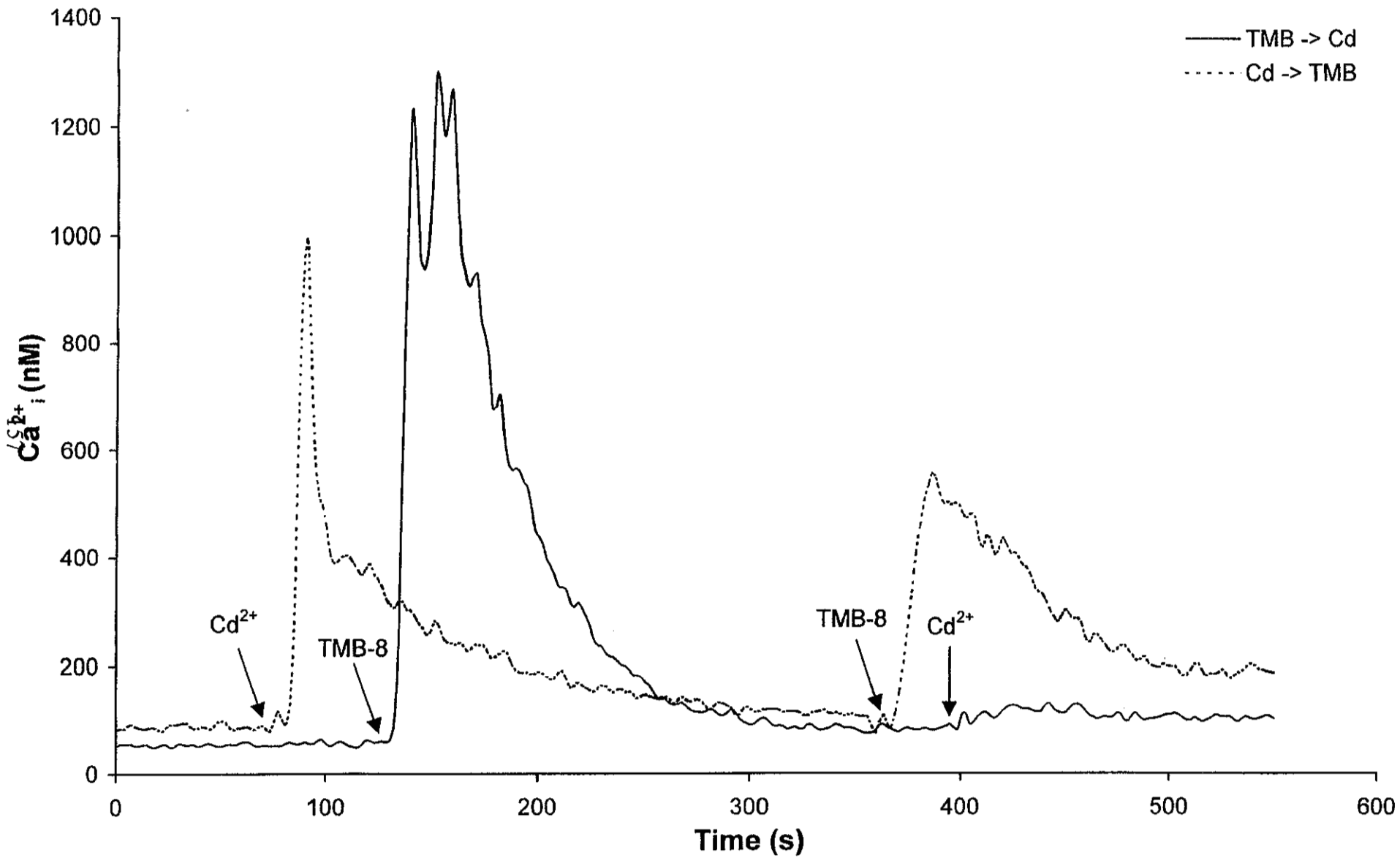
TMB -> Cd
Cd -> TMB
Ca^{2+}_i (nM)
Time (s)
Cd^{2+}
TMB-8
TMB-8
Cd^{2+}
0
200
400
600
800
1000
1200
1400
0
100
200
300
400
500
600

FIG. 7

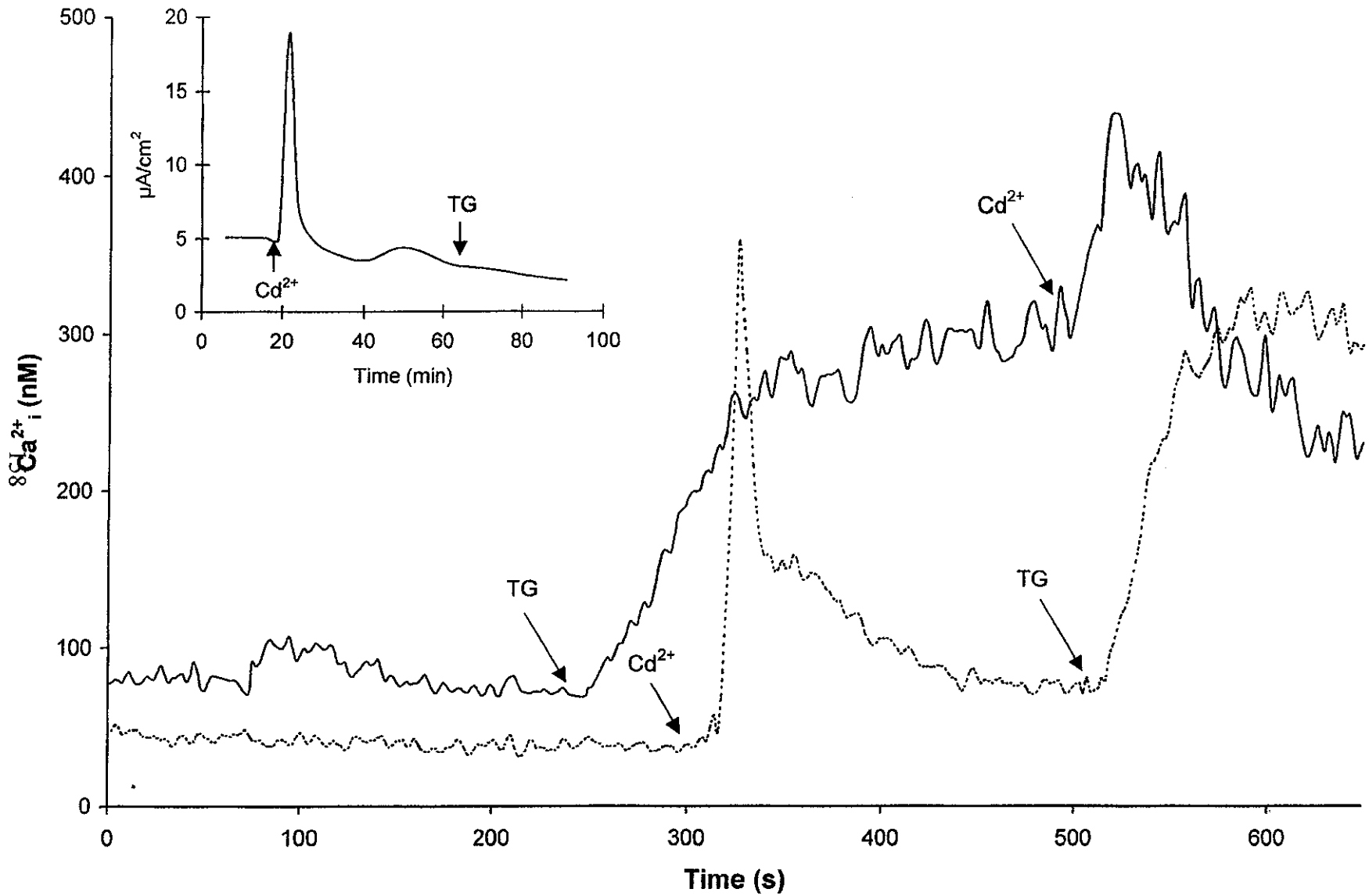
500
400
300
200
100
0
$^{8}Ca^{2+}_{i}$ (nM)
0
100
200
300
400
500
600
Time (s)
TG
Cd^{2+}
TG
Cd^{2+}
20
15
10
5
0
μA/cm²
0
20
40
60
80
100
Time (min)
TG
Cd^{2+}

FIG. 8

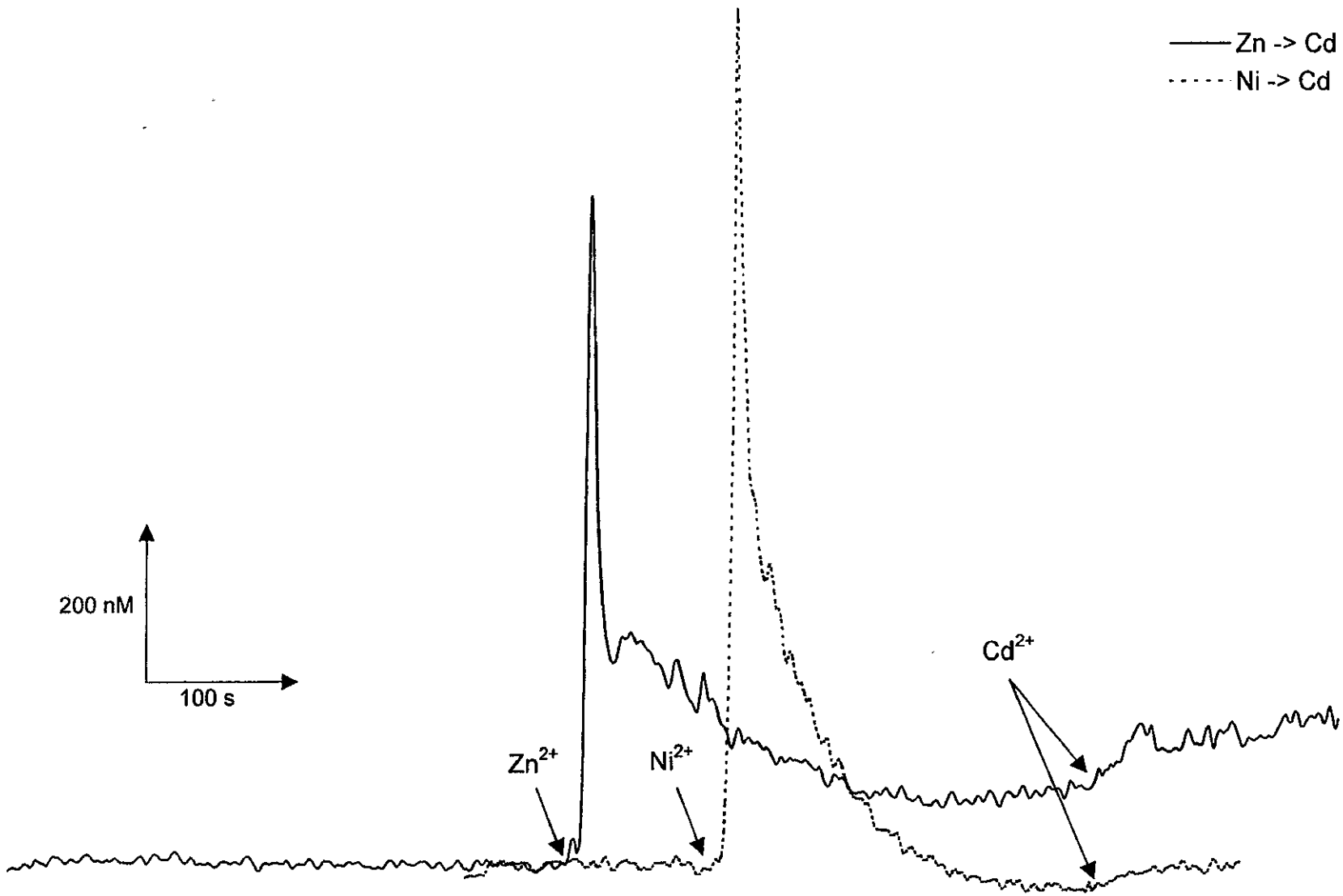

FIG. 7

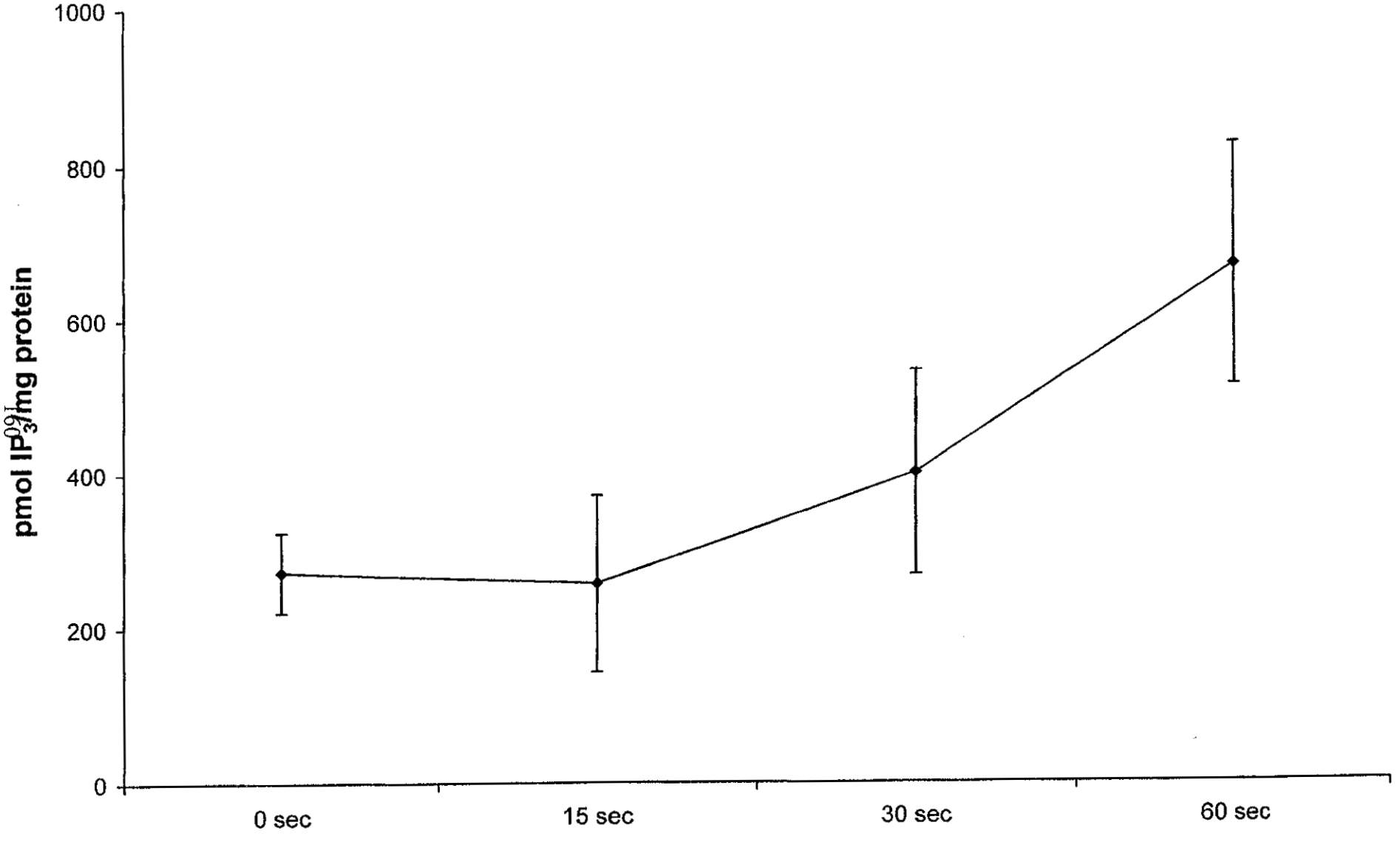
pmol IP3/mg protein
1000
800
600
400
200
0
0 sec
15 sec
30 sec
60 sec

Fig. 10

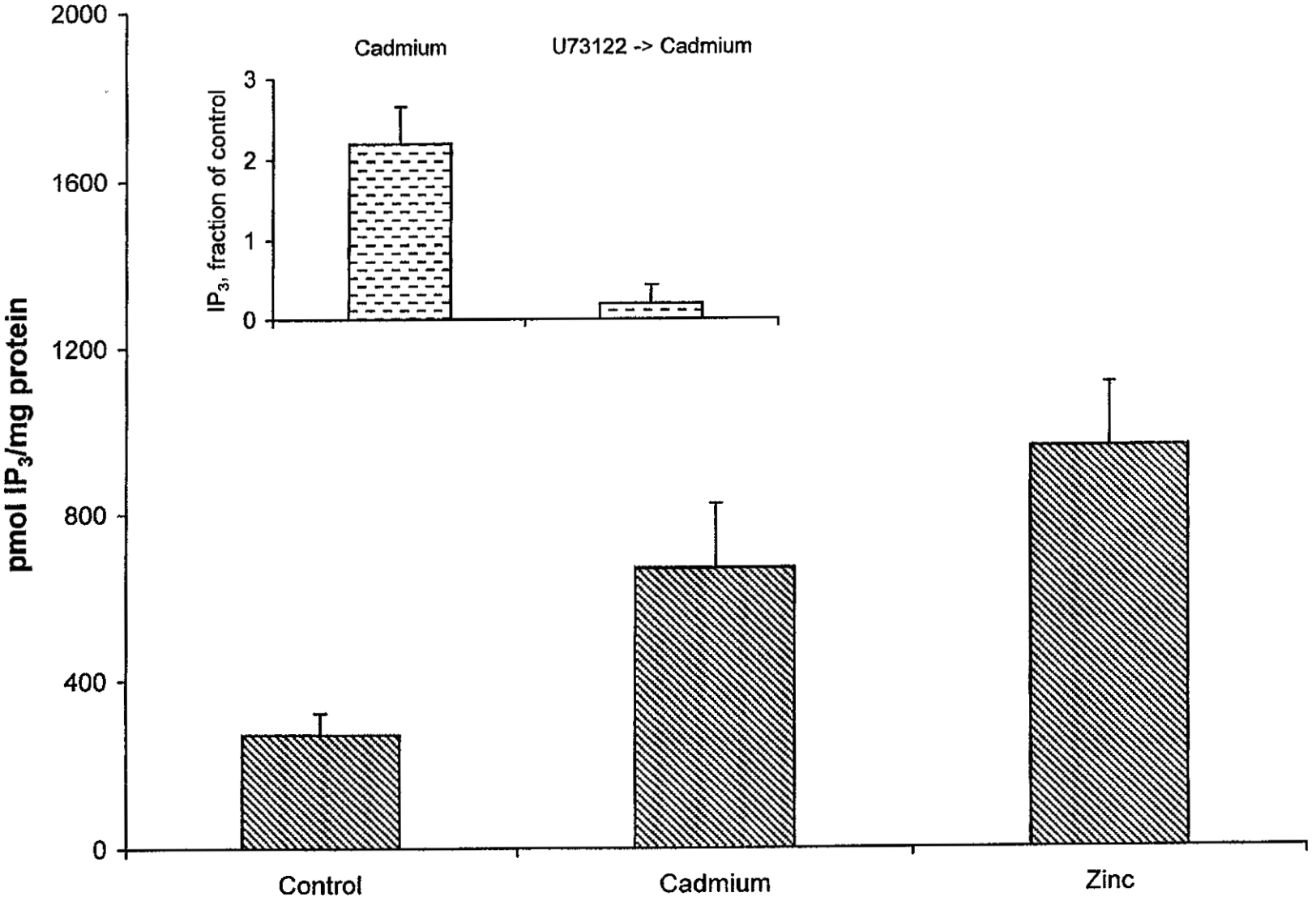
pmol IP3/mg protein
2000
1600
1200
800
400
0
Control
Cadmium
Zinc
Cadmium
U73122 -> Cadmium
IP3, fraction of control
3
2
1
0

143